THE EFFECTS OF TEMPERATURE, SLAG CHEMISTRY AND OXYGEN PARTIAL PRESSURE ON THE BEHAVIOUR OF CHROMIUM OXIDE IN MELTER SLAGS

Neill J. Bartie

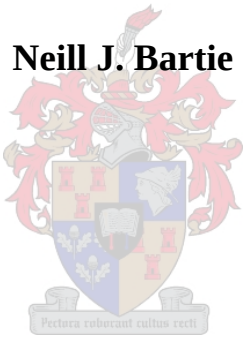

This thesis is presented in partial fulfilment of the requirements for the degree Master of Science in Engineering (Extractive Metallurgy) in the Department of Process Engineering at the University of Stellenbosch

December 2004

Supervisors: Dr. Jacques Eksteen (University of Stellenbosch, South Africa)
Dr. Sharif Jahanshahi (CSIRO Minerals Division, Australia)

Declaration

I, the undersigned, hereby declare that the work contained in this thesis is my own original work and has not previously, in part or in its entirety, been submitted at any university for a degree.

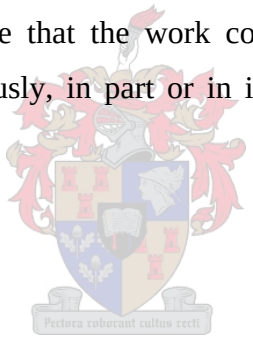

December 2004

_____

Neill J. Bartie

Abstract

This thesis details results obtained in an experimental study conducted to determine the effects of operating temperature, oxygen partial pressure, bulk chromium oxide content and bulk FeO_x/MgO ratio on the solubility of chromium oxide in melter type slags in the platinum industry.

Two PGM-containing layers in the Bushveld Complex in South Africa, the Merensky and UG2 reefs, are currently being mined for the extraction of base metals and platinum group metals (PGM). While the Merensky reef is a pyroxenitic layer, the UG2 reef is a platiniferous chromitite seam. Due to a gradual depletion in Merensky ore reserves, platinum producers have been moving towards the processing of more UG2 concentrates, which are higher in chromium oxide content. The technical difficulties associated with the smelting of concentrates with high chromium oxide contents is a matter of concern. The formation of chromite spinels in melts increases liquidus temperatures and viscosities and subsequently hampers tapping of slags and mattes from furnaces. Bottom build-up from the smelting of high chromium oxide containing concentrates could reduce effective furnace volume.

From the literature reviewed it was found that very few published investigations covered melt compositions and oxygen partial pressures similar to those encountered in the platinum industry. Relevant studies were found to deal with significantly lower bulk chromium oxide and iron oxide contents. It became clear that a need exists for information on the behaviour of chromium oxide and its effects on phase chemistry and stability in melter slags.

It was decided to study the phase equilibria through drop-quench experiments using six synthetic slags with bulk FeO_x/MgO ratios between 0.6 and 1.9 and bulk chromium oxide contents between 1.2 and 7 wt%. Temperatures investigated were 1400, 1500 and 1600°C. The oxygen partial pressure was varied between 6.8×10^{-10} atm at 1400°C to

$8.3x10^{-5}$ atm at 1600°C. Experiments were conducted in a sealed vertical tube furnace and the required oxygen partial pressure in the furnace tube was maintained by controlling the flow rates of purified CO and CO_2 gas mixtures through the tube. Reaction products were quenched after a reaction time of between 20 and 24 hours, depending on temperature, and the phase compositions were analysed by microprobe.

The experimental study revealed that chromium oxide partitions very strongly into the spinel phase relative to the liquid phase, especially at lower temperatures, and higher oxygen partial pressures and bulk chromium oxide contents. The solubility of chromium oxide in the liquid phase was found to increase with increasing temperature and decreasing oxygen partial pressure.

An increase in bulk chromium oxide contents of 1 wt%, under otherwise constant conditions, resulted in an increase in slag liquidus temperature of approximately 100°C over the range of temperatures investigated. At 1500°C and bulk chromium oxide contents of 3.7 and 6.4 wt% a reduction in oxygen partial pressure from $1.1x10^{-5}$ to $1.1x10^{-7}$ atm resulted in increases in soluble chromium oxide of 0.9 and 2.0 wt%, respectively. A further decrease in oxygen partial pressure to $6.7x10^{-9}$ atm resulted in increases in soluble chromium oxide of 2.8 and 4.7 wt%, respectively.

Experimental results were compared to values predicted by the multi-phase equilibrium (MPE) model developed by CSIRO, and found to agree well. Slag basicity was not varied experimentally and therefore the model was used to predict its effect on the solubility of chromium oxide in the liquid phase and the stability of crystalline phases. At constant temperature, an increase in basicity resulted in a decrease in the solubility of chromium oxide in the liquid phase as well as stabilisation of the spinel phase.

It was concluded that practicable combinations of one or more of four main factors, namely increased operating temperature and decreased bulk chromium oxide content, slag basicity and oxygen partial pressure, should be applied and evaluated in a plant

environment to optimise furnace operation. The MPE model would be a valuable tool in predicting the outcomes of such investigations.

Opsomming

Hierdie tesis detaileer die resultate wat verkry is uit ‘n eksperimentele studie uitgevoer om die effek van bedryfstemperatuur, die parsiële druk van suurstof, die algehele chroomoksied inhoud en die algehele FeO_x/MgO verhouding op die gedrag van chroomoksied in smelter slakke in die platinum industrie te bestudeer.

Twee PGM-bevattende ertslae in die Bosveldkompleks in Suid Afrika, die Merensky en UG2 riwwe, word huidiglik gemyn vir die ekstraksie van basismetale en platinumgroep metale (PGM). Die Merensky rif is ‘n piroksenitiese laag terwyl die UG2 rif ‘n platinumbevattende chromitiet laag is. As gevolg van ‘n geleidelike afname in reserwes van Merensky erts beweeg platinumprodusente al meer na die verwerking van groter hoeveelhede UG2 erts. Die tegniese probleme wat gepaard gaan met die smelting van konsentrate met hoë chroomoksied inhoud kan ‘n rede tot kommer wees. Die vorming van chromiet spinelle in die slak- en matfases verhoog likuidus temperature en viskositeite en bemoeilik die tap van hierdie fases uit oonde. Die opbou van soliede fases verlaag ook die effektiewe oondvolume.

Uit die literatuurstudie is gevind dat gepubliseerde studies waarin slak samestellings en parsiële suurstofdrukke wat betrekking het op die platinumindustrie bespreek is, baie beperk is. Dit is gevind dat relevante navorsing gedoen is met aansienlik laer algehele chroom- en ysteroksied konsentrasies. Gevolglik het dit duidelik geword dat ‘n behoefte bestaan vir inligting oor die gedrag van chroomoksied in oonde en die effekte daarvan op fasechemie en –stabiliteit in smelter slakke.

Daar is besluit om eksperimente uit te voer deur die gebruik van ses sintetiese slakke met algehele FeO_x/MgO verhoudings tussen 0.6 en 1.9 en algehele chroomoksied konsentrasies tussen 1.2 en 7.0 % (op ‘n massabasis). Temperature van 1400, 1500 en 1600°C en suurstof parsiële drukke tussen 6.8×10^{-10} atm by 1400°C en 8.3×10^{-5} atm by 1600°C is ondersoek. Eksperimente is uitgevoer in ‘n geseëlde vertikale buisoond en die

vereiste suurstofdruk in die oond is gehandhaaf deur beheer van die vloeitempos van gesuiwerde CO en CO_2 gas deur die oond. Reaksieprodukte is in water geblus na ‘n reaksietyd van tussen 20 en 24 ure, afhangende van die reaksietemperatuur. Fasesamestellings is bepaal deur mikrosonde analises.

Die eksperimentele studie het bewys dat chroomoksied baie sterk in die spinelfase konsentreer relatief tot die vloeistoffase, veral by laer temperature, suurstofdrukke en algehele chroomoksied konsentrasies. Dit is gevind dat die oplosbaarheid van chroomoksied in die vloeistoffase toeneem met toenemende temperatuur en afnemende suurstofdruk.

‘n Toename in die algehele chroomoksied konsentrasie van 1 massa%, onder andersins onveranderde toestande, het ‘n toename van ongeveer 100°C in likuidus temperature veroorsaak tussen 1400 en 1600°C. By 1500°C en algehele chroomoksied konsentrasies van 3.7 en 6.4 massa%, het ‘n verlaging in suurstofdruk vanaf $1.1x10^{-5}$ tot $1.1x10^{-7}$ atm respektiewelike toenames in die chroomoksied oplosbaarheid van 0.9 en 2.0 massa% veroorsaak. ‘n Verdere verlaging in suurstofdruk tot $6.7x10^{-9}$ atm het respektiewelike toenames in chroomoksied oplosbaarheid van 2.8 en 4.7 massa% veroorsaak.

Eksperimentele resultate is vergelyk met waardes wat voorspel is deur die multifase ewewigsmodel (MPE), ontwikkel deur CSIRO, en goeie ooreenstemming is gevind. Verskillende slak basisiteite is nie eksperimenteel ondersoek nie en daarom is die model gebruik om die effek daarvan op die oplosbaarheid van chroomoksied in die vloeistoffase asook die stabiliteit van kristallyne fases te bepaal. By konstante temperatuur het ‘n toename in slak basisiteit ‘n afname in chroomoksied oplosbaarheid veroorsaak en die spinelfase gestabiliseer.

Die aanbeveling is gemaak dat ‘n kombinasie van een of meer van vier hooffaktore, naamlik hoër bedryfstemperature en laer algehele chroomoksied konsentrasies, slak basisiteit en suurstofdruk, in die praktyk toegepas en geëvalueer moet word om sodoende

optimum bedryfkondisies te bepaal. Die multifase ewewigsmodel is ‘n nuttige instrument wat gebruik kan word om die resultate van sulke ondersoeke te voorspel.

Acknowledgements

My sincere thanks to the following people and organisations:

To Lonmin Platinum, in particular Mr. Kevin Hay and Dr. Michael Turner Jones, for giving me the great opportunity to further my skills at CSIRO in Melbourne, Australia, and for financial support during my time abroad.

To my supervisors, Dr. Sharif Jahanshahi, Dr. Shouyi Sun and Dr. Jacques Eksteen for suggesting the project and for inviting me to conduct the work in Australia. Also, for their guidance and support during the course of the experimental work and the writing of this thesis.

To AMIRA International and the sponsors of the P479A project (Impala Platinum, Anglo Platinum, Kumba Resources, BHP Steel and Rio Tinto) without whom this project would not have been undertaken. To CSIRO Minerals, for making a major financial contribution to the P479A project.

To Ling Zhang, Steve Wright, Michael Somerville, Justen Bremmell, Colin Nexhip, Rowan Davidson, Ty Tran, Dongsheng Xie and Rodney Hundermark for their assistance in the theoretical and experimental aspects of the work and for their friendship. Also, to personnel of the Analytical Science Group at CSIRO, in particular Luda Malichev, Nick Wilson, Colin McRae, Steve Peacock and Lisa Marolda for their assistance in preparing and analysing many samples.

To Dr. Johan Nell and Steve McCullough for their good advice and useful comments prior to commencement of the work and during the writing of this thesis.

My sincere gratitude to all my friends in Melbourne, especially Trina Dearricott and Rita Spiteri, for their true friendship and support during my time in Australia.

To my mother, Delene,

for her unconditional love and support in everything I do

Table of Contents

Chapter 1

INTRODUCTION

1.1 The Merensky and UG2 reefs

The Bushveld Complex, a large mineral deposit situated in the northern region of South Africa, contains the world's largest known reserves of Platinum Group Metals (hereafter referred to as PGMs). The major PGM containing layers are the Merensky and UG2 (upper group 2) reefs. The Merensky reef is a pyroxenitic layer, the major silicate minerals being pyroxenes [$(Fe,Mg)SiO_3$] and plagioclase [$CaAl_2Si_2O_8$]. The UG2 reef is a platiniferous chromitite seam, the main constituent being chromite [$(Fe{\cdot}Mg)^{2+}O{\cdot}(Cr{\cdot}Fe{\cdot}Al)^{3+}{}_2O_3$] with a chromium-to-iron ratio of approximately 1.35. In both reefs, the majority of PGM minerals are associated with the base metal sulphides (Liddell *et. al.*, 1986).

The UG2 reef is between 15 and 255 cm thick and lies 15 to 330m below the Merensky reef, running roughly parallel to it (Corrans *et. al.*, 1982). To a depth of 1200m, reserves of Merensky and UG2 ores have been estimated at approximately 3300 Mt and 5420 Mt, respectively (Liddell et al, 1986).

Typical compositions of the two reefs are given in Table 1.1. As is evident from this table the PGM contents of the two reefs are similar, while the chromium oxide content of the UG2 reef is significantly higher than that of the Merensky reef. The Merensky reef is considerably richer in both copper and nickel.

Table 1.1: Comparison of Merensky and UG2 ore compositions (Corrans et al, 1982)

Reef	**PGM (g/t)**	**Cu (wt%)**	**Ni (wt%)**	**Cr_2O_3 (wt%)**
Merensky	4-8	0.10-0.16	0.16-0.20	0.1
UG2	4.6-7.3	0.004-0.012	0.010-0.029	27-34

The Merensky reef has been mined since the early 1920s. The first full investigation into the economic viability of concentrating and smelting ore from the UG2 reef commenced in 1979 and the reef has been exploited in its own right since early 1983, when a concentrating and smelting plant was commissioned at Western Platinum Mine, near Rustenburg, South Africa, specifically for the processing of UG2 ore. The chromium oxide (Cr_2O_3) content of UG2 concentrates has been gradually increasing since then from 2.9 wt% (Liddell et al, 1986) to current levels of up to 6 wt% from some concentrators.

Typical dry concentrate compositions are shown in Table 1.2.

Table 1.2: Typical dry concentrate compositions (furnace feed)

Reef	**PGM (g/t)**	**Cu (wt%)**	**Ni (wt%)**	**Cr_2O_3 (wt%)**
Merensky	148.5	2.5	3.9	0.7
UG2	262.0	1.8	2.8	2.0

1.2 The smelting of Merensky and UG2 concentrates

Large volumes of slag are produced during the smelting of UG2 and Merensky concentrates. The average compositions of typical melter slags (oxides normalised to 100%) are given in Table 1.3.

Table 1.3: Average Merensky and UG2 slag compositions

Reef	FeO_x (wt%)	MgO (wt%)	SiO_2 (wt%)	Al_2O_3 (wt%)	Cr_2O_3 (wt%)	CaO (wt%)
Merensky	30.7	11.3	39.1	3.0	0.9	15.0
UG2	11.8	19.4	42.6	4.3	1.8	20.1

Platinum producers have been moving towards the processing of more UG2 concentrate relative to Merensky concentrate due to the gradual depletion in Merensky ore reserves. The higher chromium content of UG2 concentrate has been a matter of concern because of the technical difficulties associated with smelting high chromium containing concentrates. These include the formation of chromite spinels in melts, which increases liquidus temperatures and slag viscosities and subsequently hampers the settling of matte and the tapping of slags and mattes from furnaces. The formation of bottom build-ups as a result of spinel formation reduces effective furnace volume and could potentially hamper PGM recovery.

Depending on furnace operating conditions, three mineral phases can form in the slag: spinels, olivines and pyroxenes. These will be briefly introduced in turn.

The spinel phase has the general formula XY_2O_4 where X represents divalent cations such as Mg^{2+}, Fe^{2+}, Mn^{2+}, Ni^{2+} or Zn^{2+}, and Y represents trivalent cations such as Fe^{3+}, Al^{3+} and Cr^{3+} and Mn^{3+}. Some typical end-member spinels include the following:

- Chromite: $FeCr_2O_4$
- Hercynite: $FeAl_2O_4$
- Magnetite: Fe_3O_4
- Picrochromite: $MgCr_2O_4$
- Spinel: $MgAl_2O_4$
- Magnesioferrite: $MgFe_2O_4$

Spinels in which both trivalent cations occupy octahedral sites are termed normal spinels. Inverse spinels are those in which trivalent cations are distributed between octahedral and tetrahedral sites (Murck and Campbell, 1986). Most of the ferrite spinels have an inverse spinel structure, while chromites have a normal structure due to the high octahedral site preference of Cr^{3+} (Stubican and Greskovich, 1975).

The presence of chromous ion (Cr^{2+}) in spinel structures under very reducing conditions has been reported. In the solid solution between $FeCr_2O_4$ and $MgCr_2O_4$ (normal spinels) Fe^{2+} and Mg^{2+} are found in tetrahedral coordination. Cr^{2+} was detected at 1300°C in equilibrium with a metal phase and assumed to have substituted for Fe^{2+} reduced to metallic iron (Ulmer and White, 1966). In the iron-free system $MgO\text{-}Al_2O_3\text{-}Cr_2O_3$ it has been shown that Cr_2O_3 does not dissolve in $MgCr_2O_4$ spinel but that Cr^{2+} readily substitutes for Mg^{2+} in tetrahedral sites in the spinel structure under reducing conditions at 1700°C (Stubican and Greskovich, 1975). Spinels are very stable at high temperature and can raise the liquidus temperature of slags considerably.

The name olivine refers to the solid solution series $(Fe,Mg)_2SiO_4$ between the two end-members fayalite (Fe_2SiO_4) and forsterite (Mg_2SiO_4). Iron and magnesium are substituted for each other without any significant effects on crystal structure. Olivine minerals have high melting points and are the first to crystallize from ferromagnesian magmas (Amethyst Galleries' Mineral Gallery, 1997).

Pyroxenes are a family of iron-magnesium silicates that have the general formula XYZ_2O_6 where X represents ions such as Mg^{2+}, Fe^{2+}, Mn^{2+}, Li^{+}, $Ca^{2+}$and Na^{+}; Y represents ions such as Al^{3+}, Fe^{3+}, Cr^{3+}, Ti^{4+}, Mg^{2+}, Fe^{2+} and Mn^{2+} and Z represents Si, Al^{3+} and Fe^{3+}. The most common form is $(Ca,Mg,Fe)_2Si_2O_6$ (Eric Weisstein's World of Science, 2004).

1.3 The effect of suspended crystals on smelting

The effect of suspended crystals in a melt is to increase its apparent viscosity and in this way the precipitation of spinel crystals in furnace slags plays a significant role. An empirical viscosity model developed by Roscoe (Roscoe, 1952) gives the relationship between viscosity and the total amount of solids present in the system and can be used to estimate the apparent viscosity. This relationship, known as the Einstein-Roscoe equation, was developed for systems at room temperature and was evaluated by Wright *et.al.* (2000) for melts containing solid particles. It indicates that the relative melt viscosity increases exponentially with an increase in the volume fraction of solid phases present in the melt. The relationship is represented by the following equation:

$$\eta_R = \frac{\eta_M}{\eta_L} = \left(1 - R \cdot \Phi_S\right)^{-n} \qquad (1.1)$$

where η_R is the relative melt viscosity, η_M is melt viscosity, η_L is the liquid viscosity without any solids present, Φ_S is the volume fraction of solids and n and R are constants related to the size and shape of solid particles. For rigid spheres of diverse sizes, values for n and R are 2.5 and 1, respectively. Wright *et al.* (2000) studied the rheological behaviour of CaO-MgO-Al_2O_3-SiO_2 melts containing $MgAl_2O_4$ spinel particles and found the Roscoe equation to provide a good fit of experimental observations. Although it was found that n and R varied slightly with particle size, parameter values of $n=2.5$ and $R=3.2$ a good estimate for particles between 100 and 400μm in size.

Tapping of slags with high viscosities becomes problematic unless high operating temperatures are maintained to destabilise solid phases, thereby reducing melt viscosity. Smelting operations become exceedingly energy intensive in such instances and this could lead to accelerated wear of protective refractory linings and tapping channels. Furthermore, containment of matte at very high operating temperatures could present additional challenges to furnace operators.

Increased slag viscosity may also impact on the settling of matte droplets in a molten slag. The terminal settling velocity, v_∞, of matte droplets in a slag with effective viscosity η_m, is given by the Stokes equation:

$$v_\infty = \frac{g d_{matte}^2 (\rho_{matte} - \rho_{slag})}{18\eta_m} \qquad (1.2)$$

where η_m is the melt viscosity (liquid + crystals), d_{matte} the matte droplet size and ρ_{matte} and ρ_{slag} the respective densities of the matte and slag phases (Perry and Green, 1984).

From this equation it is apparent that an increase in melt viscosity would result in a decrease in the velocity of a matte droplet moving through the melt, which in turn decelerates separation of the slag and matte phases. This could also lead to PGM losses due to matte being entrained in the slag phase.

~ * ~

The objective of this study was to characterise phase equilibria and the behaviour of chromium in multi-component slags representative of those encountered during sulphide-smelting in the platinum industry. Also, to determine what operating conditions may lead to the formation of solids, and to characterise the glass and solid phases, in order to provide guidelines for effective furnace operation. It was decided to use the system $MgO\text{-}FeO_x\text{-}SiO_2$ as a reference for the work conducted during this study, since it forms the basis of many metallurgical slags found in the base and precious metals industry.

Literature pertaining to systems related to that under investigation will be discussed in Chapter 2. It will be shown that most research studies have been aimed at gaining an understanding of systems in the steelmaking and ferrochrome industries and at improvements in refractory performance industry and that a gap exists in published knowledge of non-ferrous slags in the platinum and base metals industry.

In Chapter 3 the experimental procedure will be presented, including preparation of materials, as well as equipment and analytical techniques utilised.

Results from equilibrium drop-quench experiments will be given in Chapter 4. The effect of the variables studied on parameters that are considered important, as well as a comparison with data predicted by the multi-phase equilibrium (MPE) model will be discussed in Chapter 5. The model will also be used to simulate actual furnace conditions. Predicted data will also be discussed.

Conclusions drawn from this research will be presented in Chapter 6.

Chapter 2

LITERATURE REVIEW

Apart from some minor species, PGM smelting slags generally have compositions falling within the multi-component system FeO_x-MgO-SiO_2-CrO_x-Al_2O_3-CaO. The slags studied in this work contained 5 wt% each of Al_2O_3 and CaO and between 1.5 and 7.1 wt% Cr_2O_3. Silica contents varied from 44 to 50 wt% and the ratio of total iron oxide (expressed as FeO) to MgO was varied between 0.6 and 1.9. As mentioned earlier, it was decided to use the MgO-FeO_x-SiO_2 ternary system as a reference for the work conducted during this study, since it represents the main constituents of many metallurgical slags found in the base and precious metals industry.

This review focuses on literature about phase equilibria in the reference system, the effect of chromium oxide, alumina and calcium oxide additions, chromium distribution as well as the effect of oxidation state on the behaviour of phases in the system.

2.1 Background on slag structure

It has been estimated that the earth's crust contains close to 50 wt% oxygen and over 25 wt% silicon. The next most abundant elements are believed to be aluminium, iron, calcium, sodium, potassium and magnesium in decreasing order. The metal-bearing minerals are usually sulphides, oxides or silicates but some metals, such as gold and platinum, occur as elements in ore deposits due to the instability of noble metal compounds.

Slags consist mainly of oxides and are used in most pyrometallurgical processes, including matte smelting and conversion in the extraction of copper, nickel and platinum group metals from sulphide ores. Slags fulfil two major functions:

- In extraction processes they take up gangue minerals which are not reduced to metals, and
- In refining processes they absorb, under the right conditions, unwanted constituents of metals and mattes.

In order for a slag to fulfil these functions, the following properties are important (Parker):

- It must possess a low enough viscosity (*i.e.* be sufficiently fluid) to allow easy separation from the metal or matte phase and to increase mass transfer rates across phase interfaces.
- It must become fluid at a low enough temperature for the process to be run economically, that is with as little as possible energy input and refractory wear. Fluxes may be added to lower liquidus temperatures and slag viscosities.
- The slag density should be sufficiently different from that of the metal or matte to allow easy separation.
- It must have the correct composition and structure to dissolve impurities at low activity and to allow for any required slag/metal or slag/matte reactions to take place. Ideally it should have a low solubility for the oxide of the metals being extracted and a high solubility for unwanted constituents.

Oxides generally fall into covalent and ionic groups. Most of the important covalent oxides, such as SiO_2, GeO_2, B_2O_3, P_2O_5 and As_2O_3, have oxygen atoms bonded to form three-dimensional networks. In liquid form these oxides usually have high viscosities and low electrical conductivities. Other metal oxides are generally ionic and are less viscous and more electrically conductive in liquid form (Jones).

Silica (SiO_2) forms the basis of most slags and is considered an acidic oxide, which will absorb oxygen ions supplied by other (basic) oxides according to the reaction:

$$SiO_2 + 2O^{2-} = SiO_4^{4-} \quad (2.1)$$

or $$Si^{4+} + 4O^{2-} = SiO_4^{4-} \quad (2.2)$$

The SiO_4^{4-} ion or its polymers is dominant in glasses. Oxygen atoms are tetrahedrally arranged around the silicon atom in strongly covalent bonds. The SiO_4^{4-} unit is very stable but prone to polymerisation. The structure of silica when solid is a hexagonal lattice of silicon atoms, each with four tetrahedrally coordinated oxygen atoms, extending symmetrically in three dimensions. When molten the rigid lattice is lost but the SiO_4^{4-} tetrahedra remain intact. The extent to which the tetrahedra remain linked to one another depends on temperature (Gilchrist). The solid and molten structures of the silica matrix are shown in Figure 2.1.

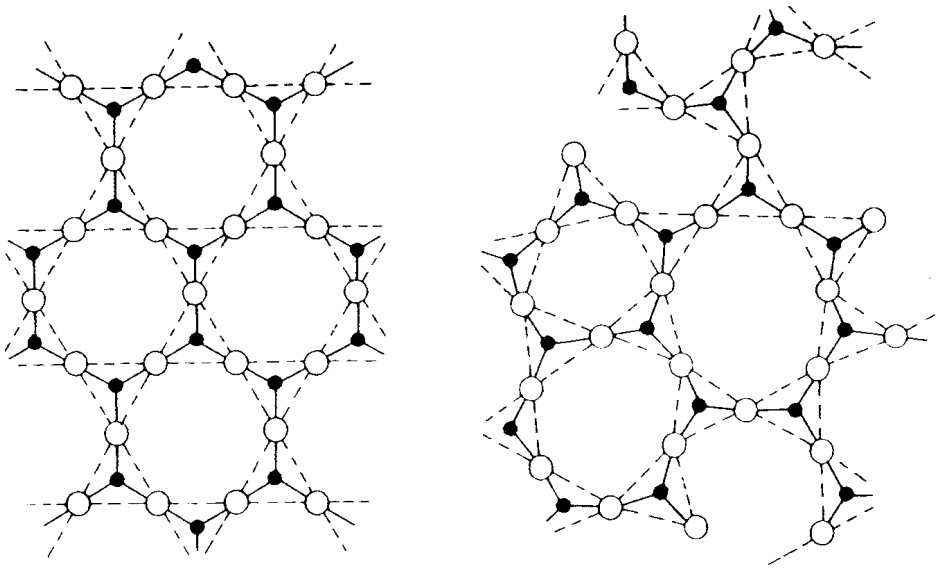

Figure 2.1: Solid and molten structure of a silica matrix (Gilchrist)

Other oxides such as CaO, MgO, MnO, FeO, ZnO, PbO, Cu_2O, Na_2O and K_2O are considered basic oxides because of their ability to provide oxygen ions when dissolved in slags. These oxides dissociate according to the reaction:

$$XO = X^{2+} + O^{2-} \qquad (2.3)$$

Two divalent metal cations (X^{2+}) can combine with one silica anion (SiO_4^{4-}) to form an orthosilicate ($2XO \cdot SiO_2$).

Acid slags are those that contain more acidic oxide than the orthosilicate composition ($2XO \cdot SiO_2$). These slags have little or no free O^{2-} ions but have a high capacity to incorporate them into their structures. Basic slags, on the other hand, contain more basic oxide than the orthosilicate composition. In such slags there is an excess of oxygen ions that are not part of the silicate anion structure. For example, acid slags with high fluidity may attack refractories made from basic oxides – the basic oxides dissociate and supply O^{2-} ions to the silicate slag (Parker).

Some oxides, such as Al_2O_3 and Fe_2O_3 are known to behave amphoterically; they act as basic oxides in acid slags and as acidic oxides in basic slags (Parker).

2.2 Phase equilibrium in the system FeO_x-MgO-SiO_2

The system MgO-FeO-SiO_2 (hereafter referred to as the reference system) was first studied in detail by Bowen and Schairer in 1934. Their study was conducted under reducing conditions, in equilibrium with liquid iron. They found three series of solid solutions, namely the magnesio-wüstite series (FeO-MgO), the olivine series (Mg_2SiO_4-Fe_2SiO_4) and the pyroxene series ($MgSiO_3$-$FeSiO_3$). Both the magnesio-wüstite and the olivine solid solution series are complete *i.e.* each end-member in the series exhibits complete solution into the other, while the pyroxene series is partially complete with limited solubility of $FeSiO_3$ in $MgSiO_3$ (Bowen and Schairer, 1935).

The liquidus surface of the ternary diagram for this system is confined by the phase boundaries for the above-mentioned three series as well as those for cristobalite and tridymite. Also included at high SiO_2 concentrations is the miscibility gap where two liquid phases co-exist. The ternary phase diagram is shown in Figure 2.2.

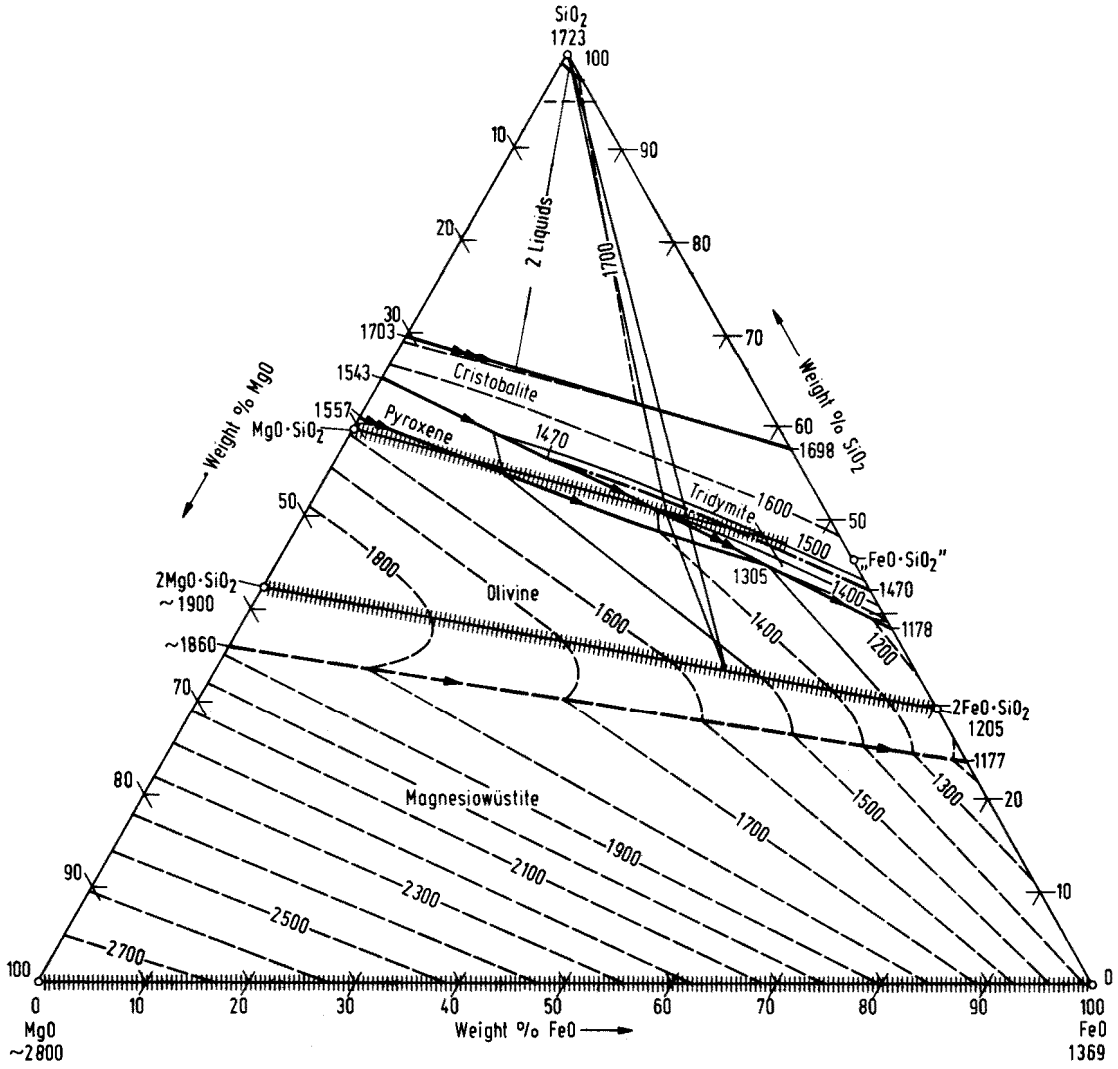

Figure 2.2: Ternary phase diagram for the system MgO-FeO-SiO_2 (Slag Atlas, 1995)

The effect of higher oxygen partial pressure on phase equilibria was taken into account when the system MgO-FeO-Fe_2O_3-SiO_2 was studied at temperatures between 1159°C and 1775°C and oxygen partial pressures over the range 1 to $10^{-8.9}$ atm by Muan and Osborne (1956). It was found that liquidus temperatures decreased as Fe^{2+} replaced Mg^{2+} and oxygen pressure was decreased. The lowest liquidus temperatures were therefore found where both the MgO content and the oxygen pressure were lowest (Muan and Osborne, 1956).

Speidel and Osborn (1967) conducted an investigation into element distribution among co-existing phases in the system MgO-FeO-Fe_2O_3-SiO_2 in equilibrium with a gas phase as a function of temperature and oxygen fugacity. The study focussed on phase composition changes during equilibrium cooling. Amongst the crystalline phases observed were olivine, pyroxene, magnesioferrite and tridymite. It was found that the ratio Mg:Fe in all of the condensed phases decreased as temperature and oxygen fugacity decreased. Speidel and Osborn found that olivine in equilibrium with pyroxene, magnetite and liquid was found to be higher in iron content than co-existing pyroxene in all cases.

A similar study of equilibrium phase compositions and thermodynamic properties of pyroxene and olivine in the system MgO-FeO_x-SiO_2, in equilibrium with metallic iron, was conducted by Nafziger and Muan (1967) at sub-solidus temperatures (between 1150 and 1250°C). It was found that virtually no Fe^{3+} was present in olivine and pyroxene under these conditions. Element distributions in olivine-pyroxene assemblages are thus believed to be valid at higher oxygen partial pressures as well (Nafziger and Muan, 1967).

In summary, the phase fields of olivine, pyroxene, magnesiowüstite, tridymite and cristobalite were found to exist in this system under reducing conditions. At sub-solidus temperatures magnesioferrite was also found as a crystalline phase. Liquidus temperatures in the system were found to decrease with decreasing oxygen potential and decreasing MgO content.

2.3 Chromium-free systems and the oxidation state of iron in melts

Shim and Ban-Ya (1980) studied the solubility of MgO and ferric-ferrous redox equilibria in liquid slags in the FeO_x-SiO_2-CaO-MgO system in equilibrium with liquid iron. Their findings included that the solubility of MgO decreases with increasing total slag iron content as well as slag basicity. Their results are shown in Figure 2.3.

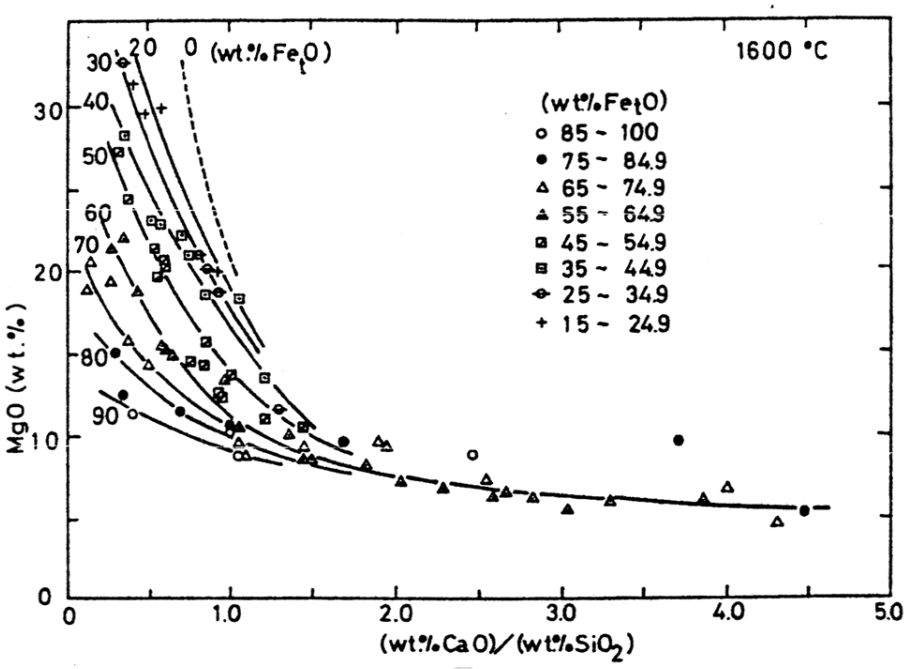

Figure 2.3: The effect of FeO_x content and basicity on the solubility of MgO at 1600°C (Shim and Ban-Ya, 1980)

The Fe^{3+}/Fe^{2+} ratio in these slags was found to increase with increasing oxygen potential, slag basicity and decreasing total iron content. At a given oxygen potential, the Fe^{3+}/Fe^{2+} ratio in the reference system (FeO_x-MgO-SiO_2) was found to decrease with increasing silica content. Empirical relationships were proposed for the solubility of MgO and the Fe^{3+}/Fe^{2+} ratio in FeO_x-MgO slags as functions of temperature over the range 1536°C to 1660°C (Shim and Ban-Ya, 1980).

Zao *et al.* (1999) studied the effect of MgO and Al_2O_3 on slag liquidus temperatures in the systems MgO-FeO_x-CaO-SiO_2 and Al_2O_3-MgO-FeO_x-CaO-SiO_2. They concluded that MgO expands the fayalite primary phase field towards higher SiO_2 contents and increases liquidus temperatures by approximately 24°C per weight percent MgO added. Addition of Al_2O_3 decreased liquidus temperatures in the fayalite primary phase field. It was reported that the effects of MgO and Al_2O_3 on liquidus temperatures of fayalite slags are independent of one another.

A study by Liu *et. al.* (2001) of the activity of FeO and the solubility of MgO in slags in the system $FeO\text{-}SiO_2\text{-}CaO\text{-}MgO\text{-}Al_2O_3$ (saturated with MgO) revealed that the solubility of MgO increases slightly with decreasing FeO content. The main constituents of slags used in this study were MgO, CaO and SiO_2 with Al_2O_3 and FeO_x contents below approximately 8 wt%. It was found that the CaO content had the greatest effect on MgO solubility - an increase in slag CaO content resulted in a decrease in MgO solubility. These results are in agreement with those of Shim and Ban-Ya (1980) mentioned earlier. Knowledge of the solubility of MgO in slags is important in limiting refractory consumption, as the correct addition of MgO to slags would reduce dissolution of magnesia from refractory materials.

Jahanshahi and Wright (1992) studied equilibrium Fe^{3+}/Fe^{2+} ratios in $Al_2O_3\text{-}CaO\text{-}FeO_x\text{-}SiO_2$ and $Al_2O_3\text{-}CaO\text{-}FeO_x\text{-}MgO\text{-}SiO_2$ slags at temperatures between 1400°C and 1500°C and at oxygen partial pressures ranging between $3x10^{-9}$ and 10^{-5} atm. Slags used in this study were high in Al_2O_3, CaO and SiO_2 with total Fe contents in the range 0.75 to 24 wt%. They mentioned the fact that the Fe^{3+}/Fe^{2+} ratio increases with increasing oxygen potential, according to the expression:

$$(\frac{Fe^{3+}}{Fe^{2+}})^2 \propto (\frac{p_{CO_2}}{p_{CO}}) \qquad (2.4)$$

which represents the equilibrium reaction:

$$Fe_2O_3 = 2FeO + ½O_2. \qquad (2.5)$$

Figure 2.4 shows the variation of Fe^{3+}/Fe^{2+} with total iron content as found by these authors.

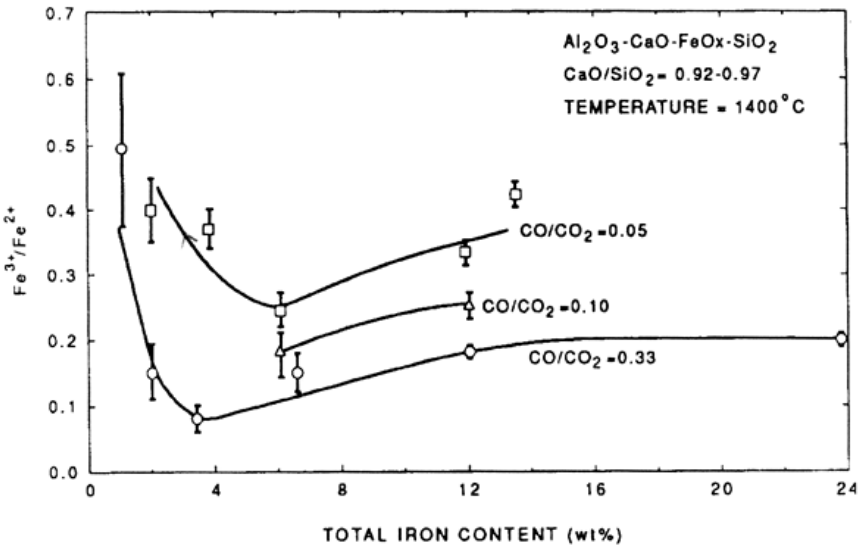

Figure 2.4: Variation of Fe^{3+}/Fe^{2+} with total Fe content of slags at 1400°C (Jahanshahi and Wright, 1992)

Their results showed that the Fe^{3+}/Fe^{2+} ratio decreases sharply as the total iron contents of slags increased from 0.75 to approximately 2 wt% and remains practically constant with an increase in total iron content from 6 wt% to 24 wt% (Jahanshahi and Wright, 1992).

Yang and Belton (1998) investigated Fe^{3+}/Fe^{2+} ratios in CaO-Al_2O_3-SiO_2 and MgO-CaO-Al_2O_3-SiO_2 slags between 1300°C and 1500°C in equilibrium with oxygen potentials ranging between pCO_2/pCO = 0.01 and air. Their study was conducted using calcium-silicate slags with alumina contents between 17 and 23 wt% and iron oxide and magnesia contents below 10 wt%. They obtained the following expression for Fe^{3+}/Fe^{2+} ratio as a function of slag basicity and pCO_2/pCO:

$$\log\left(\frac{Fe^{3+}}{Fe^{2+}}\right) = 0.3(\pm 0.02)Y + 0.45(\pm 0.01)\log\left(\frac{pCO_2}{pCO}\right) - 1.24(\pm 0.01) \qquad (2.6)$$

where Y = (CaO+MgO)/SiO_2 under the following conditions:

- Molar CaO/SiO_2 ratio between 0.45 and 1.52
- 10-15 mol% Al_2O_3
- Up to 12 mol% MgO
- Total Fe between 3 and 10 wt%

Iron redox equilibria was found to be essentially independent of both temperature, over the range 1350°C and 1600°C, and iron content at total iron concentrations between 3 and 10 wt% (Yang and Belton, 1998). This is in partial agreement with Jahanshahi and Wright's observation with total iron contents of between 6 and 24 wt% (Jahanshahi and Wright, 1992). In basic melts (CaO/SiO_2=1.3) with alumina contents between 10.4 and 14.4 wt% the authors reported Al_2O_3 to simply act as a diluent. In acid melts (CaO/SiO_2=0.64) Al_2O_3 appeared to act as a strong basic compound (Yang and Belton, 1998).

Kim and Sohn (1998) studied the effects of lime, alumina and magnesia additions on the solubility of copper, Fe^{3+}/Fe^{2+} ratio and minor element behaviour in silica-saturated iron silicate slags (36 wt% SiO_2). Experiments were conducted in equilibrium with liquid copper over a range of oxygen partial pressures between 10^{-12} and 10^{-6} atm. Both the solubility of Cu and the Fe^{3+}/Fe^{2+}-ratio were found to decrease with the additions of CaO, Al_2O_3 and MgO. The decrease in Fe^{3+}/Fe^{2+} ratio was found to be less significant at lower oxygen partial pressures. Mention was made of the fact that an increase in silica content of silica-saturated iron silicate slags results in a decrease in the Fe^{3+}/Fe^{2+} ratio (Kim and Sohn, 1998).

Roeder and Osborn (1966) studied the system Mg_2SiO_4-FeO-Fe_2O_3-$CaAl_2SiO_8$-SiO_2 at oxygen partial pressures between 10^{-9} and $10^{-0.7}$ atm and temperatures below 1185°C. They introduced both CaO and Al_2O_3 (in a 1:1 mole ratio) to the reference system. Their findings included that pyroxene and spinel exist simultaneously down to oxygen partial pressures of approximately 10^{-9} atm (Roeder and Osborn, 1966). At lower oxygen partial pressures pyroxene starts to precipitate with other silicates, rather than with spinel (Ulmer, 1970).

Karlemo and Taskinen (2000) simulated a nickel slag cleaning operation and found that for SiO_2 contents between 40 and 45%, the addition of Al_2O_3 lowers liquidus temperatures more significantly than CaO. At higher SiO_2 contents, however, the addition

of Al_2O_3 resulted in rapid increases in liquidus temperatures (Karlemo and Taskinen, 2000).

Kongoli and Yazawa (2000) studied the effect of oxygen partial pressure (pO_2), MgO and Al_2O_3 on the system FeO_x-SiO_2-CaO by means of thermodynamic modelling. It was found that at constant Fe/SiO_2 ratio in smelting and converting slags, both Al_2O_3 and CaO decrease the liquidus temperature under reducing conditions on the olivine precipitation surface ($pO_2 < 10^{-9}$ atm), whilst increasing liquidus temperatures under more oxidising conditions on the spinel saturation surface (pO_2 between 10^{-8} and 10^{-6} atm). At intermediate oxygen partial pressures, alumina was found to stabilise the spinel phase and decrease the liquid region in the spinel saturation area. MgO was found to increase liquidus temperatures under both oxidising and reducing conditions, the effect being more pronounced at lower pO_2. These authors emphasised the fact that additions of Al_2O_3, CaO and MgO would only decrease liquidus temperatures in cases where slags are silica-saturated. In silica non-saturated iron-silicate slags additions of these oxides increase liquidus temperatures in the spinel precipitation field and increase the risk of spinel (magnetite) formation (Kongoli and Yazawa, 2000).

In summary, the addition of CaO (*i.e.* an increase in slag basicity) to the reference system at a given temperature and oxygen potential resulted in decreases in the solubility of MgO and increases in the Fe^{3+}/Fe^{2+} ratio in melts. In smelting and converting slags, CaO was found to decrease liquidus temperatures on the olivine precipitation surface, whilst increasing liquidus temperatures on the spinel precipitation surface.

Redox equilibria data show that, in basic melts with Al_2O_3 contents between 10 and 14 wt%, Al_2O_3 was found to act as a diluent, while in acid slags it was found to act as a strong basic compound. At silica contents between 40 and 45 wt%, Al_2O_3 was found to decrease liquidus temperatures, while at higher silica contents additions of Al_2O_3 resulted in sharp increases in liquidus temperatures. At intermediate oxygen partial pressures, Al_2O_3 stabilised the spinel phase and increased liquidus temperatures; under more reducing conditions it decreased liquidus temperatures.

2.4 Iron-free systems and the oxidation state of chromium in melts

Chromium can exist in a range of oxidation states, the most commonly observed Cr^{2+}, Cr^{3+} and Cr^{6+}. Therefore, it is to be expected that phase equilibria in chromium-containing systems would be strongly dependent on oxygen partial pressure (Nell and De Villiers, 1993). The most stable oxide of chromium is Cr_2O_3, as the trivalent chromium cation exists over a wide range of temperature and composition. Under oxidising conditions, such as in air, a considerable proportion of chromium also exists in higher valence states, mostly as Cr^{6+}, especially when the slag basicity is high (Pretorius *et al.*, 1992). Schwerdtfeger and Mirzayousef-Jadid (2000) reported that calcium silicate slags contain significant amounts of Cr^{6+} at oxygen partial pressures above 10^{-2} atm (as reviewed by Jahanshahi *et al.*, 2004).

At high temperatures and under strongly reducing conditions, such as in equilibrium with liquid metal, chromium also exists in the divalent state (Pretorius *et al.*, 1992).

Phase equilibria in the system $CaO\text{-}CrO\text{-}Cr_2O_3\text{-}SiO_2$, in contact with liquid chromium and in atmospheres with oxygen partial pressures between 10^{-13} and 10^{-10} atm, were studied by De Villiers and Muan (1992). It was found that liquidus and solidus temperatures in this system were between 100°C and 200°C lower than for the same system in air, depending on melt basicity. Considerable solid solution of chromium oxide in CaO and other calcium silicates was observed with the system in equilibrium with metallic chromium, the reason being partial substitution of Cr^{2+} for Ca^{2+} in these structures. Under slightly more oxidising conditions it was found that, despite the fact that most of the chromium was still present in the divalent state, phases containing Cr^{2+} did not exist at liquidus temperatures. The extent of substitution of Cr^{2+} for Ca^{2+} was also found to decrease significantly. Further increases in oxygen partial pressure showed an increase in the Cr^{3+}/Cr^{2+} ratio (De Villiers and Muan, 1992). In summary it was found that the transition from Cr^{3+} to Cr^{2+} as oxygen partial pressure decreased resulted in

significant decreases in liquidus and solidus temperatures and increased the solubility of chromium in the liquid phase.

The lowest oxygen partial pressure studied in the present work was in the region of 10^{-10} atm and therefore, it is expected that chromium was present predominantly in the trivalent state during this study.

In a further analysis of the $CaO\text{-}CrO\text{-}Cr_2O_3\text{-}SiO_2$ system, Nell and De Villiers (1993) confirmed that two Cr^{2+}-containing phases exist at low oxygen partial pressures, namely $CaCr^{2+}Si_4O_{10}$ and $(Ca_{0.4}Cr^{2+}_{0.6})Cr^{3+}_2O_4$. Under more oxidising conditions these phases were found to react and form more oxidised phases and liquidus temperatures were found to increase (Nell and De Villiers, 1993).

Pretorius and Muan (1992) investigated the solubility and activity-composition relations of CrO_x in the systems $CaO\text{-}CrO_x\text{-}SiO_2$ and $CaO\text{-}Al_2O_3\text{-}CrO_x\text{-}SiO_2$. Their study was conducted at 1500°C and oxygen partial pressures of $10^{-9.56}$, $10^{-11.50}$ and $10^{-12.50}$ atm for the first system and $10^{-11.50}$ atm and $10^{-12.58}$ atm for the second system. It was found that the solubility of chromium oxide increased significantly due to an increase in Cr^{2+} content with decreases in oxygen partial pressure and the basicity of melts. The addition of alumina (up to 20 wt%) to the system $CaO\text{-}CrO_x\text{-}SiO_2$ resulted in a decrease in the solubility of chromium oxide in melts. At an oxygen partial pressure of $10^{-12.5}$ atm and a temperature of 1500°C, the solubility of chromium oxide (expressed as Cr_2O_3) in the alumina-free system was approximately 42 wt%, while additions of between 10 and 20 wt% Al_2O_3 resulted in a decrease in solubility to between 28 and 30 wt% (Pretorius and Muan, 1992).

Figure 2.5 shows their results for the effect of pO_2 and melt basicity on Cr_2O_3 in melts containing 10 and 20 wt% alumina at 1500°C.

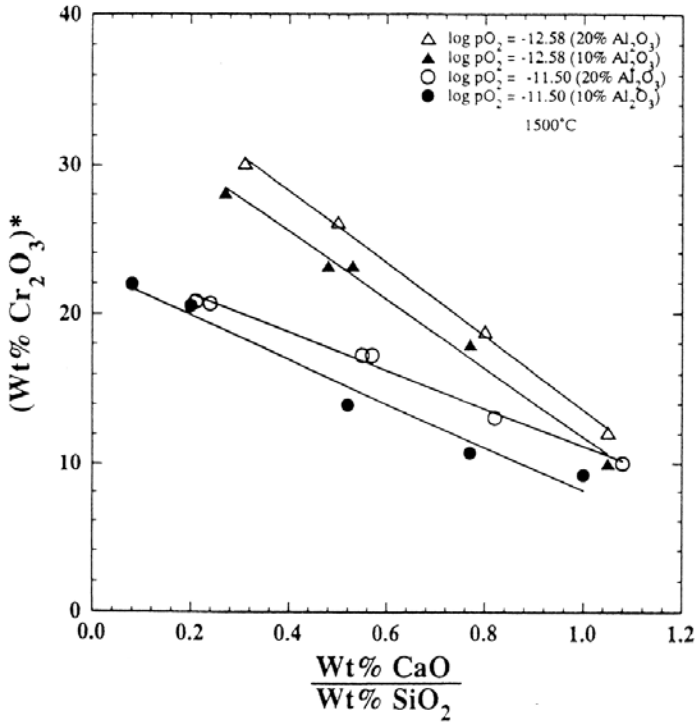

Figure 2.5: Chromium oxide in melts as a function of pO_2 and melt basicity for the system CaO-Al_2O_3-CrO_x-SiO_2 at 1500°C, melts sesquioxide-saturated where $Cr_2O_3^*$ is the total amount of chromium oxide expressed as Cr_2O_3.
(Pretorius and Muan, 1992)

In a further discussion of the above mentioned systems, Pretorius *et al.* (1992) described the Cr^{2+}/Cr^{3+} ratio in melts as a function of oxygen partial pressure, slag basicity and Al_2O_3 content. Their analysis showed that, at a given oxygen partial pressure, the proportion of Cr^{2+} decreases with increasing slag basicity. This is similar to observations made for iron oxide in silicate melts under reducing conditions at high temperatures. The Al_2O_3 content of these slags had little effect on the Cr^{2+}/Cr^{3+} ratio (Pretorius *et al.*, 1992).

Xiao and Holappa (1993) also reported that the proportion of Cr^{2+} decreases with increasing slag basicity in the system CaO-CrO_x-SiO_2. With a substitution of CaO for SiO_2, slags were found to readily saturate with CrO_x, due to its low solubility at high CaO contents. At constant temperature and slag basicity, the fraction of Cr^{2+} was found to decrease significantly with an increase in total chromium oxide content. Although partial substitution of MgO for CaO caused a decrease in the activities of CrO and Cr_2O_3,

addition of up to 20 wt% MgO to the system had no significant effect on the Cr^{2+}/Cr^{3+} ratio. Alumina additions of between 0 and 10 wt% led to a decrease in the amount of divalent chromium in the system, while additions between 10 and 20 wt% did not have any further effect on the oxidation state of chromium (Xiao and Holappa, 1993).

In their study of the activity of chromium oxide in the system $CaO\text{-}SiO_2\text{-}Al_2O_3\text{-}MgO\text{-}CrO_x$ at temperatures between 1550°C and 1650°C, Pei and Wijk (1994) reported similar results to those discussed above. They found that the proportion of chromium present in the divalent state increased with decreasing slag basicity and oxygen partial pressure, and with increasing temperature. An increase in the total CrO_x content resulted in a decrease in Cr^{2+} content of melts, as shown in Figure 2.6 (Pei and Wijk, 1994).

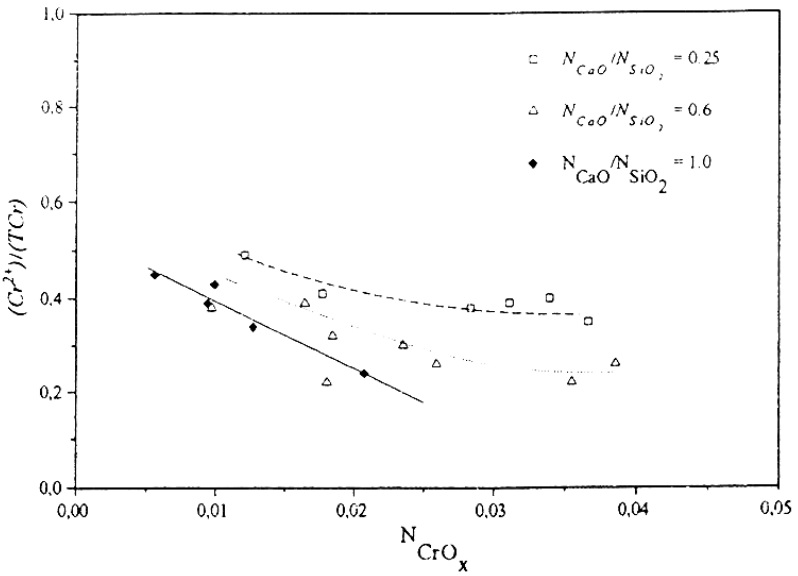

Figure 2.6: Proportion of divalent chromium in melts at 1600°C and $pO_2=10^{-11}$ atm (Pei and Wijk, 1994)

The solubility of $MgCr_2O_4$ in $MgO\text{-}Al_2O_3\text{-}SiO_2\text{-}CaO$ slags was measured by Morita *et al.* (1988) at 1600°C in air. The addition of CaO to the system $MgO\text{-}Al_2O_3\text{-}SiO_2$ led to an increase in chromite solubility. In alumina-containing slags, Cr^{3+} in $MgCr_2O_4$ was found to be substituted by Al^{3+} in proportion to the total Al_2O_3 content of the melt (Morita *et al.*, 1988).

Morita *et al.* (1988) also investigated the solubility of $MgCr_2O_4$ in slags in the above system at 1600°C under reducing conditions. In $MgO\text{-}SiO_2$ melts, saturated with $2MgO{\cdot}SiO_2$, the solubility of $MgCr_2O_4$ was found to increase with decreasing oxygen partial pressure. Addition of CaO to the system under these conditions resulted in a decrease in total soluble chromium. Figure 2.7 shows their results for the effect of oxygen partial pressure on the solubility of $MgCr_2O_4$ in melts.

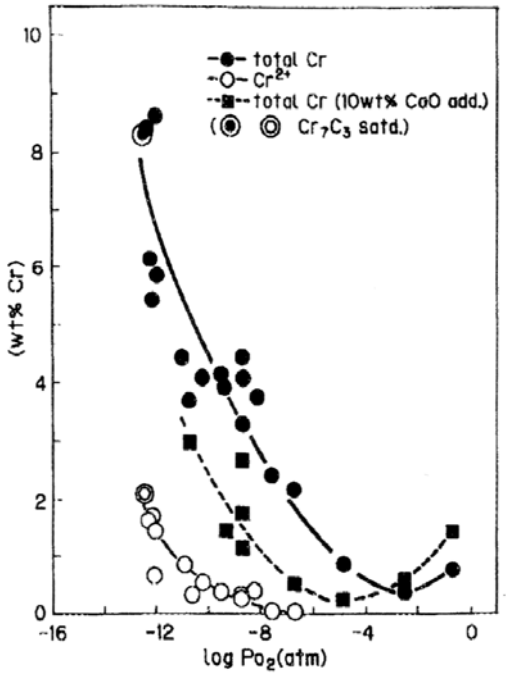

Figure 2.7: The effect of pO_2 on the solubility of $MgCr_2O_4$ in $MgO\text{-}SiO_2\text{-}CaO\text{-}CrO_x$ melts, saturated with $2MgO{\cdot}SiO_2$, at 1600°C (Morita *et al.*, 1988)

To summarise this section it can be said that chromium oxide significantly increases liquidus temperatures of slags under oxidising conditions. The solubility of CrO_x was found to increase with increasing temperature, decreasing oxygen partial pressure and decreasing melt basicity. The addition of Al_2O_3 (up to approximately 10 wt%) to chromium-containing calcium-silicate slags resulted in a decrease in CrO_x solubility in melts due to an increase in the Cr^{3+}/Cr^{2+} ratio.

Jahanshahi *et al*. (2004) reviewed recent studies on the physico-chemical properties of molten slags and oxide solid solutions. Their review indicated that the Cr^{3+}/Cr^{2+} ratio in calcium silicate slags is dependent upon oxygen partial pressure, basicity as well as bulk chromium oxide content. The dependence of the Cr^{3+}/Cr^{2+} ratio on oxygen partial pressure was found to be close to ideal. At 1600°C, a chromium oxide content of between 1 and 3 wt% and a CaO/SiO_2 ratio of 0.66 the Cr^{3+}/Cr^{2+} ratio was inferred to be approximately 0.1 at an oxygen partial pressure of 10^{-11} atm. At a given temperature, pO_2 and bulk CrO_x content, the oxidation state of chromium was found to increase with an increase in basicity. As mentioned earlier, the Cr^{6+} concentration was found to become significant at oxygen partial pressures above approximately 10^{-2} atm.

2.5 Iron and chromium-containing ternary and multi-component systems

Eguchi *et al*. (1977) studied phase equilibria in the system $FeO\text{-}Cr_2O_3\text{-}SiO_2$ in equilibrium with liquid iron under a nitrogen atmosphere. Their findings included that the solubility of Cr_2O_3 in slags in this system were 1.5, 3 and 5 wt% at temperatures of 1230°C, 1300°C and 1400°C, respectively.

Pathy and Ward (1964) studied the distribution of chromium between liquid iron and synthetic $CaO\text{-}MgO\text{-}FeO_x\text{-}SiO_2\text{-}Cr_2O_3$ steelmaking slags (>40 wt% CaO) in equilibrium with ferrochromium alloys of different compositions. The solubility of Cr_2O_3 in slags was found to be less than 10 wt% at 1736°C. They found that, in slags not saturated with Cr_2O_3, the Cr content of slags increased with increasing iron oxide in slag.

According to Arculus *et. al.* (1974) the addition of only small amounts of chromium oxide to the reference system, $FeO_x\text{-}MgO\text{-}SiO_2$, in air resulted in the appearance of a spinel field. Figure 2.8 shows the tetrahedron representing the system $MgO\text{-}FeO_x\text{-}Cr_2O_3\text{-}SiO_2$ with FeO_x expressed as Fe_3O_4.

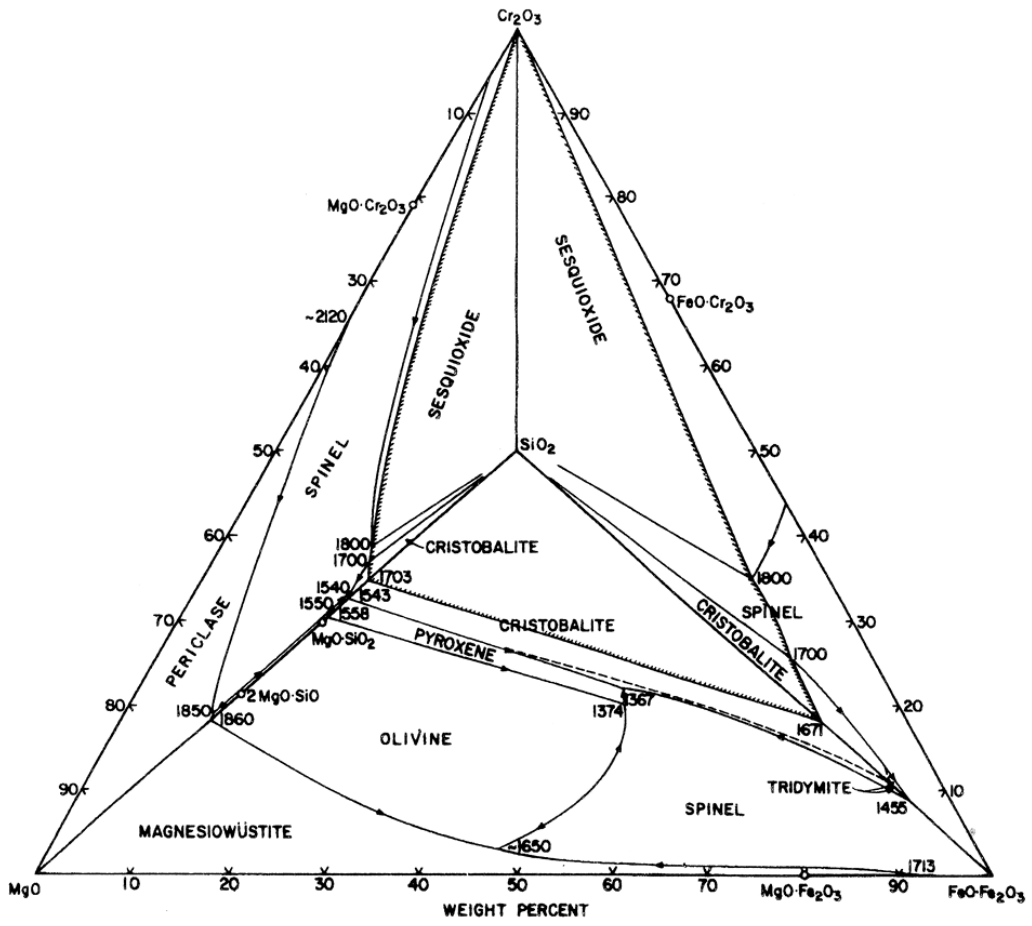

Figure 2.8: The system $MgO\text{-}FeO_x\text{-}Cr_2O_3\text{-}SiO_2$ in air at 1 atm total pressure. Left face after Keith (1954), right face after Muan and Sõmiya (1960) and base after Muan and Osborn (1956), as reviewed by Arculus *et al*. (1974)

While the compositions of olivine and pyroxene were almost unaffected by the addition of Cr_2O_3, the spinel phase was found to have a very broad range of composition, from chromium-free magnesioferrite ($MgFe_2O_4$) to iron-free picrochromite ($MgCr_2O_4$), due to extensive solid solution. In moving to the left face of Figure 2.8, over the olivine and pyroxene volumes, the Cr_2O_3 content of the liquid phase was found to be approximately 1.4 wt%. When plotted on the surface $Cr_2O_3\text{-}MgO\text{-}Fe_3O_4$ (the front face of Figure 2.8) spinel compositions were found to lie on a straight line extending from $MgCr_2O_4$ (20 wt% MgO) to a point in close agreement with the composition of $MgFe_2O_4$, which contains 13 wt% MgO. The maximum Cr_2O_3 content of olivine and pyroxene was found to be approximately 0.35 wt% under these conditions, less than the Cr_2O_3 content of the co-existing liquid phase in each case (Arculus *et al.*, 1974).

Further studies (Arculus and Osborn, 1975) into this system indicated that a decrease in oxygen partial pressure from 0.21 atm to approximately 10^{-5} atm brought about a decrease in the MgO content of spinels in equilibrium with pyroxene and liquid. Conclusions made by these authors included that spinel solid solutions are continuous between the end-members $MgCr_2O_4$, $FeCr_2O_4$, $MgFe_2O_4$ and Fe_3O_4 in equilibrium with olivine and pyroxene as crystalline phases or pyroxene and silica as crystalline phases. The Fe^{3+}/Fe^{2+} ratio in the spinel phase was found to increase with a decrease in temperature.

In their studies of the behaviour of chromium in reduced slag-metal systems, Rankin and Biswas (1978, 1979) equilibrated CaO-SiO_2-Al_2O_3-CrO_x-FeO slags with Fe-Cr-Si alloys at 1600°C. Slags had CaO/SiO_2 ratios between 0 and approximately 2 with Al_2O_3 contents up to saturation in the slag. The chromium content of reduced slags was found to decrease with increasing basicity and with decreasing temperature. Their results for the effect of slag composition on the equilibrium chromium content of the slag are shown in Figure 2.9.

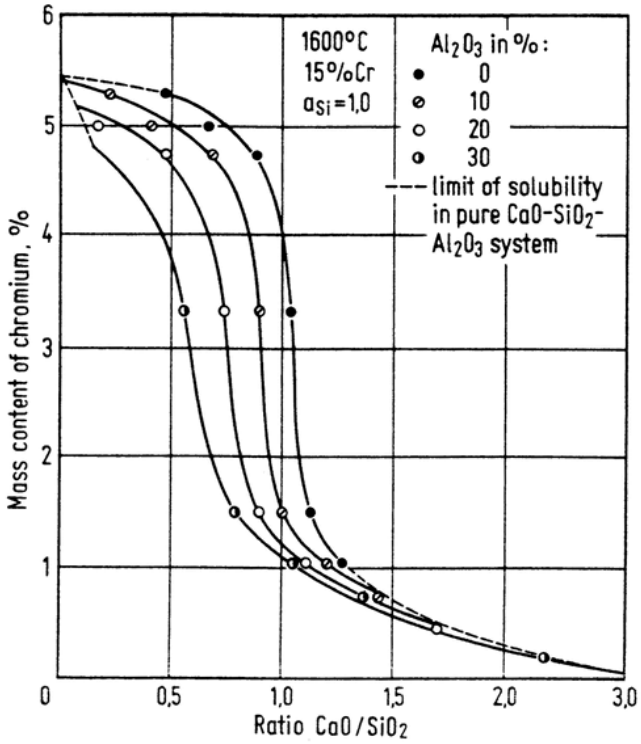

Figure 2.9: The effect of slag composition on slag chromium content (Rankin and Biswas, 1979)

In reduced slags (*i.e.* in equilibrium with alloys) chromium is present predominantly in the divalent state, but it is expected that equilibrium exists between Cr^{2+} and Cr^{3+}. The authors proposed an average of $CrO_{1.07}$ under such conditions. Under more oxidising conditions the activities of both CrO and Cr_2O_3 increase until the activities of either oxide becomes unity, or a reaction takes place between CrO and/or Cr_2O_3 with another slag component to form a product with unit activity. The latter was proposed to most likely take place to produce $FeCr_2O_4$, $MgCr_2O_4$ or a distorted spinel of the form $(xFeO,yCrO)\cdot Cr_2O_3$ (Rankin and Biswas, 1978). Other researchers have reported the presence of Cr^{2+} in $FeCr_2O_4$-$MgCr_2O_4$ spinels at 1300°C in equilibrium with a metal phase (Ulmer and White, 1966).

Murck and Campbell (1986) equilibrated chromite with natural basic liquids along the QFM (quartz-fayalite-magnetite) oxygen buffer from 1150°C to 1500°C and at 1250°C and 1400°C from the NNO (nickel-nickel oxide) to IW (iron-wüstite) oxygen buffers. They examined the influence of temperature, oxygen fugacity and bulk composition on

the solubility of chromite in these liquids. At constant temperature, the chromium content of the glass phase was found to increase with decreasing oxygen fugacity, especially at lower pO_2. The chromium content of olivines was found to increase with increasing temperature, though not as strongly as with melts, and with decreasing oxygen potential. The sharpest increases in $[Cr]_{glass}$ and $[Cr]_{olivine}$ was found at oxygen partial pressures below approximately 10^{-8} atm and 1400°C. Figures 2.10a and 2.10b show their results for the solubility of chromium in the glass phase as functions of temperature and oxygen partial pressure (fugacity), respectively.

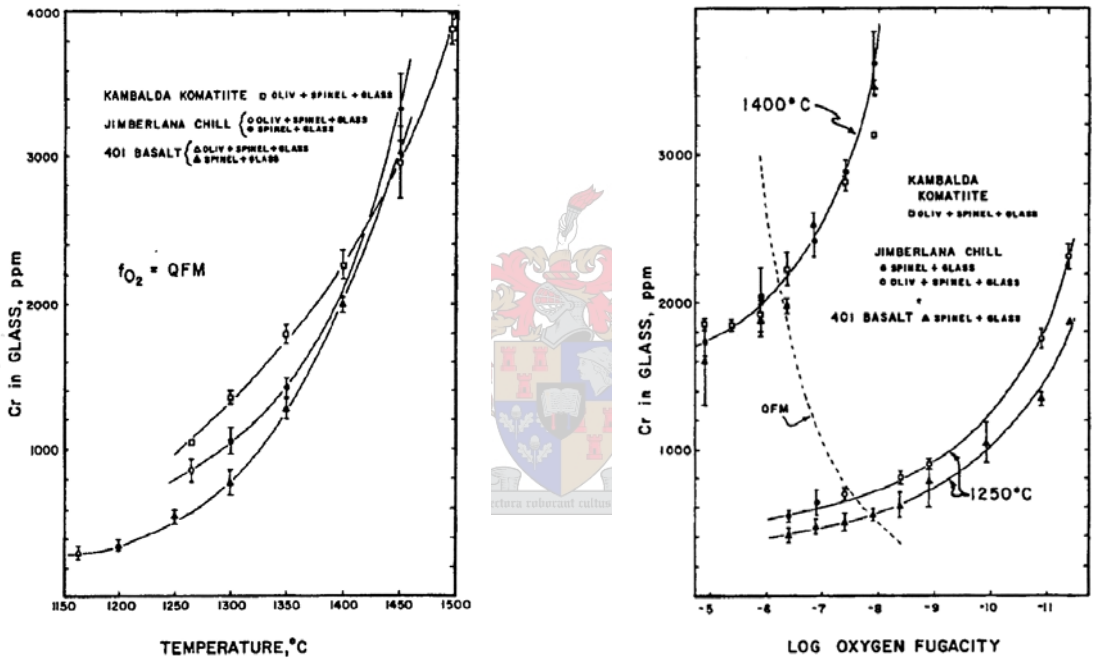

Figure 2.10: The effect of (a) temperature and (b) oxygen fugacity on Cr in the glass phase for three different natural basic liquids (Murck and Campbell, 1986)

An increase in temperature along the QFM buffer from 1150°C to 1500°C (causing an increase in pO_2 from approximately 10^{-9} to $10^{-5.5}$ atm) resulted in an increase in the Cr_2O_3 and MgO contents and a decrease in FeO, Fe_2O_3 and Al_2O_3 in spinels. The Fe^{3+}/Fe^{2+} ratio was found to increase with increasing oxygen potential (Murck and Campbell, 1986).

Schwessinger and Muan (1992) investigated the distribution of Mg, Fe, Al and Cr among olivine, pyroxene, spinel and the liquid phase in the system MgO-FeO-Fe_2O_3-Al_2O_3-

Cr_2O_3-SiO_2 at temperatures ranging from 1309 to 1471°C at a constant CO_2/H_2 ratio of 10 (pO_2 ranging from $10^{-7.78}$ at 1300°C to $10^{-5.69}$ at 1500°C). Starting slags contained between 13 and 30 wt% MgO, 40 to 50 wt% SiO_2, 1 to 3.3 wt% FeO_x and Cr_2O_3 and Al_2O_3 contents between 3.3 and 6.7 wt%. Their findings included that chromium is strongly partitioned into the spinel phase relative to coexisting liquid, olivine and pyroxene. The solubility of Cr_2O_3 in the liquid was found to be between 0.3 and 0.8 wt% and it increased with decreasing Al_2O_3 in the liquid phase. Aluminium was found to be enriched in liquid and spinel relative to olivine and pyroxene. The Al/Cr ratio in spinel was found to decrease with increasing silica activity in melts, indicating that at a given Al/Cr ratio, melts higher in SiO_2 would precipitate spinels richer in Cr (Schwessinger and Muan, 1992).

Rait *et al*. (1997) investigated the effect of chromium oxide addition to iron-making slags in the system CaO-MgO-Al_2O_3-SiO_2-FeO_x. Slags with a CaO/SiO_2 ratio of 1, and Al_2O_3 and FeO_x contents of approximately 20 wt% and 5 wt%, respectively were considered. In air, an addition of 1 wt% CrO_x resulted in an increase in liquidus temperature of approximately 200°C in the spinel field, while under an atmosphere of CO_2 the liquidus temperature of the same slag increased by 50°C. Chromium was found to partition strongly into spinel relative to the liquid phase. The spinel Cr_2O_3 content was found to increase with decreasing Al_2O_3 and FeO_x in spinel and was higher in iron-free slags. The solubility of chromium in the liquid phase was found to be between 0.4 and 0.9 wt% in spinel-saturated slags at 1600°C and decreased with increasing MgO content, while no correlation with oxygen partial pressure was observed. In this investigation an increase in temperature led to an increase in spinel Cr_2O_3 content, while Cr_2O_3 in the liquid phase seemed to be unaffected (Rait *et al.*, 1997).

Jakeš and Reid (1974) studied chromium partitioning between olivine and pyroxene and the redox state of lunar rocks. It was assumed that Cr^{2+} is preferentially incorporated into olivine, while Cr^{3+} partitions mainly into pyroxenes. The partitioning of Cr between olivine and pyroxene was assumed to be a function of the Cr^{2+}/Cr^{3+} ratio in a system. Chromium in pyroxenes was reported to decrease with the ratio Mg/(Mg+Fe), while

chromium in olivines were found to increase with decreasing Mg/(Mg+Fe) ratio in the olivine (Jakeš and Reid, 1974).

From the review presented in this section it is evident that the addition of small amounts of CrO_x to melts results in the formation of chromite spinel and drastic increases in liquidus temperatures. Chromium was found to partition strongly into the spinel phase but also reports to other solid phases such as olivine and pyroxene in small concentrations. Temperature tends to affect both the solubility of chromium in the liquid phase and the composition of the spinel phase. The solubility of CrO_x in the liquid phase increases with decreases in oxygen partial pressure, basicity, and Al_2O_3 and MgO contents, and with increasing temperature.

2.6 Spinel solid solutions and other systems with spinel as a crystalline phase

Most chromium containing spinels consist primarily of the oxides MgO, FeO, Fe_2O_3, Cr_2O_3 and Al_2O_3 and usually occur in nature with olivine and/or pyroxene. Other oxides are usually present only in minor amounts in chromite spinel structures. Theoretically, many possible spinel compounds (end-members) exist, but the following are predominant (Irvine, 1965):

- Chromite: $FeCr_2O_4$
- Hercynite: $FeAl_2O_4$
- Magnetite: Fe_3O_4
- Picrochromite: $MgCr_2O_4$
- Spinel: $MgAl_2O_4$
- Magnesioferrite: $MgFe_2O_4$

Muan and Sõmiya (1960) studied phase relations in the system FeO_x-Cr_2O_3-SiO_2 in air. Data projected onto the ternary diagram for the system Fe_3O_4-Cr_2O_3-SiO_2 revealed the presence of silica (as tridymite and cristobalite), the spinel solid solution ($FeO{\cdot}Fe_2O_3$-

$FeO{\cdot}Cr_2O_3$) and the sesquioxide solid solution (Fe_2O_3-Cr_2O_3) as crystalline phases. It was found that the addition of Cr_2O_3 to FeO_x-SiO_2 mixtures resulted in rapid increases in liquidus temperatures. Of the crystalline phases found in this system, silica had a constant composition corresponding to SiO_2, while the spinel and sesquioxide phases were members of solid solution series. The melting temperature of the stoichiometric compound $FeCr_2O_4$ was reported to be in the region of 2070°C (Muan and Sõmiya, 1960).

Toker *et al.* (1991) studied the system Fe-Cr-O under very reducing conditions (at oxygen partial pressures down to approximately 10^{-12} atm) by equilibrating liquid Fe-Cr alloys with iron chromite solid solutions at 1600°C and 1700°C. The spinel phases identified in this investigation were found to be in the high-chromium range of the solid solution series Fe_3O_4-Cr_3O_4 *i.e.* between stoichiometric iron chromite ($FeCr_2O_4$) and Cr_3O_4. Sharp decreases in liquidus temperatures of the chromites in equilibrium with Fe-Cr alloys were attributed to an increase in divalent chromium content in the liquid slag with a decrease in oxygen potential (Toker *et al.*, 1991).

A thermodynamic assessment of available data and modelling of phase relationships in the system Fe-Cr-O was conducted by Taylor and Dinsdale (1993). They found that at low oxygen partial pressures Fe-Cr alloys exist in equilibrium with a corundum phase closely resembling Cr_2O_3, while at higher oxygen partial pressures alloys exist in equilibrium with a spinel phase, close to $FeCr_2O_4$ in composition, and a wüstite-based halite phase containing a small percentage of chromium. At higher oxygen partial pressures the spinel phase was found to extend from $FeCr_2O_4$ to Fe_3O_4 and the corundum phase showed a complete range of solubility between Cr_2O_3 and Fe_2O_3. The spinel phase was found to be non-stoichiometric, showing an excess of oxygen above the expected metal-to-oxygen ratio of 3:4 (Taylor *et al.*, 1993).

From their study of the chemical and structural properties of the system Fe_2O_3-Cr_2O_3, Musić *et al.* (1993) reported that over the entire composition range, solid solutions of the type $(Fe_{1-x}Cr_x)_2O_3$ were formed. All samples were one-phase systems. This indicates that

Fe^{3+} and Cr^{3+} are easily interchangeable in the solid solution. Riboud and Muan (1964) also mentioned the easy substitution of Cr^{3+} for Fe^{3+} in crystalline phases due to the completeness of the solid solution series Fe_2O_3-Cr_2O_3 at temperatures above 1000°C.

Keith (1954) studied phase relations in the system MgO-Cr_2O_3-SiO_2 and found the stability fields of Cr_2O_3, MgO and $MgCr_2O_4$ to dominate the ternary diagram. His study was aimed at improving refractory materials made from chromite or chromite-forsterite mixtures. He concluded that pyroxenes and other minerals with low MgO:SiO_2 ratios should be considered undesirable impurities in these materials as they contribute to liquid formation. The addition of MgO and Cr_2O_3 to these materials would be beneficial in refractory applications as it would move bulk compositions into fields where chromite ($FeCr_2O_4$), forsterite (Mg_2SiO_4) and periclase (MgO) are stable and temperatures of initial melting are high (Keith, 1954). In the current study the aim is to determine conditions that favour the formation of a liquid phase and therefore, according to Keith's findings, lower Cr_2O_3 and MgO contents would be desirable.

A study of the system MgO-Al_2O_3-Cr_2O_3 by Wilde and Rees (1943), aimed at developing the use of Cr in chrome-magnesite refractories, revealed that in the binary system Al_2O_3-Cr_2O_3 complete solid solution exists between the end-members. In the binary system MgO-Al_2O_3 only one compound was found to exist, namely $MgAl_2O_4$, and that MgO was not soluble in this compound. Similarly in the binary system MgO-Cr_2O_3 the only compound observed was $MgCr_2O_4$. They reported that a complete solid solution series exists between $MgAl_2O_4$ and $MgCr_2O_4$ in the ternary system (Wilde and Rees, 1943).

Alper *et al*. (1964) studied phase relations in the system MgO-$MgCr_2O_4$ under a nitrogen atmosphere. Their results indicated that 47 wt% Cr_2O_3 could enter the MgO lattice in solid solution at 2350°C. The solid solution was found to decrease to 32 wt% Cr_2O_3 at 2165°C, and 11, 5 and 2.5 wt% at 1600, 1400 and 1200°C, respectively. At 1000°C no chromium oxide was found in solid solution with MgO. Liquidus temperatures in this system were found to be in excess of 2355°C. Their proposed phase diagram for this system is shown in Figure 2.11.

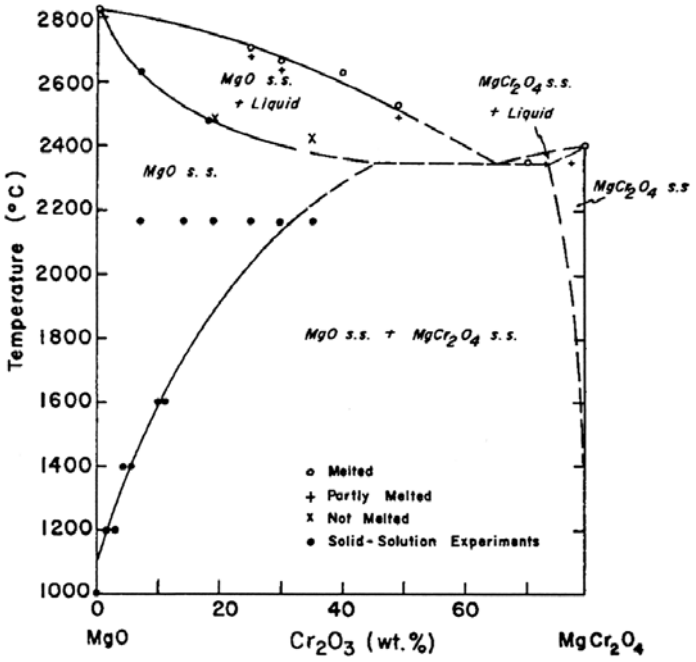

Figure 2.11: Phase equilibrium diagram for the system MgO-$MgCr_2O_4$ (Alper *et al.*, 1964)

The effect of addition of Cr_2O_3 on the properties of MgO-Al_2O_3 spinels was studied by Sarkar *et al.* (2002). Up to 4 wt% Cr_2O_3 was added to mixtures with MgO:Al_2O_3 molar ratios of 2:1, 1:1 and 1:2, all sintered at 1550, 1600 and 1650°C. It was found that Cr_2O_3 reported to the spinel phase in all cases, indicating full solubility of Cr_2O_3 in the spinel phase. This was confirmed by the fact Cr_2O_3 was uniformly distributed throughout spinel grains and grain boundaries. For the alumina-rich composition, Cr_2O_3 was also found to decrease the temperature at which complete solid solution of Al_2O_3 in the spinel phase occurs. This was confirmed by the fact that the corundum phase did not exist at 1600°C and 1650°C when Cr_2O_3 was added to the alumina-rich MgO-Al_2O_3 mixture. The same was not observed for MgO in the MgO-rich mixture (Sarkar *et al.*, 2002).

Navrotsky (1975) noted that at temperatures above approximately 1300°C, a complete solid solution is formed between Cr_2O_3 and Al_2O_3. The solid solution series between Cr_2O_3 and Fe_2O_3, on the other hand, is limited at high temperature by the reduction of hematite to magnetite and by the formation of Fe_3O_4-$FeCr_2O_4$ spinels (Navrotsky, 1975).

In their series of studies of the systems $MgAl_2O_4$-$MgCr_2O_4$-Ca_2SiO_4, $MgFe_2O_4$-$MgCr_2O_4$-Ca_2SiO_4 and $MgAl_2O_4$-$MgFe_2O_4$-Ca_2SiO_4 in air, White *et al.* (1955, 1964, 1966) found that in each case the two spinels form a continuous series of solid solutions and formed a binary eutectic with Ca_2SiO_4, separating the primary crystallization fields of spinel and Ca_2SiO_4. In the first two systems the temperature of initial and final melting of the eutectic was found to increase by approximately 300°C as Cr_2O_3 replaced Al_2O_3 and Fe_2O_3 in spinel. The solubility of spinel in the glass phase was found to decrease with an increase in bulk Cr_2O_3 content. In the system $MgAl_2O_4$-$MgFe_2O_4$-Ca_2SiO_4, the temperature of initial and final melting increased by approximately 40°C as the spinel composition changed from $MgFe_2O_4$ to $MgAl_2O_4$. It was inferred that in the quaternary system $MgAl_2O_4$- $MgFe_2O_4$- $MgCr_2O_4$-Ca_2SiO_4 the three spinel species would exhibit complete solid solution (El-Shahat and White, 1966).

Jacob *et al*. (1987) determined tie lines between spinel ($FeAl_2O_4$-$FeCr_2O_4$) and corundum (Al_2O_3-Cr_2O_3) phases at 1550°C and an oxygen partial pressure of $7.6x10^{-10}$ atm. Their results are shown in Figure 2.12.

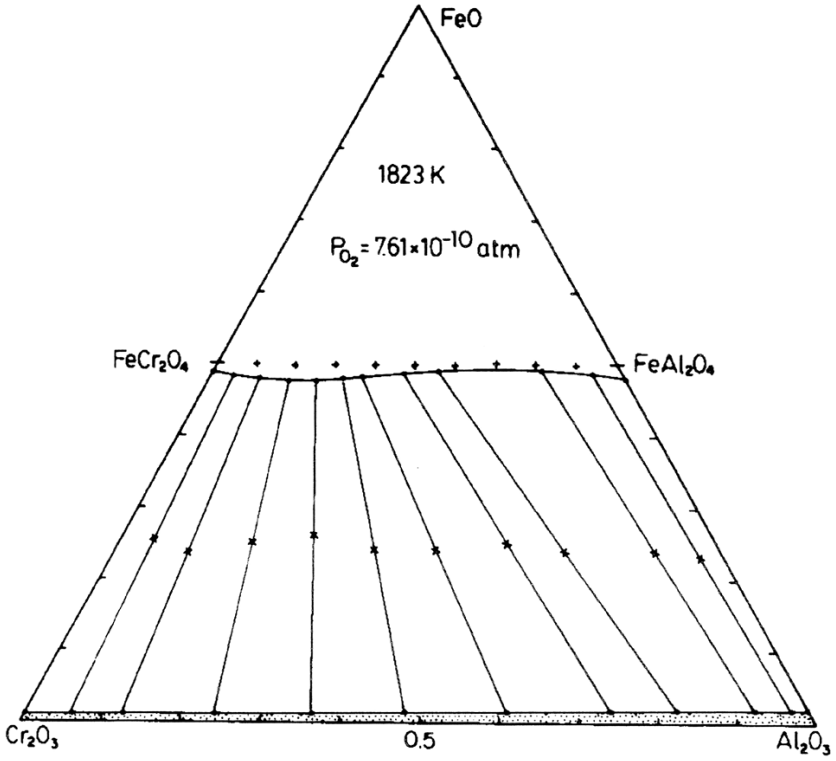

Figure 2.12: Tie-lines between the corundum and spinel phases in the system FeO-Cr_2O_3-Al_2O_3 at 1550°C (Jacob *et al.*, 1987)

At this temperature (1550°C) some solubility of corundum in the spinel phase, and vice versa, was observed. Compared to similar data by the same authors at 1100°C, tie lines between equilibrium phases show a trend towards linking phases with similar Cr/Al ratios at the higher temperature (Jacob *et al.*, 1987).

Phase equilibria and activities of constituents in the $FeCr_2O_4$-$MgCr_2O_4$-$MgAl_2O_4$ spinel solid solution saturated with $(Cr,Al)_2O_3$ was studied at 1300°C, in equilibrium with liquid metal by Hino *et al*. (1995). It was found that the corundum phase exhibited slight solubility in the spinel solid solution, while the spinel phase had no measurable solubility in the corundum phase. Figure 2.13 shows phase relations in the system Cr_2O_3-$FeCr_2O_4$-$MgCr_2O_4$-Al_2O_3 at 1300°C.

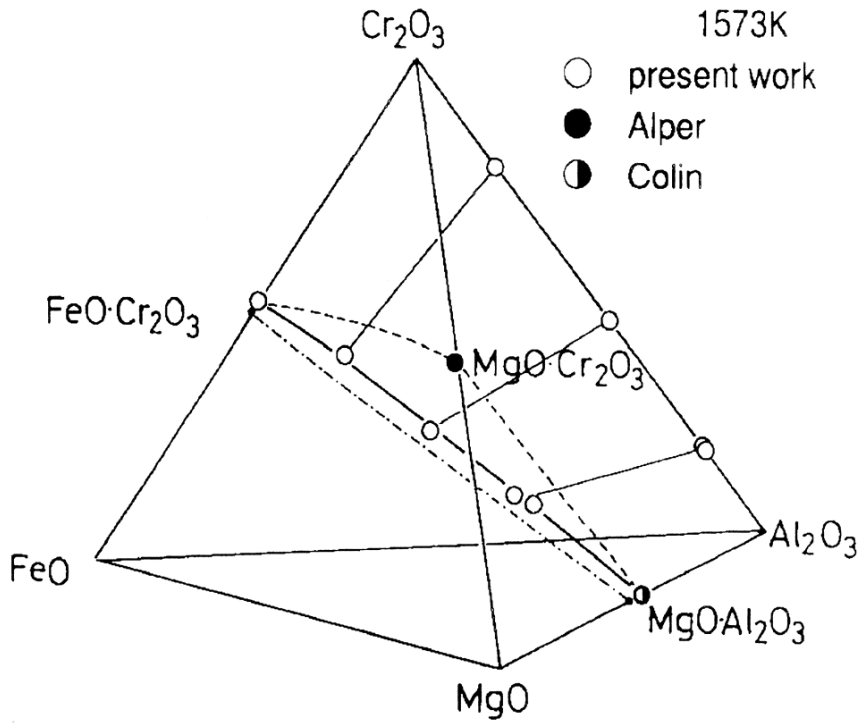

Figure 2.13: Phase relations in the system Cr_2O_3-$FeCr_2O_4$-$MgCr_2O_4$-Al_2O_3 in equilibrium with liquid iron at 1300°C
(Hino *et al.*, 1995)

Hanson and Jones (1998) parameterized the partitioning of trivalent and divalent chromium between olivine and liquid in spinel-saturated melts over a wide range of liquid compositions and redox conditions. The presence of Cr^{2+} was found to be suppressed by Fe^{3+}. The behaviour of chromium as a function of oxygen fugacity was reported to be similar in iron-free and iron-bearing systems. It was noted that the chromium content of spinel-saturated liquids is governed by temperature, composition and oxygen fugacity but is buffered by spinel and insensitive to the bulk chromium content of the system.

To summarize this section, Cr_2O_3 was found to stabilise the spinel phase and partition into the spinel phase very strongly. Significant increases in liquidus temperatures (up to ~300°C) were observed when Cr_2O_3 replaced Al_2O_3 and Fe_2O_3 in the spinel structure. The solubility of spinel in the liquid phase was found to decrease with increasing bulk Cr_2O_3 content of melts. Under reducing conditions the solubility of chromium oxide in

the liquid phase increased due to an increase in the portion of chromium in the divalent state.

While much was discussed with regard to phase equilibria, the modelling thereof still requires elucidation.

2.7 Computer simulation of phase equilibria

A number of phase equilibrium modelling software products are available. Most of these are updated on a regular basis, especially with regard to binary and ternary interactions in melts. The multi-phase equilibrium (MPE) model, developed by CSIRO, was the preferred software because of its availability, its robustness in terms of equilibrium modelling and its ability to predict slag viscosities.

The MPE modelling package was developed for the calculation of multi-phase equilibrium in metallurgical systems. An important feature of the package is that it has the added benefit of being able to predict viscosities of homogeneous liquids as well as solid-containing melts using structural parameters obtained from the thermodynamic model in conjunction with the stability of oxide phases (Zhang *et al.*, 2001).

Multi-phase equilibrium is calculated by Gibbs free energy minimisation based on the SOLGASMIX algorithm. The mixing behaviour in solution phases such as slag, spinel, alloy and matte is described by means of certain solution models selected for each of the phases.

Although beyond the scope of this work, the models chosen to represent each of the phases will be mentioned briefly (as reviewed by Zhang *et. al*, 2001). It has been shown that the cell model can represent the thermodynamic behaviour of complex molten ferrous slags with reasonable accuracy, while using only binary interaction parameters. The cell model was therefore selected for the slag phase. Solid solution models for halite,

spinel, olivine, melilite and pseudo-brookite are included in the MPE model, represented using the compound energy model (CEM) and regular solution type model. A model proposed by Pelton and Bale (1986) was used for liquid ferrous alloys. Two databases are used in conjunction with the model - the first covers highly alloyed iron-based alloys and the second is used to describe the behaviour of liquid steel with low-level impurities or alloying elements. The matte phase is modelled using the quasi-chemical model proposed by Kongoli *et al.* (1998) (Zhang *et al.*, 2001).

Comprehensive databanks of published results pertaining to thermodynamics, slag composition-activity relations and transport properties have been compiled. The information has been critically assessed to support development of the model (Zhang *et al.*, 2002). To date, the model has been validated against data on industrial slags and oxide solid solutions containing up to 17 oxide components (Al_2O_3, CaO, CoO, Cu_2O, Cr_2O_3, CrO, FeO, Fe_2O_3, MgO, NiO, PbO, Ti_2O_3, TiO_2, P_2O_5, ZnO, MnO and SiO_2) (Chen *et al.*, 2004).

One of the more recent achievements in the development of this model has been the expansion to include chromium oxide. This is of particular interest to platinum producers due to a shift towards smelting concentrates with high chromium contents, which brings with it operational difficulties because of the formation of spinel crystals in furnace slags, as discussed in Chapter 1 and shown in the preceding literature review.

Any model requires experimental data for either parameter fitting or validation and it is intended that the data generated during this study will be used to fine-tuning of the MPE model.

2.8 Summary

From the literature reviewed it is evident that research studies have been aimed primarily at gaining an understanding of phase relations in systems related to the steelmaking and

ferrochrome industries, as well as the refractory industry. These studies generally cover compositions in the high CaO and Al_2O_3 regions with lower MgO, FeO_x and SiO_2 contents than slags in the platinum industry.

Only very few published investigations, mostly of geological interest, have been found to cover melt compositions and oxygen potentials similar to those encountered in melters in the platinum industry. Amongst these is the work of Murck and Campbell (1986), although bulk chromium oxide contents were significantly lower (*i.e.* less than 0.38 wt%) than those found in slags of interest for this study. Similarly, Hanson and Jones (1998) studied systems with chromium contents below approximately 0.63 wt%. Schwessinger and Muan (1992) studied systems with much lower iron oxide contents.

Therefore, it is clear that a need exists for experimental data on the behaviour of chromium in multi-component melts found in the platinum industry. The chief objective of this study was to characterise phase equilibria and the behaviour of chromium in multi-component slags similar to those found in the platinum industry, to determine which conditions may lead to the formation of solids and to characterise the resulting glass (liquid) phase and solid (mineral) phases, and their respective amounts.

In order to meet these objectives it was decided to apply the widely used drop-quench technique for the determination of phase stability and phase composition under selected experimental conditions. The technique allows the researcher to examine the phase chemistry under pre-defined conditions by producing a snapshot of the phases present at the moment that the sample was quenched and frozen.

Variables investigated were temperature, bulk FeO_x/MgO ratio, bulk CrO_x content and oxygen partial pressure with SiO_2 contents between 44 and 50 wt%. The aim was to develop a better understanding of phase stability and chemistry in these slags as well as factors that may have a bearing on successful plant operation.

Chapter 3

EXPERIMENTAL PROCEDURE

3.1 Introduction

Phase equilibria were studied using the drop-quench method. This method is commonly used for the study of phase equilibria in metallurgical systems and of the investigations reviewed in Chapter 2, no less than thirty-seven made use of this technique.

An attempt was made to reach gas-liquid equilibrium under carefully controlled conditions of temperature and oxygen partial pressure. Experiments were conducted at temperatures of 1400, 1500 and 1600°C.

From the literature review it is clear that oxygen partial pressure has a pronounced effect on the solubility of chromium oxide in the liquid phase. It was considered important to quantify this effect in melts with chromium oxide contents closer to what is expected to be found in the platinum industry (*i.e.* up to approximately 6 wt% Cr_2O_3). To this end, the ratio of CO_2 to CO in the gas phase was kept constant at levels of 0.5, 2, 10 and 20, resulting in oxygen partial pressures ranging from 2.7×10^{-10} to 8.3×10^{-5} atm.

Samples were rapidly quenched in cold water in order to produce snapshots of phase relations existing at each selected experimental condition.

3.2 Starting materials

Starting slag mixtures were chosen to be similar in composition to the bulk composition of non-ferrous slags in the platinum industry. Master slag compositions were chosen to have FeO_x/MgO-ratios of 0.5, 1 and 2 and SiO_2 contents of between 45 and 50 wt%. The alumina and lime contents were kept constant at approximately 5 wt% of each. Chromium oxide (expressed as Cr_2O_3) contents were 1.5, 3.7, 6.4 and 7.1 wt%.

Two chromium-free slags (B1 and B2) were used as references to validate the experimental technique against established literature data. Slag B1 contained only FeO_x, MgO and SiO_2 while slag B2 contained CaO and Al_2O_3 in addition to FeO_x, MgO and SiO_2.

Master slags were prepared by mixing appropriate amounts of dry reagent grade MgO, SiO_2, $CaCO_3$, Al_2O_3 and Cr_2O_3. Wüstite (FeO) was prepared by reducing pure hematite (Fe_2O_3) at 850°C for 48 hours under a CO-CO_2 atmosphere with a CO_2/CO ratio of 1.5. Whether sufficient reduction of hematite had taken place was confirmed by means of X-ray diffraction (XRD) analyses (see Appendix B). All reagents except for iron oxide were blended and pulverised together, while iron oxide was carefully pulverised separately to minimise oxidation. The required amount of iron oxide was then combined with the oxide mixture and blended for approximately 40 minutes to ensure homogeneity.

Mixtures were pre-melted in MgO crucibles at temperatures close to liquidus temperatures estimated from data for the MgO-FeO-SiO_2 ternary system so as to minimise dissolution of MgO from crucibles into slags. Master slag compositions are given in Table 3.1.

Table 3.1: Master slag compositions

Master Slag	MgO	Cr_2O_3	Fe_2O_3	SiO_2	CaO	Al_2O_3	FeO_x/MgO
	(weight %)						
1	24.5	1.2	17.0	47.7	4.8	4.8	0.6
2	18.7	1.5	23.0	47.3	4.7	4.8	1.1
3	14.1	1.3	30.5	45.1	4.4	4.5	1.9
4	19.5	3.7	23.0	44.1	4.8	4.9	1.1
5	18.0	6.4	21.0	44.7	4.9	4.9	1.1
6	14.1	7.1	19.0	49.8	5.0	5.0	1.2
B1	18.4	-	32.0	49.3	-	-	1.6
B2	16.5	-	28.9	44.6	5.0	5.1	1.6

* Total Fe expressed as Fe_2O_3

3.3 Equipment

A vertical tube resistance furnace, fitted with three U-shaped molybdenum disilicide heating elements, was utilized for drop-quench experiments. The work tube (60mm inner diameter) was manufactured from recrystallised alumina and fitted with water-cooled brass end-caps. The bottom end cap was closed off with a thin plastic film and a blank flange during experiments. The purpose of the plastic film was to maintain the gas seal when the bottom flange was removed directly before quenching. The exit gas stream was directed through bubblers to monitor whether a proper gas seal was maintained throughout each experiment. A schematic diagram of the tube furnace is shown in Figure 3.1 and photographs of the experimental setup can be found in Appendix C.

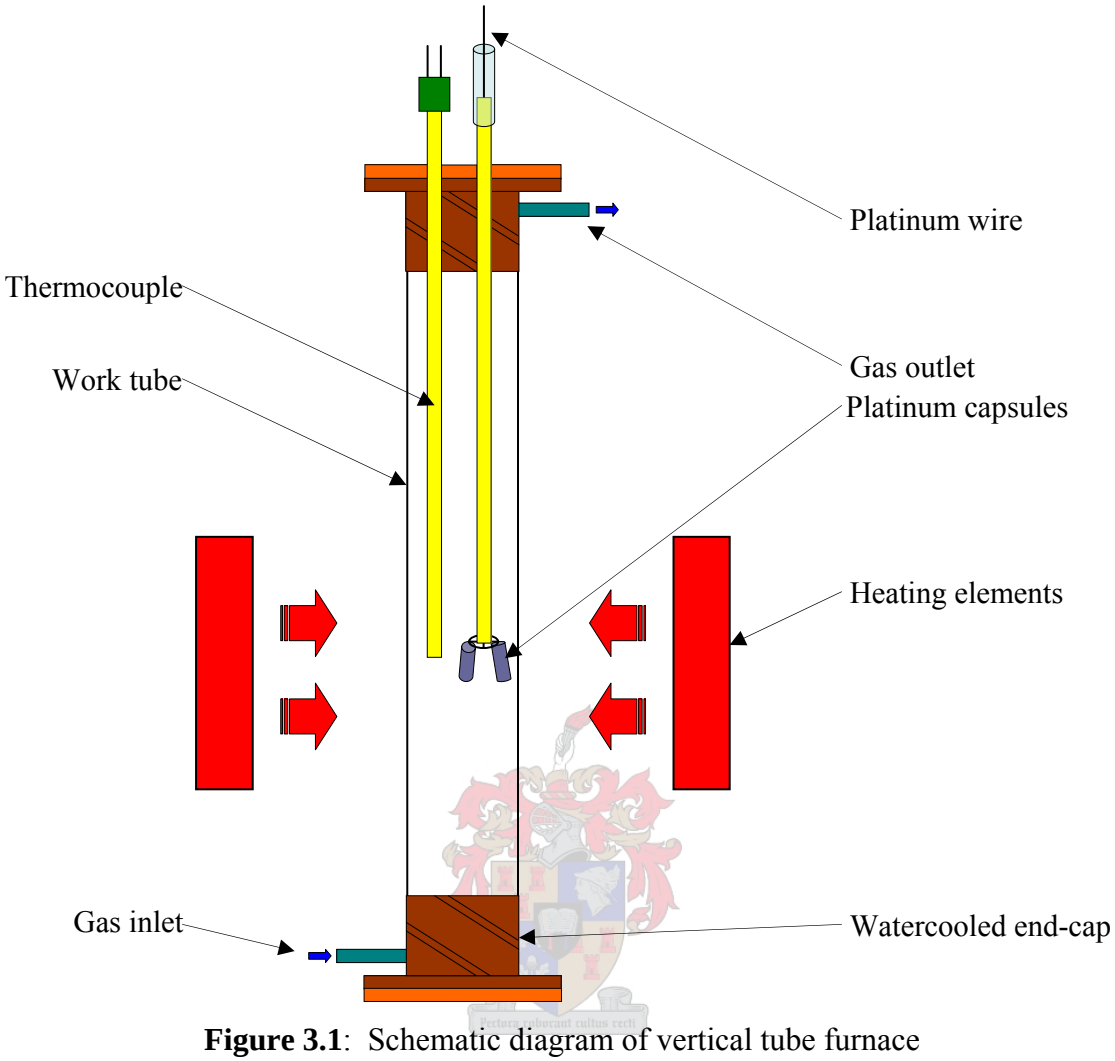

Figure 3.1: Schematic diagram of vertical tube furnace

The temperature in the hot zone was measured using a B-type (Pt-6%Rh/Pt-30%Rh) thermocouple, with a maximum application temperature of 1700°C, inserted from the top of the furnace tube. Thermocouples were calibrated against the melting point of copper (1083°C) by producing cooling curves for molten copper from approximately 1120°C. A description of the method used is given in Appendix B. All thermocouples were found to be accurate to ±1°C and no corrections were required.

The length of the hot zone was determined to be approximately 4 cm when the furnace was heated to 900°C (Appendix B). Its temperature was accurately controlled to the setpoint temperature (± 1°C) utilising a Eurotherm programmable controller. The maximum attainable operating temperature in the hot zone was approximately 1630°C.

The required partial pressure of oxygen inside the furnace tube was maintained by accurately controlling the flows of CO (99.5%) and CO_2 (99.8%) through gas cleaning trains and pre-calibrated mass flow controllers. The calculation of oxygen partial pressure from thermodynamic relations is discussed in Appendix A. The oxygen partial pressures obtained at temperatures and CO_2/CO ratios relevant to this investigation is shown in Table 3.2.

Table 3.2: Oxygen partial pressure (atm) at relevant temperatures and CO_2/CO ratios

Temperature (°C)	**CO_2/CO**			
	0.5	**2**	**10**	**20**
1400	6.82×10^{-10}	1.09×10^{-8}	2.72×10^{-7}	1.09×10^{-6}
1500	6.72×10^{-9}	1.08×10^{-7}	2.69×10^{-6}	1.08×10^{-5}
1600	5.20×10^{-8}	8.32×10^{-7}	2.08×10^{-5}	8.32×10^{-5}

Calibration curves for each gas channel were drawn by measuring the flowrate of the relevant gas through a burette at different controller setpoints. Results were found to be repeatable with increasing and decreasing controller setpoints and the relationship between controller setpoint and actual flowrate was found to be linear in all cases, within the ranges used (Appendix B). The required flowrate of each gas was calculated using a fixed total gas flowrate and the CO_2/CO ratio. Flow controller setpoints were then calculated using the calibration curves.

Gases were purified utilising tubes of silica gel and magnesium perchlorate to effectively remove moisture, and through copper windings at 500°C to remove traces of oxygen. The silica gel was replaced regularly, before any colour change due to moisture absorption was detected. Copper windings were replaced approximately once per month, or regenerated with pure CO gas, to ensure effective gas conditioning.

Starting slag samples were contained in capsules rolled from platinum foil with a thickness of 0.025mm. Each capsule had a volume of approximately $0.4cm^3$ and held roughly 1 gram of pulverized premelted slag. Samples were suspended in the hot zone

using platinum wire in an alumina sheath, reacted for the required period of time and then dropped into a bath of cold water to quench.

3.4 Analytical techniques

Small grains of slag from each sample were mounted, sectioned and polished for examination under reflected light optical microscope. Slag particles were carefully placed in small plastic containers. The containers were filled with liquid resin and excess air removed by vacuum. After baking, resin mounts were removed from the plastic containers and polished using six different grits of sandpaper.

Samples were viewed under optical microscope and photographs taken. Polished mounts were subsequently coated with a thin layer of carbon for conduction during microprobe analyses.

Remaining slag samples were pulverised and submitted to CSIRO's Analytical Services for bulk slag analysis and ferrous iron (Fe^{2+}) determination using wet-chemical analysis.

3.4.1 Phase identification

Equilibrium phases were identified using reflective optical microscopy and scanning electron microscope (SEM) images. The spinel and glass phases were easily identified as bright white angular crystals and light grey regions, respectively. Distinction between the olivine and pyroxene phases proved to be more difficult visually as both types of crystals appeared medium to dark grey in colour. This difficulty was overcome by determining cation-to-silica ratios in identified phases, so establishing whether it was olivine or pyroxene.

The formula for olivine is $(Fe,Mg)_2SiO_4$ in which the atomic ratio (Fe + Mg)/Si is 2. For pyroxene the formula is $(Fe,Mg)_2Si_2O_6$ and the same ratio is unity. Calculation of this

ratio facilitated easy identification of the olivine phase, as in most cases the calculated ratio agreed very well with the theoretical value.

In many of the slag samples, cation-to silica ratios for the liquid phase also equated to values close to 1. Where crystalline phases were visually distinguished from the glassy phase and found to have ratios very close to 1, they were assumed to be pyroxenes. In most cases these crystals were very similar in composition to the liquid phase. Phase compositions were taken as the average of 3 to 5 point analyses per phase.

3.4.2 Phase chemistry

Compositions of the glass and crystalline phases were determined using a JEOL Superprobe. Operating conditions were an accelerating potential of 15kV and a current of 20nA. The beam was focussed, with a 1 to 2 μm analysis volume. The probe was calibrated for Mg, Fe, Si, Ca, Al and Cr using the mineral standards listed below.

- Mg: $MgAl_2O_4$ (spinel)
- Fe: Fe_2O_3 (hematite)
- Si: $CaSiO_3$ (wollastonite)
- Ca: $CaSiO_3$ (wollastonite)
- Al: $MgAl_2O_4$ (spinel)
- Cr: Cr_2O_3

3.4.3 Bulk chemical analyses

Bulk chemical compositions were determined by XRF (X-Ray Fluorescence Spectroscopy) for SiO_2, Al_2O_3, Fe_2O_3, CaO, Cr_2O_3 and MgO as well as several other minor oxides not relevant to this study.

Separation of slag from the platinum foil proved to be extremely laborious in certain cases, especially with experiments conducted at 1600°C and under the most reducing

conditions, when the platinum foil became very brittle, possibly due to reaction with iron. In these cases samples submitted for chemical analysis contained significant amounts of platinum, which had to be corrected for. These samples were fused with sodium peroxide, digested in nitric acid and analysed using Vista ICP-OES (Inductively Coupled Plasma – Optical Emission Spectrometer). Samples were analysed for Pt, Al, Ca, Cr, Fe and Mg. Analyses were reported on a platinum free basis. Elemental concentrations were converted to oxides and silica content was calculated by difference.

3.4.4 Ferrous iron (Fe^{2+}) determinations

Ferrous iron content was determined using a dichromate titration method. Samples were digested under non-oxidising conditions using a nitrogen gas blanket to prevent ingress of air into the digestion solution. Hydrofluoric acid (HF) was used to dissolve silicate phases and hydrochloric acid (HCl) to dissolve remaining iron containing phases. Titrations were carried out manually, using a standard potassium dichromate solution with barium diphenylamine sulphonate as the indicator. The chemical reaction occurring during this titration is the following:

$$6\,Fe^{2+} + Cr_2O_7^{2-} + 14\,H^+ \leftrightarrow 2\,Cr^{3+} + 6\,Fe^{3+} + 7\,H_2O \qquad (3.1)$$

This reaction can be separated into two half-reactions. Dichromate ions act as the oxidising agent and its reduction can be written as follows:

$$Cr_2O_7^{2-} + 14\,H^+ + 6\,e^- \leftrightarrow 2\,Cr^{3+} + 7\,H_2O \qquad (3.2)$$

Ferrous iron (Fe^{2+}) is oxidised to ferric iron (Fe^{3+}) by the dichromate ion:

$$Fe^{2+} \leftrightarrow Fe^{3+} + e^- \qquad (3.3)$$

The amount of dichromate ion consumed to oxidise all the ferrous iron to ferric iron was calculated from the titration, and represented one sixth of the amount of Fe^{2+} ions originally present in the sample.

Chapter 4

RESULTS

Experimental data for all drop-quench experiments will be given in this chapter. It was imperative to determine the reaction time required to achieve chemical equilibrium prior to conducting actual experiments. The series of experiments conducted for this purpose will be dealt with in Section 4.1.

Experiments conducted with the two chromium-free slags (slags B1 and B2) will be discussed in Section 4.2. Results from these experiments were used for validation of the experimental technique. Both slag B1 and B2 had bulk FeO_x/MgO ratios of 1.6.

The next section will deal with a series of experiments conducted in a gas atmosphere with CO_2/CO ratio of 2. The aim of these experiments was to determine the effects of bulk FeO_x/MgO ratio, bulk chromium oxide content and temperature on phase chemistry and phase stability.

In Section 4.4 results will be presented for the series of experiments in which the gas phase CO_2/CO ratio was varied. These experiments were conducted in order to study the effect of oxygen partial pressure on the solubility of chromium oxide in the liquid phase and on phase stability.

It should be mentioned that the bulk slag compositions and bulk Fe^{3+}/Fe^{2+} ratios shown in the data tables that follow are not considered to be very accurate. Very often the sample that was mounted and polished consisted of almost half of the total amount of sample available after equilibration experiments. Reflected light microscopy indicated that samples were not always homogeneous and therefore, may not always have been truly representative of reaction products. This will be discussed in more detail in Section 4.5. The apparent loss of iron during equilibration, assumed to be due to iron-platinum alloy formation, was calculated using original master slag

compositions and bulk slag compositions after reaction but for the reasons mentioned above these values may not be accurate.

A summary of phases found under the experimental conditions studied will be given in Section 4.6. Photomicrographs of a few slags containing both spinel and olivine crystals can be found in Appendix D.

The results for a full set of experiments conducted with a reaction time of 3 hours will be presented in Appendix E. It only became apparent after completion of these experiments that a 3-hour reaction time may not have been sufficient to reach equilibrium. Although these results will not be discussed, it may provide the reader with an indication of the approach to equilibrium.

For the data presented in this Chapter, full closure of material balances is not possible. Material balance reconciliation may provide a solution to alleviate this problem.

For reference, master slag compositions as shown in Table 3.1 are repeated below.

Table 3.1: Master slag compositions

Master Slag	MgO	Cr_2O_3	Fe_2O_3	SiO_2	CaO	Al_2O_3	FeO_x/MgO
	(weight %)						
1	24.5	1.2	17.0	47.7	4.8	4.8	0.6
2	18.7	1.5	23.0	47.3	4.7	4.8	1.1
3	14.1	1.3	30.5	45.1	4.4	4.5	1.9
4	19.5	3.7	23.0	44.1	4.8	4.9	1.1
5	18.0	6.4	21.0	44.7	4.9	4.9	1.1
6	14.1	7.1	19.0	49.8	5.0	5.0	1.2
B1	18.4	-	32.0	49.3	-	-	1.6
B2	16.5	-	28.9	44.6	5.0	5.1	1.6

* Total Fe expressed as Fe_2O_3

In the data tables that follow, total iron oxide will be expressed as Fe_2O_3, unless indicated otherwise, and total chromium oxide as Cr_2O_3.

4.1 Reaction time required to reach equilibrium

A series of five experiments was conducted in order to determine the reaction time required to reach chemical equilibrium in slags before quenching. Samples of master slags 2 and 5 were reacted for periods of 4.7, 17, 20, 24 and 46 hours at 1400°C and an oxygen partial pressure of $1.1x10^{-8}$ atm. Phase compositions and bulk Fe^{3+}/Fe^{2+} ratios were determined for each product sample.

Phase compositions were taken as the arithmetic mean of between 4 and 5 analyses per phase. Results from these five experiments for master slags 2 (1.5 wt% bulk chromium oxide) and 5 (6.4 wt% bulk chromium oxide) are summarized in Tables 4.1 and 4.2

Table 4.1: Determination of equilibration time with master slag 2 at 1400°C and oxygen partial pressure of $1.1x10^{-8}$ atm

Reaction time (h)	**Phase**	**MgO (wt%)**	**Cr_2O_3 (wt%)**	**Fe_2O_3 (wt%)**	**SiO_2 (wt%)**	**CaO (wt%)**	**Al_2O_3 (wt%)**	**Fe^{3+}/Fe^{2+}**
4.7	Bulk	18.96	1.42	22.13	47.91	4.76	4.82	0.28
	Glass	19.21	0.30	21.84	48.96	4.92	4.77	
	Spinel	11.56	50.05	33.69	0.17	0.16	4.36	
17	Bulk	19.06	1.38	22.08	47.73	4.86	4.89	0.27
	Glass	9.11	0.40	24.71	51.12	8.04	6.62	
	Spinel	10.51	44.71	37.99	0.19	0.14	6.47	
	Olivine	43.62	0.20	17.07	38.91	0.14	0.06	
20	Bulk	19.23	1.51	21.95	47.64	4.83	4.84	0.34
	Glass	18.95	0.32	21.46	49.05	5.20	5.02	
	Spinel	11.96	49.36	32.70	0.25	0.13	5.60	
	Olivine	44.71	0.13	15.86	39.14	0.13	0.03	
23.8	Bulk	19.38	1.60	22.02	47.43	4.75	4.82	0.29
	Glass	18.55	0.32	21.66	49.11	5.25	5.11	
	Spinel	11.52	46.45	35.83	0.20	0.14	5.87	
	Olivine	45.70	0.27	15.30	38.54	0.13	0.06	
46	Bulk	17.21	1.26	23.88	49.25	4.07	4.33	0.02
	Glass	17.67	0.74	20.75	49.65	5.77	5.42	
	Spinel	11.00	57.11	24.52	0.14	0.11	7.12	
	Olivine	43.18	0.40	17.55	38.67	0.16	0.04	

Results obtained for master slag 5 are given in Table 4.2.

Table 4.2: Determination of equilibration time with master slag 5 at 1400°C and oxygen partial pressure of $1.1x10^{-8}$ atm

Reaction time (h)	Phase	MgO (wt%)	Cr_2O_3 (wt%)	Fe_2O_3 (wt%)	SiO_2 (wt%)	CaO (wt%)	Al_2O_3 (wt%)	Fe^{3+}/Fe^{2+}
4.7	Bulk	-	-	-	-	-	-	-
	Glass	19.91	0.90	16.19	51.46	6.35	5.19	
	Spinel	12.59	52.47	29.14	0.15	0.15	5.50	
	Olivine	46.03	0.56	13.11	40.10	0.15	0.04	
17	Bulk	22.02	5.40	18.66	44.23	4.86	4.83	0.27
	Glass	8.63	0.35	19.69	53.23	10.31	7.78	
	Spinel	12.02	50.49	29.49	0.19	0.20	7.62	
	Olivine	45.49	0.28	14.43	39.53	0.20	0.07	
20	Bulk	22.03	5.30	18.34	44.46	4.99	4.89	0.34
	Glass	18.39	0.50	19.83	48.91	6.75	5.62	
	Spinel	11.93	50.49	30.43	0.16	0.15	6.84	
	Olivine	45.52	0.35	14.63	39.27	0.19	0.04	
23.8	Bulk	22.90	6.32	19.19	42.40	4.57	4.61	0.29
	Glass	17.61	0.51	19.10	49.51	7.33	5.94	
	Spinel	11.89	50.85	29.39	0.23	0.18	7.46	
	Olivine	45.34	0.37	14.98	39.05	0.20	0.07	
46	Bulk	16.79	6.17	18.13	48.78	4.17	5.97	0.07
	Glass	19.21	1.30	13.55	53.54	6.25	6.15	
	Spinel	13.74	63.96	15.59	0.13	0.11	6.47	
	Olivine	47.36	0.68	12.30	39.49	0.14	0.04	

No bulk composition or ferric/ferrous ratio could be determined for a reaction period of 4.7 hours due to the fact that the remaining quenched sample was too small for analysis.

Figures 4.1 and 4.2 show the variation of glass phase composition with time for slags 2 and 5, respectively.

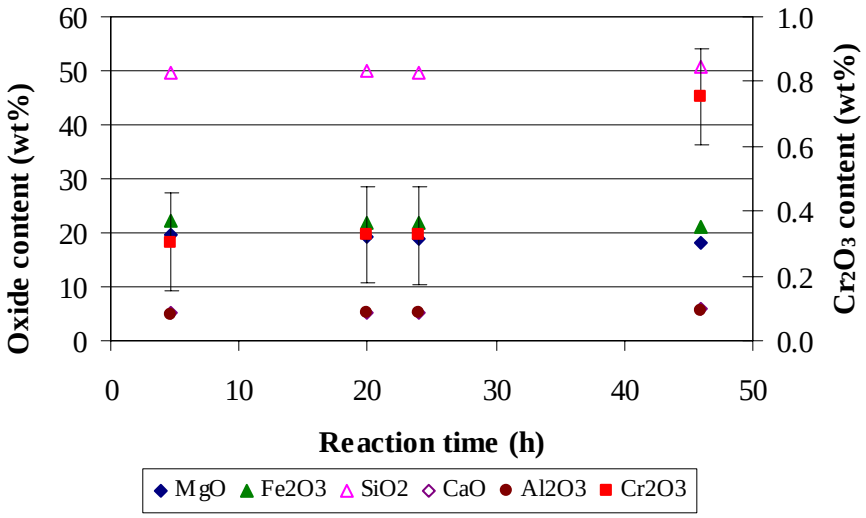

Figure 4.1: Variation of glass phase composition with reaction time at 1400°C and pO_2=1.1x10^{-8} atm (master slag 2)

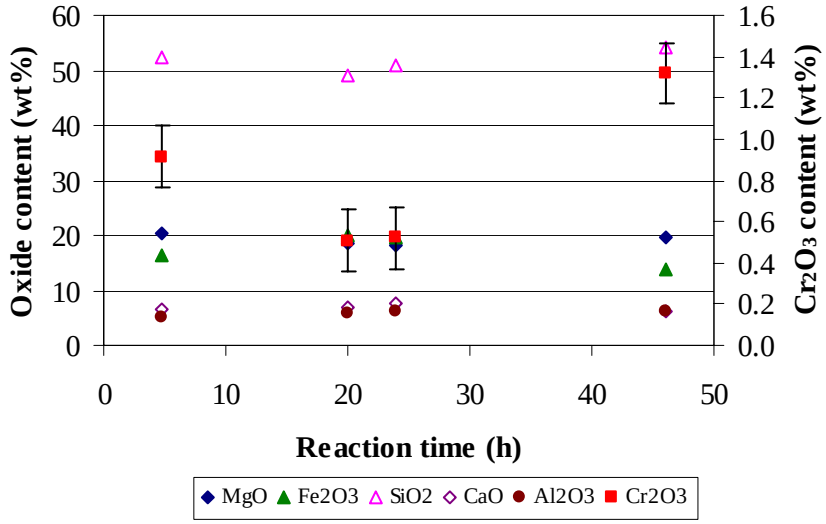

Figure 4.2: Variation of glass phase composition with reaction time at 1400°C and pO_2=1.1x10^{-8} atm (master slag 5)

From Figure 4.1 for master slag 2 it is evident that the composition of the glass phase remained essentially constant up to approximately 24 hours of reaction, after which the chromium oxide content started to increase from approximately 0.3 wt% to 0.8 wt% after 46 hours of reaction.

Figure 4.2 indicates that for master slag 5 the liquid composition stabilized in terms of iron oxide (expressed as Fe_2O_3) and chromium oxide (expressed as Cr_2O_3) between 20

and 24 hours of reaction. Between 24 and 46 hours of reaction the CrO_x content increased from 0.5 to 1.3 wt%, while the FeO_x content decreased from 19.6 to 13.8 wt%. This is believed to be as a result of iron loss by alloying with the platinum crucible.

Figures 4.3 and 4.4 show the variation of spinel phase composition with reaction time.

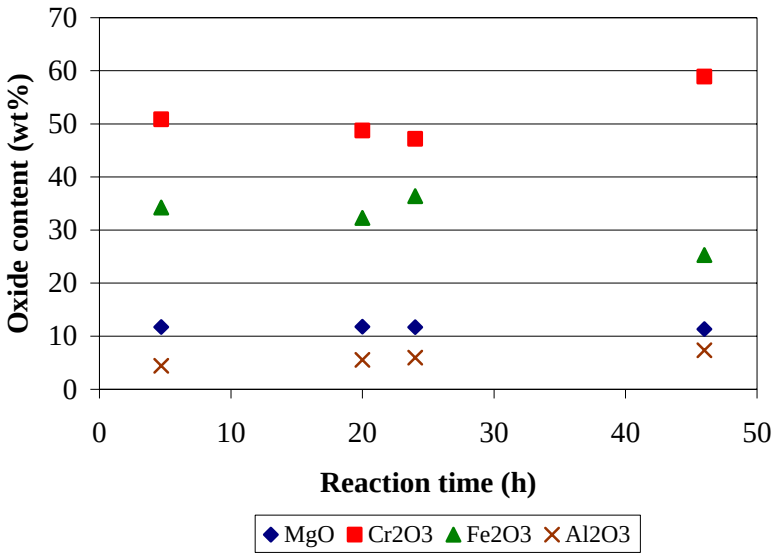

Figure 4.3: Variation of spinel phase composition with reaction time at 1400°C and $pO_2=1.1x10^{-8}$ atm (master slag 2)

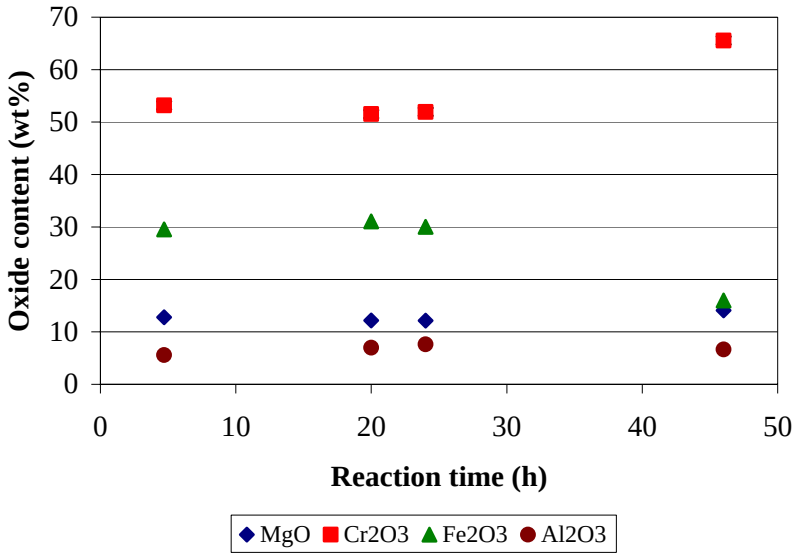

Figure 4.4: Variation of spinel phase composition with reaction time at 1400°C and pO_2=1.1x10^{-8} atm (master slag 5)

Figures 4.3 and 4.4 for the spinel phase show similar trends. In both cases the spinel phase composition remained constant for up to 24 hours of reaction time. At a bulk chromium oxide content of 1.5 wt% (master slag 2) the spinel CrO_x content increased from 47.2 to 58.9 wt% and FeO_x content decreased from 36.4 to 25.3 wt%, between 24 and 46 hours of reaction. A gradual increase in Al_2O_3 content of approximately 0.07 wt%/h was also observed.

At a bulk chromium oxide content of 6.4 wt% (master slag 5) the spinel CrO_x content was found to increase from 51.9 to 65.6 wt% and the FeO_x content decreased from 30.0 to 16.0 wt% between 24 and 46 hours of reaction.

Figure 4.5 shows the variation of bulk Fe^{3+}/Fe^{2+} with reaction time at 1400°C and oxygen partial pressure of 1.1x10^{-8} atm.

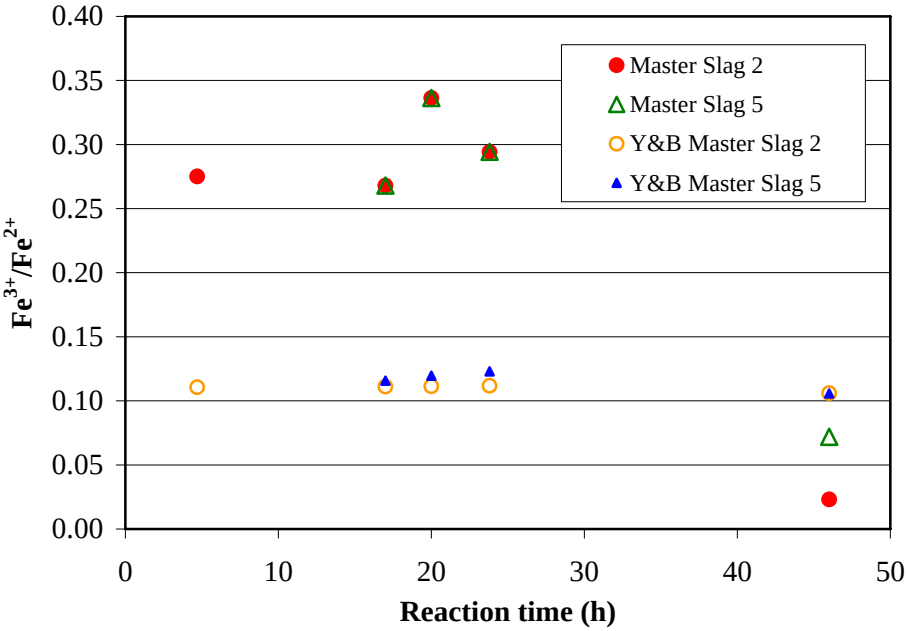

Figure 4.5: Variation of bulk Fe^{3+}/Fe^{2+} with reaction time at 1400°C and $pO_2=1.1x10^{-8}$ atm

From Figure 4.5 it is evident that the bulk ratio of ferric-to-ferrous iron remained stable within analytical error at values close to 0.3 for up to 24 hours of reaction. Between 24 and 46 hours of reaction, Fe^{3+}/Fe^{2+} decreased to values of 0.02 and 0.07 for master slags 2 and 5, respectively. Also shown in Figure 4.5 are Fe^{3+}/Fe^{2+} ratios predicted using the relationship given by Yang and Belton (1998), indicated as "Y&B" in Figure 4.5. Fe^{3+}/Fe^{2+} ratios for each experiment were calculated using the equation proposed by Yang and Belton (equation 2.5). Data obtained during this study do not seem to agree well with the predicted values, but it should be noted that Yang and Belton's study was conducted using calcium-silicate slags with Al_2O_3 contents close to 20 wt% and MgO and iron oxide contents below 10 wt%.

From the above observations it was decided to conduct experiments with reaction periods not less than 20 hours and not more than 24 hours.

4.2 Experiments with chromium-free slags

Master slags B1 and B2 were reacted at 1400°C and an oxygen partial pressure of $1.1x10^{-8}$ atm ($CO_2/CO=2$) for a period of 24 hours. The aim of these experiments was to determine whether phase compositions agreed with published data.

Experimental results are shown in Table 4.3.

Table 4.3: Normalised phase compositions obtained through equilibration of master slags B1 and B2

Slag	Phase	MgO (wt%)	FeO_x (wt%)	SiO_2 (wt%)
B1	Bulk*	17.3	27.3	55.4
	Glass	19.7	29.3	51.0
	Pyroxene	24.9	19.6	55.5
B2	Bulk*	17.9	25.2	56.9
	Glass	20.1	27.4	52.5
	Olivine	41.5	19.4	39.1

* bulk compositions were determined by XRF and compositions of other phases by microprobe analysis

As is evident from Table 4.3 equilibration of slag B1 (in the system FeO_x-MgO-SiO_2) resulted in the formation of pyroxene as the only crystalline phase. During equilibration of slag B2 (in the system FeO_x-MgO-SiO_2-CaO-Al_2O_3) olivine formed as the only crystalline phase.

The normalized compositions of phases shown in Table 4.3 are shown on the ternary diagram for the system FeO-MgO-SiO_2 in Figure 4.6.

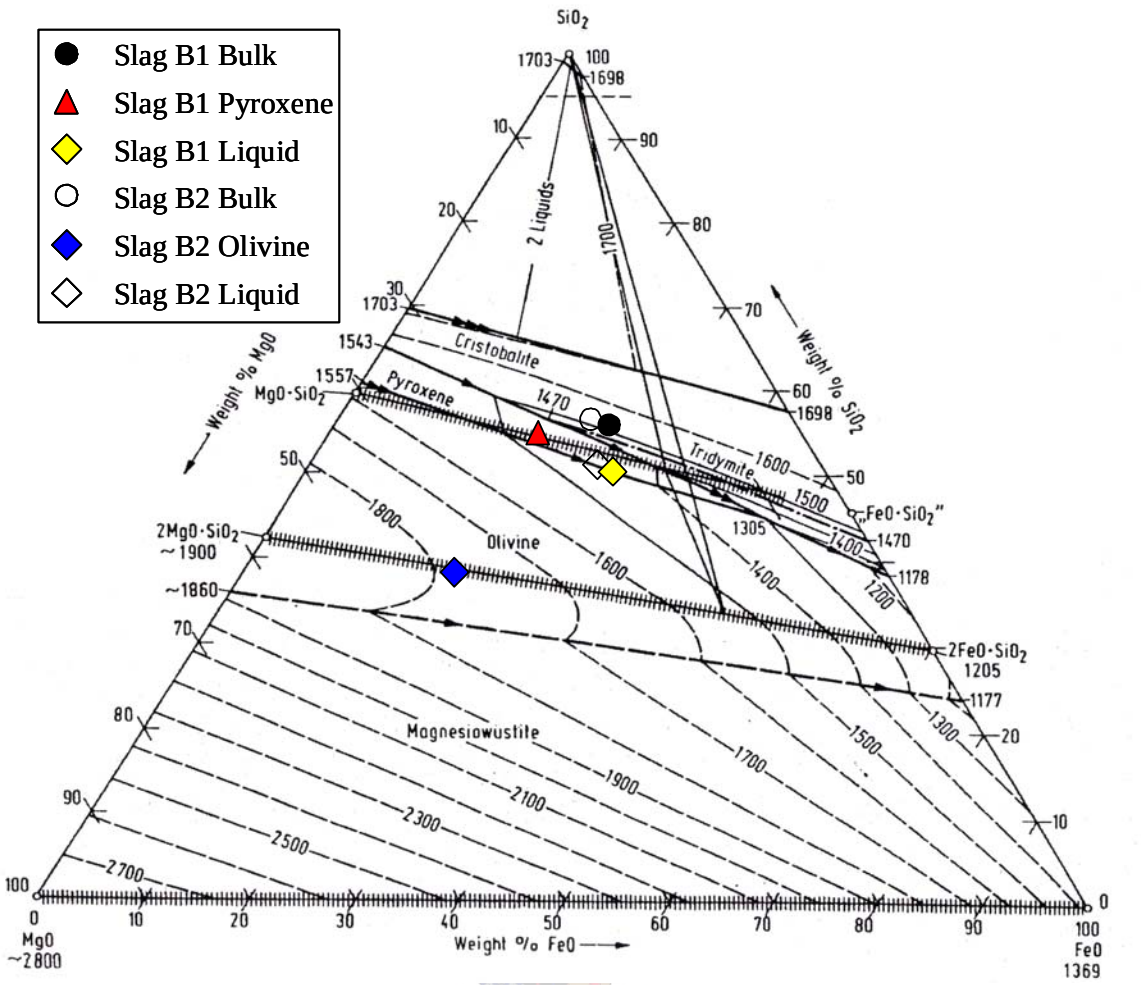

Figure 4.6: Phase compositions superimposed on the ternary diagram for the system FeO_x-MgO-SiO_2 (original diagram from Slag Atlas, 1995)

As can be seen from Figure 4.6 the composition of pyroxene was found to lie on the solid solution line for that phase. The slight deviation of the experimentally found composition of olivine from the solid solution line may be attributed to the normalization from the five-component system as well as the effects of CaO and Al_2O_3 on the activities of SiO_2, MgO and FeO_x.

Optical microscopy revealed that samples consisted mainly of a liquid phase. Crystalline phases could only be identified utilizing the scanning electron microscope (SEM). The bulk and liquid phase compositions were therefore expected to be very close to one another. As indicated in Figure 4.6, actual bulk compositions were significantly different from liquid compositions and this is believed to be due to uncalibrated differences between the results obtained through XRF and microprobe analyses.

If it is assumed that bulk and liquid compositions were in fact very similar, application of the lever rule would support the observation that very few olivine and pyroxene crystals were observed.

The above observations indicate that experimental data points agree well with previously determined compositions of crystalline phases, and therefore the experimental technique is considered to provide satisfactory results.

4.3 Experiments at a constant CO_2/CO ratio of 2 in the gas phase

As mentioned earlier the aim of these experiments was to determine the effects of the bulk FeO_x/MgO ratio, bulk CrO_x content and temperature on phase compositions and phase stability. In master slags 1, 2 and 3 the bulk FeO_x/MgO ratios were 0.6, 1.1 and 1.9, respectively and the bulk chromium content was kept constant, while in slags 2, 4, 5 and 6 the chromium oxide contents were 1.5, 3.7, 6.4 and 7.1 wt%, respectively while the FeO_x/MgO ratio was kept constant.

Results from experiments conducted at 1400°C are given in Table 4.4.

Table 4.4: Phase compositions obtained through equilibration of master slags 1 through 6 at 1400°C and $CO_2/CO=2$ ($pO_2=1.1x10^{-8}$ atm)

Master Slag	Phase	MgO (wt%)	Cr_2O_3 (wt%)	Fe_2O_3 (wt%)	SiO_2 (wt%)	CaO (wt%)	Al_2O_3 (wt%)	Fe^{3+}/Fe^{2+}
1	Bulk	23.83	0.97	15.20	49.63	5.20	5.18	0.11
	Glass	22.21	0.79	14.77	50.13	5.90	6.21	
	Spinel	15.12	58.03	15.65	0.20	0.10	10.91	
	Olivine	48.31	0.39	10.81	40.28	0.15	0.06	
2	Bulk	19.38	1.60	22.02	47.43	4.75	4.82	0.23
	Glass	18.55	0.32	21.66	49.11	5.25	5.11	
	Spinel	11.52	46.45	35.83	0.20	0.14	5.87	
	Olivine	45.70	0.27	15.30	38.54	0.13	0.06	
3	Bulk	14.77	1.07	28.13	46.73	4.62	4.68	0.05
	Glass	14.24	0.94	24.44	50.39	4.76	5.23	
	Spinel	8.68	60.95	25.43	0.12	0.09	4.73	
4	Bulk	19.99	4.04	20.58	45.43	4.91	5.05	-
	Glass	20.47	1.04	18.76	49.12	5.24	5.36	
	Spinel	12.75	60.37	19.28	0.14	0.10	7.36	
5	Bulk	22.90	6.32	19.19	42.40	4.57	4.61	0.29
	Glass	17.61	0.51	19.10	49.51	7.33	5.94	
	Spinel	11.89	50.85	29.39	0.23	0.18	7.46	
	Olivine	45.34	0.37	14.98	39.05	0.20	0.07	
6	Bulk	14.20	7.28	18.66	49.83	4.99	5.03	-
	Glass	14.98	0.76	17.42	55.64	5.75	5.44	
	Spinel	11.75	56.67	28.02	0.12	0.13	3.30	

From Table 4.4 it can be seen that both the spinel and olivine phases crystallized with the equilibration of slags 1, 2 and 5. The only crystalline phase observed with slags 3, 4 and 6 at 1400°C was spinel. Significant variation is observed in Fe^{3+}/Fe^{2+} data, most likely due to inaccuracy of the analytical technique when spinel crystals, which are difficult to dissolve during digestion, are present. No Fe^{3+}/Fe^{2+} determinations could be done for slags 4 and 6 due to samples being too small for bulk and Fe^{3+}/Fe^{2+} analyses.

Table 4.5: Phase compositions obtained through equilibration of master slags 1 through 6 at 1500°C and $CO_2/CO=2$ ($pO_2=1.1x10^{-7}$ atm)

Master Slag	Phase	MgO (wt%)	Cr_2O_3 (wt%)	Fe_2O_3 (wt%)	SiO_2 (wt%)	CaO (wt%)	Al_2O_3 (wt%)	Fe^{3+}/Fe^{2+}
1	Bulk	22.81	1.26	17.22	50.12	4.10	4.48	0.81
	Glass	25.30	1.15	12.93	49.87	5.49	5.25	
	Spinel	15.81	66.00	11.46	0.28	0.13	6.32	
2	Bulk	17.05	1.43	25.18	48.06	3.98	4.30	1.43
	Glass	19.88	1.40	17.42	51.00	5.18	5.12	
3	Bulk	13.07	1.23	29.40	48.36	3.82	4.11	0.68
	Glass	15.82	1.24	22.85	50.09	5.06	4.94	
4*	Bulk	18.73	3.42	18.79	49.95	4.46	4.64	0.30
	Glass	19.87	1.41	13.80	53.67	5.80	5.44	
5	Bulk	17.38	8.83	18.80	46.07	4.25	4.66	0.27
	Glass	20.34	2.11	16.23	50.25	5.79	5.29	
	Spinel	13.43	65.11	15.48	0.16	0.10	5.71	
6	Bulk	13.42	7.30	17.96	52.32	4.35	4.66	0.40
	Glass	14.46	3.45	11.78	59.01	5.65	5.65	
	Spinel	12.43	67.86	16.08	0.13	0.12	3.38	

* The formation of a spinel phase was suspected but not observed

As is evident from Table 4.5 crystalline phases were less stable at 1500°C when compared to the results at 1400°C. Slags 2, 3 and 4 were above their liquidus temperatures, as microprobe analyses did not show the presence of any crystalline phases. It is worth noting that the olivine phase was unstable in all these slags at 1500°C. Once again, significant variation is observed in Fe^{3+}/Fe^{2+} data.

Data for slags 2, 3 and 4 indicate differences between bulk and liquid phase analyses, especially in terms of iron oxide content. A likely explanation is that some iron was lost due to alloy formation with the platinum foil. The apparent loss of iron was between 15 and 21 wt% of the initial master slag iron content. Another contributing factor could be the fact that bulk slag analyses were determined by XRF, while liquid phase compositions were determined by microprobe. The XRF and microprobe may have different biases and precisions.

Table 4.5 shows that both the chromium oxide and iron oxide contents of slag 4 as determined for the bulk and liquid phases differed significantly even though no crystalline phases were observed. This suggests that a crystalline phase may have been present in the sample but not identified. This assumption is supported by the fact that spinel crystals were observed at 1600°C, as will be shown in the next set of data.

Results obtained at 1600°C are given in Table 4.6.

Table 4.6: Phase compositions obtained through equilibration of master slags 1 through 6 at 1600°C and $CO_2/CO=2$ ($pO_2=8.3x10^{-7}$ atm)

Master Slag	Phase	MgO (wt%)	Cr_2O_3 (wt%)	Fe_2O_3 (wt%)	SiO_2 (wt%)	CaO (wt%)	Al_2O_3 (wt%)	Fe^{3+}/Fe^{2+}
1	Bulk	21.72	1.45	19.16	48.05	4.74	4.87	0.09
	Glass	22.15	1.32	17.56	48.80	4.91	5.25	
2	Bulk	20.40	3.14	20.87	46.06	4.67	4.86	0.10
	Glass	21.21	1.51	19.05	48.01	5.04	5.19	
3	Bulk	-	-	-	-	-	-	-
	Glass	15.61	1.33	27.59	45.91	4.68	4.88	
4	*Bulk*	*14.34*	*3.25*	*14.57*	*31.28*	*3.28*	*33.27*	-
	Glass	*12.89*	*0.75*	*12.37*	*34.59*	*3.92*	*35.48*	
	Spinel	*21.94*	*2.66*	*9.55*	*0.05*	*0.01*	*65.79*	
5	Bulk	18.16	11.18	18.50	42.47	4.66	5.04	-
	Glass	19.43	2.58	18.14	49.00	5.48	5.37	
	Spinel	12.90	65.88	17.00	0.13	0.08	4.00	
6	Bulk	14.53	6.53	16.75	51.35	5.13	5.72	-
	Glass	15.40	2.78	16.58	53.99	5.69	5.55	
	Spinel	13.70	65.66	15.66	0.12	0.07	4.78	

Table 4.6 indicates that slags 1, 2 and 3 were above their liquidus temperatures at 1600°C, while spinel crystals were observed in slags 4, 5 and 6.

Results obtained for slag 4 during this particular experiment show total disagreement with compositions expected from the original slag composition and other experiments conducted using slag 4. Because of the fact that XRF and microprobe results are in reasonable agreement, this observation cannot be attributed to analytical error. The

only logical conclusion that can be made is that some form of contamination occurred during sample preparation, but the exact cause is uncertain.

Bulk chromium oxide contents determined for slags 2 and 5 are notably different from expected values, while other oxides show reasonable agreement with master slag compositions. The possibility does exist that bulk samples after equilibration were not truly representative as difficulties were in some instances experienced in separating slags from platinum foil, especially at high reaction temperatures and low oxygen partial pressures. No crystalline phases were observed for slag 2 and the glass phase chromium oxide content was the same as that of the master slag. Therefore it is reasonable to assume that an error occurred in the preparation or analysis of the bulk sample.

4.4 Experiments at different CO_2/CO ratios in the gas phase

The aim of these experiments was to study the effect of oxygen partial pressure on phase chemistry and stability at a constant bulk FeO_x/MgO ratio. Slags 2, 4, 5 and 6 were selected for this purpose and reacted at temperatures of 1400°C, 1500°C and 1600°C and CO_2/CO ratios of 0.5, 2, 10 and 20.

4.4.1 Results obtained at 1400°C

Results obtained at 1400°C are given in Tables 4.7 to 4.10.

Table 4.7: Phase compositions obtained through equilibration of master slags 2, 4, 5 and 6 at 1400°C and a CO_2/CO ratio of 0.5 (pO_2=6.8x10^{-10} atm)

Master Slag	Phase	MgO (wt%)	Cr_2O_3 (wt%)	Fe_2O_3 (wt%)	SiO_2 (wt%)	CaO (wt%)	Al_2O_3 (wt%)	Fe^{3+}/Fe^{2+}
2	Bulk	19.64	1.36	18.85	50.10	4.97	5.08	Nil
	Glass	20.65	3.68	17.39	47.55	5.23	5.50	
4	Bulk	19.40	4.65	22.45	44.00	4.63	4.87	0.09
	Glass	*13.53*	*46.12*	*17.40*	*13.97*	*1.49*	*7.48*	
	Spinel	13.23	60.75	17.27	0.16	0.12	8.47	
5	Bulk	18.90	6.81	17.15	46.84	5.11	5.19	0.26
	Glass	21.23	0.69	19.78	47.83	5.27	5.20	
	Spinel	13.11	54.11	22.85	0.17	0.12	9.64	
6	Bulk	14.08	9.90	19.04	47.27	4.76	4.95	0.43
	Glass	19.46	4.01	16.74	48.80	5.42	5.57	
	Spinel	13.21	66.63	15.44	0.15	0.12	4.45	

The above results indicate that at 1400°C and an oxygen partial pressure of 6.8x10^{-10} atm the spinel phase formed only at bulk chromium oxide contents above 3.7 wt%. Data for slag 2 (bulk CrO_x content of 1.5 wt%) show that no crystalline phases formed under these conditions. The liquid composition shown for slag 4 is unrealistic, possibly due to analytical error or contamination, and was not taken into account in the discussion of results.

The difference in iron oxide contents between the master slags and bulk analyses indicate iron losses of approximately 13.6 and 18.2 percent of the initial contents for slags 2 and 4, respectively. Iron losses for slags 5 and 6 were negligible. Indications are that the ferric-to-ferrous iron ratio increased with increasing bulk chromium oxide content. However, this may be due to difficulty in digesting spinel crystals and the possible oxidation of Fe^{2+} to Fe^{3+} during the digestion.

Table 4.8: Phase compositions obtained through equilibration of master slags 2, 4, 5 and 6 at 1400°C and a CO_2/CO ratio of 2 (pO_2=1.1x10^{-8} atm)

Master Slag	Phase	MgO (wt%)	Cr_2O_3 (wt%)	Fe_2O_3 (wt%)	SiO_2 (wt%)	CaO (wt%)	Al_2O_3 (wt%)	Fe^{3+}/Fe^{2+}
2	Bulk	19.38	1.60	22.02	47.43	4.75	4.82	0.23
	Glass	18.55	0.32	21.66	49.11	5.25	5.11	
	Spinel	11.52	46.45	35.83	0.20	0.14	5.87	
	Olivine	45.70	0.27	15.30	38.54	0.13	0.06	
4	Bulk	19.99	4.04	20.58	45.43	4.91	5.05	-
	Glass	20.47	1.04	18.76	49.12	5.24	5.36	
	Spinel	12.75	60.37	19.28	0.14	0.10	7.36	
5	Bulk	22.90	6.32	19.19	42.40	4.57	4.61	0.29
	Glass	17.61	0.51	19.10	49.51	7.33	5.94	
	Spinel	11.89	50.85	29.39	0.23	0.18	7.46	
	Olivine	45.34	0.37	14.98	39.05	0.20	0.07	
6	Bulk	14.20	7.28	18.66	49.83	4.99	5.03	-
	Glass	14.98	0.76	17.42	55.64	5.75	5.44	
	Spinel	11.75	56.67	28.02	0.12	0.13	3.30	

At 1400°C and an oxygen partial pressure of 1.1x10^{-8} atm spinel formed with slags 4 and 6, while spinel and olivine formed with slags 2 and 5. Apparent iron losses were calculated to be between 2 and 8 percent of the initial iron content. The Fe^{3+}/Fe^{2+} ratio could not be determined for slags 4 and 6 due to samples being too small to analyse.

Table 4.9: Phase compositions obtained through equilibration of master slags 2, 4, 5 and 6 at 1400°C and a CO_2/CO ratio of 10 (pO_2=2.7x10^{-7} atm)

Master Slag	Phase	MgO (wt%)	Cr_2O_3 (wt%)	Fe_2O_3 (wt%)	SiO_2 (wt%)	CaO (wt%)	Al_2O_3 (wt%)	Fe^{3+}/Fe^{2+}
2	Bulk	19.05	1.47	22.39	47.54	4.77	4.78	0.27
	Glass	19.07	0.51	21.61	48.89	5.01	4.91	
	Spinel	11.96	46.95	35.38	0.15	0.11	5.45	
4	Bulk	18.87	3.54	20.96	47.86	4.25	4.52	0.67
	Glass	20.82	0.61	21.43	47.07	5.23	4.84	
	Spinel	12.57	43.75	37.39	0.17	0.11	6.01	
5	Bulk	17.44	5.80	18.73	49.10	4.30	4.63	0.23
	Glass	19.16	1.03	18.30	50.84	5.46	5.20	
	Spinel	12.41	59.12	23.71	0.15	0.11	4.49	
6	Bulk	14.11	7.45	18.88	49.60	4.93	5.02	0.76
	Glass	14.22	0.61	16.66	57.35	5.79	5.36	
	Spinel	12.14	52.43	31.98	0.12	0.15	3.18	

Results presented in Table 4.9 indicate that the spinel phase was stable in all experiments conducted at 1400°C and an oxygen partial pressure of 2.7x10^{-7} atm. Apparent iron losses, likely due to FePt alloy formation, were found to be between 1 and 8 percent of the initial master slag iron content.

Table 4.10: Phase compositions obtained through equilibration of master slags 4 and 5 at 1400°C and a CO_2/CO ratio of 20 (pO_2=1.1x10^{-6} atm)

Master Slag	Phase	MgO (wt%)	Cr_2O_3 (wt%)	Fe_2O_3 (wt%)	SiO_2 (wt%)	CaO (wt%)	Al_2O_3 (wt%)	Fe^{3+}/Fe^{2+}
4	Bulk	-	-	-	-	-	-	-
	Glass	20.33	0.82	20.79	47.61	5.21	5.22	
	Spinel	12.46	54.00	26.46	0.14	0.08	6.85	
5	Bulk	-	-	-	-	-	-	-
	Glass	19.57	1.00	16.98	51.46	5.64	5.36	
	Spinel	12.77	58.59	22.71	0.16	0.09	5.68	

At an oxygen partial pressure of 1.1x10^{-6} atm at 1400°C the spinel phase was found to be stable for slags 4 and 5. Samples were too small to determine bulk compositions and Fe^{3+}/Fe^{2+} ratios. Slags 2 and 6 were not equilibrated at a CO_2/CO ratio of 20.

4.4.2 Results obtained at 1500°C

Results obtained at 1500°C are shown in Tables 4.11 to 4.14.

Table 4.11: Phase compositions obtained through equilibration of master slags 2, 4, 5 and 6 at 1500°C and a CO_2/CO ratio of 0.5 (pO_2=6.7x10^{-9} atm)

Master Slag	Phase	MgO (wt%)	Cr_2O_3 (wt%)	Fe_2O_3 (wt%)	SiO_2 (wt%)	CaO (wt%)	Al_2O_3 (wt%)	Fe^{3+}/Fe^{2+}
2	Bulk	19.54	1.50	19.53	49.52	4.93	4.98	0.34
	Glass	19.52	1.70	13.33	54.55	5.28	5.62	
4	Bulk	21.06	4.41	19.30	44.72	5.19	5.31	0.08
	Glass	21.62	1.73	18.45	47.60	5.22	5.37	
5	Bulk	19.07	7.98	17.30	45.20	5.12	5.33	0.14
	Glass	20.01	2.33	16.06	50.42	5.58	5.59	
6	Bulk	14.68	7.53	16.59	50.91	5.15	5.16	Nil
	Glass	13.56	3.07	13.01	59.28	5.17	5.92	
	Spinel	11.78	68.07	16.92	0.11	0.04	3.09	

The liquidus temperatures of slags 4 and 5 at a CO_2/CO ratio of 0.5 appeared to be between 1400°C and 1500°C as this temperature increase resulted in the destabilization of the spinel phase. Spinel remained stable for slag 6 at 1500°C. Losses of iron, again assumed to be due to alloy formation, were found to be between 10 and 13 percent of master slag iron contents.

The significant dissimilarities between bulk and liquid phase chromium oxide contents determined for slags 4 and 5 once again suggest that unidentified chromium oxide containing crystalline phases may have been present in samples, although no such phases were observed optically or using scanning electron microscopy (SEM). As will be indicated in Table 4.15, spinel crystals were indeed observed in slag 5 at 1600°C.

Table 4.12: Phase compositions obtained through equilibration of master slags 2, 4, 5 and 6 at 1500°C and a CO_2/CO ratio of 2 (pO_2=1.1x10^{-7} atm)

Master Slag	Phase	MgO (wt%)	Cr_2O_3 (wt%)	Fe_2O_3 (wt%)	SiO_2 (wt%)	CaO (wt%)	Al_2O_3 (wt%)	Fe^{3+}/Fe^{2+}
2	Bulk	17.05	1.43	25.18	48.06	3.98	4.30	1.43
	Glass	19.88	1.40	17.42	51.00	5.18	5.12	
4	Bulk	18.73	3.42	18.79	49.95	4.46	4.64	0.30
	Glass	19.87	1.41	13.80	53.67	5.80	5.44	
5	Bulk	17.38	8.83	18.80	46.07	4.25	4.66	0.27
	Glass	20.34	2.11	16.23	50.25	5.79	5.29	
	Spinel	13.43	65.11	15.48	0.16	0.10	5.71	
6	Bulk	13.42	7.30	17.96	52.32	4.35	4.66	0.40
	Glass	14.46	3.45	11.78	59.01	5.65	5.65	
	Spinel	12.43	67.86	16.08	0.13	0.12	3.38	

The olivine crystals found at 1400°C with slags 2 and 5 were not observed at 1500°C and slag 2 was found to be above its liquidus temperature at 1500°C. Slags 5 and 6 were below their liquidus temperatures at 1500°C as spinel crystals were observed after equilibration. Iron losses were between 4.5 and 13.5 percent of the original content, decreasing with increasing bulk chromium oxide content. As discussed in Section 4.3, unobserved spinel crystals may have been present in slag 4 under these conditions. It will be shown in Table 4.16 that spinel crystals were observed in the same slag at 1600°C and therefore this explanation may be valid.

Table 4.13: Phase compositions obtained through equilibration of master slags 2, 4, 5 and 6 at 1500°C and a CO_2/CO ratio of 10 (pO_2=2.7x10^{-6} atm)

Master Slag	Phase	MgO (wt%)	Cr_2O_3 (wt%)	Fe_2O_3 (wt%)	SiO_2 (wt%)	CaO (wt%)	Al_2O_3 (wt%)	Fe^{3+}/Fe^{2+}
2	Bulk	19.25	1.44	21.61	48.03	4.83	4.84	0.17
	Glass	19.38	0.84	21.48	48.48	4.92	4.91	
	Spinel	12.25	59.09	23.64	0.16	0.12	4.75	
4	Bulk	19.95	3.96	21.52	44.77	4.85	4.95	0.18
	Glass	20.18	0.80	21.11	47.63	5.21	5.06	
5	Bulk	18.40	7.47	20.27	44.00	4.90	4.96	0.30
	Glass	19.23	1.03	19.92	49.23	5.60	5.00	
	Spinel	12.65	58.99	23.36	0.17	0.11	4.72	
6	Bulk	14.33	6.59	17.93	50.96	5.07	5.11	0.37
	Glass	14.63	0.97	17.70	55.47	5.82	5.41	
	Spinel	11.79	60.40	23.08	1.40	0.23	3.09	

Table 4.13 indicates that the spinel phase remained stable with an increase in temperature from 1400°C to 1500°C at a CO_2/CO ratio of 10 for slags 2, 5 and 6. Only a glassy phase was observed with slag 4 at 1500°C. Bulk slag analyses indicate differences in bulk and master slag iron contents between 3 and 6 percent. Once again, the significant difference in bulk and glass phase chromium oxide contents of slag 4 indicates that another chromium oxide containing phase may have been present in the sample. Table 4.17 shows that a spinel phase was observed in a sample of the same slag at 1600°C.

Table 4.14: Phase compositions obtained through equilibration of master slags 2, 4, 5 and 6 at 1500°C and a CO_2/CO ratio of 20 (pO_2=1.1x10^{-5} atm)

Master Slag	Phase	MgO (wt%)	Cr_2O_3 (wt%)	Fe_2O_3 (wt%)	SiO_2 (wt%)	CaO (wt%)	Al_2O_3 (wt%)	Fe^{3+}/Fe^{2+}
2	Bulk	19.10	1.44	22.13	47.74	4.80	4.80	0.16
	Glass	19.24	0.79	22.32	47.89	4.91	4.86	
4	Bulk	20.00	4.42	20.85	44.90	4.85	4.99	0.28
	Glass	19.13	0.85	19.50	49.80	5.59	5.13	
	Spinel	12.55	59.91	22.81	0.15	0.13	4.45	
5	Bulk	18.35	7.37	19.59	44.81	4.89	4.99	0.21
	Glass	20.45	0.85	20.70	47.77	5.23	5.00	
	Spinel	12.65	58.31	23.73	0.15	0.09	5.07	
6	Bulk	14.19	7.42	18.26	50.08	4.99	5.05	0.32
	Glass	15.00	1.04	18.08	55.05	5.69	5.14	
	Spinel	11.45	61.59	23.81	0.11	0.13	2.90	

Table 4.14 indicates that at an oxygen partial pressure of 1.1x10^{-5} atm and temperature of 1500°C slags 4, 5 and 6 were below their liquidus temperatures. No crystalline phases were observed for slag 2 but the lower liquid phase chromium oxide content once again suggests that another chromium-containing phase may have been present. Iron losses were found to be between 1 and 4 percent of the original content for slags 2, 5 and 6 and approximately 11 percent of the master slag composition for slag 4.

4.4.3 Results obtained at 1600°C

Results obtained at 1600°C are shown in Tables 4.15 to 4.18.

Table 4.15: Phase compositions obtained through equilibration of master slags 2, 4, 5 and 6 at 1600°C and a CO_2/CO ratio of 0.5 (pO_2=5.2x10^{-8} atm)

Master Slag	Phase	MgO (wt%)	Cr_2O_3 (wt%)	Fe_2O_3 (wt%)	SiO_2 (wt%)	CaO (wt%)	Al_2O_3 (wt%)	Fe^{3+}/Fe^{2+}
2	Bulk	17.74	2.85	21.02	48.23	5.04	5.12	0.16
	Glass	19.49	1.68	11.54	56.11	5.42	5.76	
4	Bulk	20.46	4.28	18.04	46.92	5.13	5.17	Nil
	Glass	20.45	1.08	17.99	50.07	5.08	5.33	
5	Bulk	18.90	10.00	18.44	42.70	4.86	5.10	0.11
	Glass	14.84	0.63	17.86	55.53	5.67	5.47	
	Spinel	11.06	57.27	27.48	0.13	0.13	3.94	
6	Bulk	15.16	9.98	18.37	46.65	4.78	5.06	Nil
	Glass	15.88	5.47	15.61	51.92	5.38	5.75	
	Spinel	12.30	68.04	16.06	0.23	0.09	3.27	

As expected, slag 2 did not contain any crystalline phases. As mentioned in Section 4.4.2 the possibility exists that a crystalline phase may have been present in slag 4, although not observed optically or using SEM. The bulk chromium oxide contents of slags 5 and 6 were unrealistically high, likely due to samples not being truly representative of reaction products.

As explained in Section 4.4.2 it is surprising that the spinel phase formed during equilibration of slag 5 as no crystalline phases were found at the same gas phase CO_2/CO ratio and 1500°C. The oxygen partial pressure was 5.2x10^{-8} atm at 1600°C, an order of magnitude higher than at 1500°C (pO_2=6.7x10^{-9} atm) but it is likely that temperature has a more significant effect on phase stability than oxygen partial pressure. The liquidus temperature for slag 5 must then be above 1600°C at a CO_2/CO ratio of 0.5 and not between 1400°C and 1500°C as reported earlier.

Table 4.16: Phase compositions obtained through equilibration of master slags 2, 4, 5 and 6 at 1600°C and a CO_2/CO ratio of 2 (pO_2=8.3x10^{-7} atm)

Master Slag	Phase	MgO (wt%)	Cr_2O_3 (wt%)	Fe_2O_3 (wt%)	SiO_2 (wt%)	CaO (wt%)	Al_2O_3 (wt%)	Fe^{3+}/Fe^{2+}
2	Bulk	20.40	3.14	20.87	46.06	4.67	4.86	0.10
	Glass	21.21	1.51	19.05	48.01	5.04	5.19	
4	*Bulk*	*14.34*	*3.25*	*14.57*	*31.28*	*3.28*	*33.27*	-
	Glass	*12.89*	*0.75*	*12.37*	*34.59*	*3.92*	*35.48*	
	Spinel	*21.94*	*2.66*	*9.55*	*0.05*	*0.01*	*65.79*	
5	Bulk	18.16	11.18	18.50	42.47	4.66	5.04	-
	Glass	19.43	2.58	18.14	49.00	5.48	5.37	
	Spinel	12.90	65.88	17.00	0.13	0.08	4.00	
6	Bulk	14.53	6.53	16.75	51.35	5.13	5.72	-
	Glass	15.40	2.78	16.58	53.99	5.69	5.55	
	Spinel	13.70	65.66	15.66	0.12	0.07	4.78	

As mentioned in Section 4.3, results obtained for slag 4 at 1600°C and a CO_2/CO ratio of 2 were omitted in the discussion of results. As at 1500°C, results at 1600°C show that the spinel phase was stable when slags 5 and 6 were equilibrated at this CO_2/CO ratio. The liquidus temperatures for these slags must therefore be above 1600°C.

Table 4.17: Phase compositions obtained through equilibration of master slags 2, 4, 5 and 6 at 1600°C and a CO_2/CO ratio of **10** (pO_2=2.1x10^{-5} atm)

Master Slag	Phase	MgO (wt%)	Cr_2O_3 (wt%)	Fe_2O_3 (wt%)	SiO_2 (wt%)	CaO (wt%)	Al_2O_3 (wt%)	Fe^{3+}/Fe^{2+}
2	Bulk	18.86	1.45	21.34	48.69	4.80	4.86	0.14
	Glass	18.81	1.37	21.58	48.42	4.91	4.93	
4	Bulk	19.83	4.00	21.02	45.25	4.92	4.98	0.14
	Glass	20.16	1.15	21.05	47.31	5.21	5.13	
	Spinel	12.70	62.25	20.35	0.14	0.09	4.48	
	Pyroxene	21.09	1.11	19.85	48.28	4.65	5.03	
5	Bulk	18.46	7.97	20.24	43.56	4.82	4.94	0.19
	Glass	18.90	1.55	19.62	49.30	5.55	5.09	
	Spinel	12.49	63.33	19.96	0.15	0.10	3.98	
6	Bulk	14.47	9.53	18.71	47.32	4.92	5.05	0.29
	Glass	14.74	1.15	18.70	54.34	5.81	5.26	
	Spinel	11.34	64.77	20.93	0.11	0.11	2.74	

Interesting to note from Table 4.17 is the fact that both spinel and pyroxene precipitated with the equilibration of slag 4 at 1600°C and a CO_2/CO ratio of 10, while at 1400°C and 1500°C the only crystalline phase was spinel. The presence of pyroxene at 1600°C is highly unlikely. It could be that the glass phase was mistaken for pyroxene as the compositions of the two phases shown in Table 4.17 are practically identical. The early stages of pyroxene crystallization may have occurred as a result of quenching.

For slag 2 no crystalline phases were identified, which indicates that the liquidus temperature for this slag lies between 1500°C and 1600°C at this CO_2/CO ratio.

Indications are that the liquidus temperatures for slags 5 and 6 lie above 1600°C. Bulk chromium oxide contents determined after equilibration were unrealistically high, most likely due to samples not being representative of the reaction products.

Table 4.18: Phase compositions obtained through equilibration of master slags 4 and 5 at 1600°C and a CO_2/CO ratio of 20 (pO_2=8.3x10^{-5} atm)

Master Slag	Phase	MgO (wt%)	Cr_2O_3 (wt%)	Fe_2O_3 (wt%)	SiO_2 (wt%)	CaO (wt%)	Al_2O_3 (wt%)	Fe^{3+}/Fe^{2+}
4	Bulk	19.75	4.74	21.73	44.07	4.75	4.96	0.18
	Glass	20.34	1.51	21.36	46.52	5.04	5.23	
	Spinel	12.97	61.36	20.68	0.18	0.10	4.71	
	Pyroxene	21.29	1.51	19.85	47.72	4.33	5.30	
5	Bulk	17.97	9.28	19.88	43.00	4.69	5.19	0.38
	Glass	19.04	1.59	19.99	48.61	5.39	5.38	

Similar to the finding at a CO_2/CO ratio of 10, both spinel and pyroxene precipitated with reaction of slag 4 at 1600°C and a CO_2/CO ratio of 20. As mentioned before, the presence of pyroxene at 1600°C is highly improbable. When comparing the analyses shown for the glass and pyroxene phases in Table 4.18 it appears as though the glass phase could have been mistaken for pyroxene, or that pyroxene started to crystallize due to quenching from such high temperature.

The liquidus temperature for slag 5 under these conditions was found to be between 1500 and 1600°C. The bulk chromium oxide content determined for slag 5 was unrealistically high, while in the liquid it was much lower than in the master slag, which places doubt on the observation that the liquidus temperature of slag 5 was exceeded at 1600°C.

4.5 Possible reasons for discrepancies in bulk and glass compositions

As mentioned earlier, reflected light microscopy indicated that samples were not always homogeneous and therefore, may not always have been truly representative of reaction products. Figures 4.7a and 4.7b show photographs of homogeneous and non-homogeneous samples, respectively. The figures show white spinel crystals and the grey glass phase.

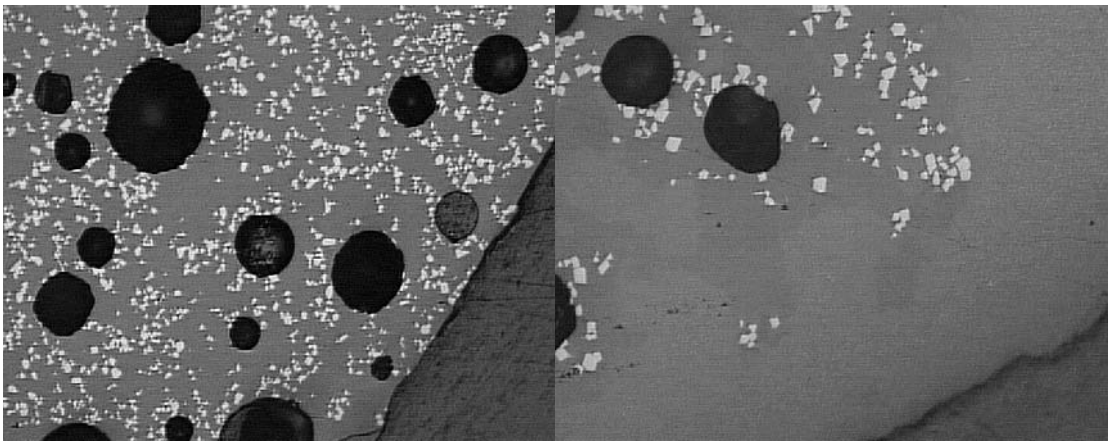

Figure 4.7a:
Example of a homogeneous sample

Figure 4.7b:
Example of a non-homogeneous sample

If the portion of a non-homogeneous sample selected for bulk analysis contained more spinel crystals than it would have been if the sample were homogeneous, the bulk chromium oxide content would be reported higher than the true content and vice versa. This is because of the fact that chromium oxide distributes strongly into the spinel phase relative to the glass phase.

This also allows for the possibility that in certain samples where a crystalline phase was in fact present, only the glass phase was observed in the portion of slag selected for microscopic examination. This would be the case where only a glass phase was observed optically but where chromium oxide in the glass phase was analysed to be lower that that of the bulk sample.

Results from Fe^{3+}/Fe^{2+} determinations were often erratic, possibly due to inherent inaccuracies in the technique. Another explanation might be the difficulty in digesting spinel crystals without oxidation of ferrous iron to ferric iron. Digestion at too high a temperature would have introduced the risk of oxidation.

4.6 Summary of phase stabilities

A summary of phases identified under each of the experimental conditions investigated is given in Table 4.19.

Table 4.19: Phases identified at different temperatures and CO_2/CO ratios

Master Slag	Temperature (°C)	CO_2/CO ratio			
		0.5	**2**	**10**	**20**
1	1400	-	GO	-	-
	1500	-	GS	-	-
	1600	-	G	-	-
2	1400	G	GSO	GS	-
	1500	G	G	GS	G
	1600	G	G	G	-
3	1400	-	GS	-	-
	1500	-	G	-	-
	1600	-	G	-	-
4	1400	GS	GS	GS	GS
	1500	G	G	G	GS
	1600	G	GS	GSP	GSP
5	1400	GS	GSO	GS	GS
	1500	G	GS	GS	GS
	1600	GS	GS	GS	G
6	1400	GS	GS	GS	-
	1500	GS	GS	GS	GS
	1600	GS	GS	GS	-

where G = glass, S = spinel, O = olivine, P = pyroxene

Qualitative trends deduced from Table 4.19 are the following:

- Olivine seems to be stable at lower temperatures and was observed only at 1400°C in this study.
- Pyroxene was observed only at 1600°C in this study. The existence of pyroxene at 1600°C is counter-intuitive, though. As mentioned earlier, the presence of pyroxene in these samples is believed to be due to the early stages of crystallisation as a result of quenching.

- When considering slags 2, 4, 5 and 6, which all had bulk FeO_x/MgO ratios of approximately 1.1, liquidus temperatures appear to increase with increasing bulk chromium oxide content as the spinel phase remains stable up to higher temperatures.
- When considering slags 1, 2 and 3, which had bulk chromium oxide contents between 1.2 and 1.5 wt%, liquidus temperatures seem to decrease as MgO in the system is replaced by iron oxide. This corresponds with findings from literature.

Chapter 5

DISCUSSION

The chief objective of this study was to quantify the behaviour of chromium in melter slags with respect to temperature, bulk FeO_x/MgO ratio, bulk chromium oxide content and oxygen partial pressure.

The distribution of chromium oxide between the spinel and glass phases will be discussed in section 5.1 and the solubility of chromium oxide in the glass phase in section 5.2. MPE-predicted values will also be shown in Section 5.2 and compared with experimental data.

The MPE model was used to simulate the effect of slag basicity under a number of furnace operating conditions. Results from these simulations will be discussed in section 5.3.

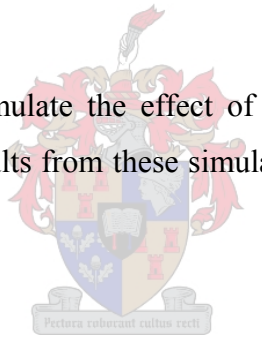

5.1 The distribution of chromium oxide between the spinel and glass phases

Figure 5.1 shows the relationship between CrO_x in the spinel phase and CrO_x in the glass phase (total chromium oxide expressed as Cr_2O_3). Data shown represent the entire range of oxygen partial pressures investigated *i.e.* from 6.8×10^{-10} atm at 1400°C to 8.3×10^{-5} atm at 1600°C. The individual effects of oxygen partial pressure and slag chemistry will also be discussed.

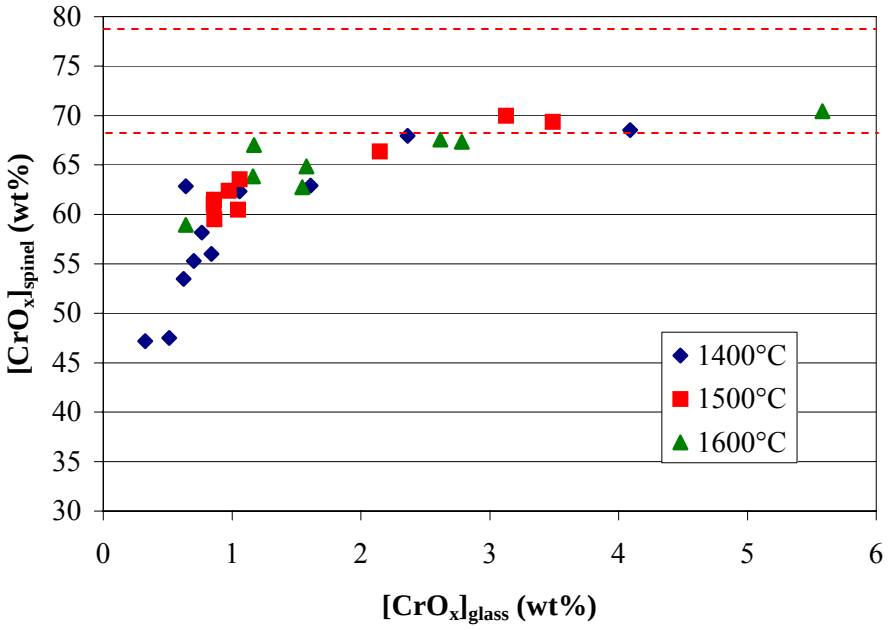

Figure 5.1: The relationship between $[CrO_x]_{spinel}$ and $[CrO_x]_{glass}$ at 1400, 1500 and 1600°C over the range of pO_2 investigated (CrO_x contents of $MgCr_2O_4$ and $FeCr_2O_4$ indicated with dashed lines at 79 and 68 wt%, respectively)

As is evident from Figure 5.1, CrO_x in spinel and CrO_x in the glass phase increased simultaneously for values of $[CrO_x]_{glass}$ up to approximately 2 wt%. The CrO_x content of the spinel phase seemed to be limited to between 66 and 70 wt% where $[CrO_x]_{glass}$ exceeded approximately 2 wt%. This effect does not seem to be significantly dependent on temperature.

It appears as though chromium oxide preferentially enters the spinel structure until a maximum spinel chromium content is reached. Chromium oxide in the glass phase then increases, leading to a decrease in $[CrO_x]_{spinel}/[CrO_x]_{glass}$. It is thought that chromium oxide will enter the spinel structure up to a point where no further Fe^{2+} or Mg^{2+} is available for it to bond with. The chromium oxide content of the glass phase will then start to increase. While the concentration of CrO_x in the spinel phase does not vary $[CrO_x]_{glass} > 2$ wt%, it is expected that the relative amount of spinel crystals will increase.

Interesting to note is the fact that the iron chromite ($FeCr_2O_4$) end-member of the spinel solid solution series contains 68wt% Cr_2O_3 while the picrochromite ($MgCr_2O_4$) end-member contains 79wt% Cr_2O_3. This might indicate that $[CrO_x]_{glass}$ starts to increase as the spinel composition approaches that of the $FeCr_2O_4$ end-member.

According to Hanson and Jones (1998), the Cr^{3+} content of the glass phase is buffered by spinel. The addition of Cr^{3+} to the system results in an increase in spinel chromium content until the Cr^{3+} saturation abundance is reached. It is assumed that additional chromium added to the system then enters the glass phase and, as mentioned, the crystallisation of spinel increases.

The relationship between $[CrO_x]_{spinel}$ and $[CrO_x]_{glass}$ obtained through variation of the bulk chromium oxide content from 1.5 to 7 wt% and the bulk FeO_x/MgO ratio from 0.6 to 1.9 at a CO_2/CO ratio of 2 is shown in Figure 5.2.

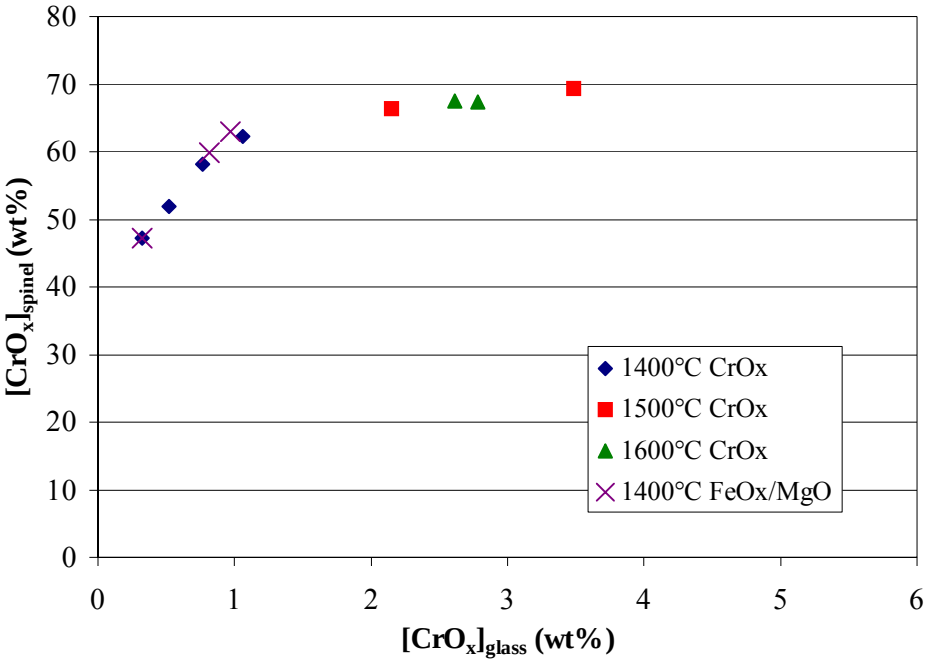

Figure 5.2: The relationship between $[CrO_x]_{spinel}$ and $[CrO_x]_{glass}$ with variations in bulk chromium oxide content and FeO_x/MgO ratio at a CO_2/CO ratio of 2.

As expected, an increase in bulk CrO_x content at 1400°C resulted in an increase in both $[CrO_x]_{spinel}$ and $[CrO_x]_{glass}$. Even though both increased the distribution ratio $[CrO_x]_{spinel}/[CrO_x]_{glass}$ decreased as bulk CrO_x content increased. Thus, the partitioning of chromium oxide into the glass phase became stronger as the limiting spinel chromium oxide content was approached.

Compositions for the glass and spinel phases obtained through variation of the bulk FeO_x/MgO ratio at 1400°C correspond with the trend found through variation of the bulk chromium oxide content. Although only three data points are shown, it can be seen that both $[CrO_x]_{spinel}$ and $[CrO_x]_{glass}$ increased as iron oxide replaced magnesia in the system. An increase in FeO_x/MgO from 0.6 to 1.9 caused the ratio $[CrO_x]_{spinel}/[CrO_x]_{glass}$ to decrease significantly (from 120 to 66), indicating that chromium oxide became more soluble in the glass phase relative to the spinel phase.

At 1500°C, the spinel phase was only observed at the two highest bulk chromium oxide contents (6.4 and 7.1 wt%) and the ratio $[CrO_x]_{spinel}/[CrO_x]_{glass}$ decreased from 30 to 20 with this increase in bulk chromium oxide content. In relative terms, $[CrO_x]_{glass}$ increased significantly from 2.1 to 3.5 wt% while $[CrO_x]_{spinel}$ increased slightly from 66 and 69 wt%, suggesting that a large proportion of the chromium oxide added to the system reported to the glass phase.

The distribution ratio $[CrO_x]_{spinel}/[CrO_x]_{glass}$ is shown as a function of oxygen partial pressure in Figure 5.3.

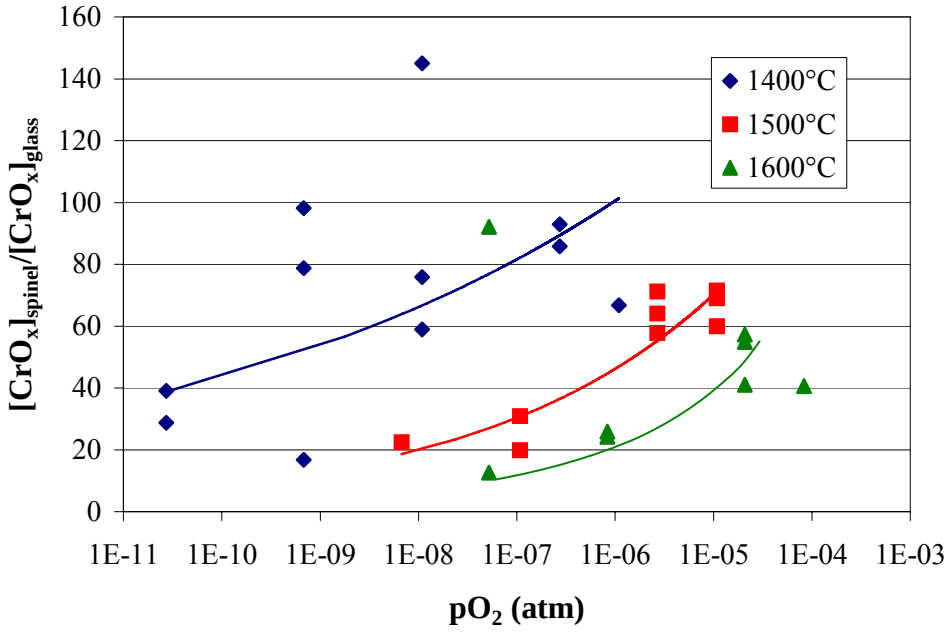

Figure 5.3: The variation of $[CrO_x]_{spinel}/[CrO_x]_{glass}$ with pO_2

Figure 5.3 shows that CrO_x is strongly partitioned into the spinel phase with $[CrO_x]_{spinel}/[CrO_x]_{glass}$ ratios much greater than unity. The highest distribution ratio was found at 1400°C and a bulk CrO_x content of 1.5 wt%. The relative amount of CrO_x that reported to the glass phase increased with a decrease in oxygen partial pressure (at constant temperature) and an increase in temperature (at constant pO_2). This is in agreement with conclusions made by Schwessinger and Muan (1992) and Rait *et al.* (1997). It should be noted that the distribution ratio shown in Figure 5.3 does not account for the relative amount of each phase present in the sample and is purely based on phase compositions.

Apart from slags with low bulk chromium oxide levels, spinel compositions were not significantly influenced by pO_2 at 1400°C and therefore, it can be assumed that the decrease in $[CrO_x]_{spinel}/[CrO_x]_{glass}$ with decreasing pO_2 was primarily due to an increase in CrO_x in the glass phase. This observation is in agreement with the findings of Hanson and Jones (1998) and is believed to be due to an increase in Cr^{2+}/Cr^{3+} in the glass phase as pO_2 is decreased.

Scatter in experimental data at constant pO_2, especially at 1400°C, is as a result of variations in bulk CrO_x contents. As mentioned, the $[CrO_x]_{spinel}/[CrO_x]_{glass}$ ratio decreased with increasing bulk CrO_x content at constant temperature and oxygen partial pressure, although CrO_x in both the glass and spinel phases increased. This implies that the amount of spinel increased, but in proportion to the amount of soluble chromium in the slag. In other words, a greater proportion of the chromium reported to the molten slag phase instead of precipitating as solids.

In summary, the partitioning of chromium oxide shifts away from the spinel phase and towards the glass phase as temperature is increased and oxygen partial pressure is decreased. There exists an apparent maximum chromium oxide content in the spinel phase. Addition of CrO_x to the system after this spinel composition has been reached leads to an increase in chromium in the liquid phase.

5.2 The solubility of chromium oxide in the glass phase

Solubility, in the strict sense of the word, refers to the maximum amount of CrO_x that can be dissolved in the slag without the formation of chromium-containing solids. In the context of this study, this term is broadened to mean the concentration of CrO_x in the glass phase in equilibrium with the saturating solid.

The solubility of CrO_x in the glass phase was determined as functions of temperature, bulk FeO_x/MgO, bulk CrO_x content and oxygen partial pressure with the aim of determining conditions that would be most favourable to dissolve chromium into the glass phase as this is of major importance in the smelting of UG2 concentrates.

MPE calculations were also performed for all the experimental conditions. In this section, experimental data will be shown using solid markers, while values predicted by the MPE model are shown with open markers.

5.2.1 The effect of temperature on the solubility of CrO_x in the glass phase

Figure 5.4 shows the variation of $[CrO_x]_{glass}$ with operating temperature at a CO_2/CO ratio of 2 for master slags 2, 4, and 5.

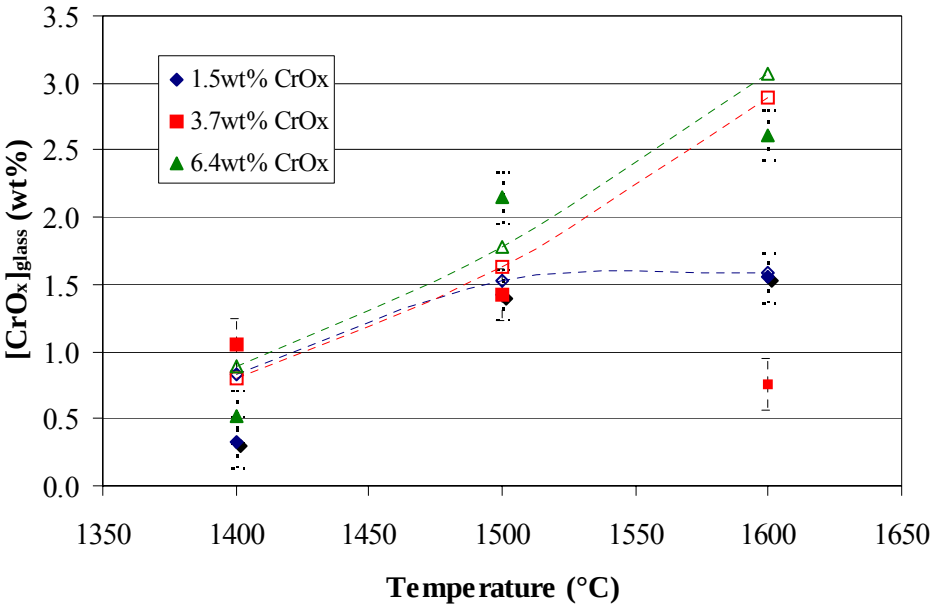

Figure 5.4: Variation of $[CrO_x]_{glass}$ with temperature at $CO_2/CO = 2$ and an average bulk FeO_x/MgO ratio of 1.1 (experimental values shown with solid markers and MPE-predicted values with open markers and dashed lines)

As expected, an increase in temperature resulted in an increase in CrO_x dissolved in the glass phase. Under moderately oxidizing conditions (CO_2/CO=2) and a bulk CrO_x content of 6.4 wt%, an increase in temperature from 1400°C to 1600°C caused $[CrO_x]_{glass}$ to increase from 0.5 to 2.1 wt%. The chromium oxide content of the glass phase increased from 0.3 to 1.5 wt% at a bulk CrO_x content of 1.5 wt% as the spinel phase dissolved above 1400°C.

The increase in $[CrO_x]_{glass}$ seems to be stronger at higher bulk CrO_x content. The slope of

the regression line at 6.4 wt% CrO_x is almost double that at 1.5 wt% CrO_x. In all cases the ratio $[CrO_x]_{glass}/[CrO_x]_{spinel}$ increased with temperature, indicating that partitioning of CrO_x into the glass phase is more favourable at higher temperature, as mentioned in the previous section.

At a CO_2/CO ratio of 10 (pO_2 between $2.7x10^{-7}$ and $2.1x10^{-5}$ atm) an increase in temperature from 1400°C to 1600°C was found to result in an average increase in $[CrO_x]_{glass}$ of only 0.6 wt%, this effect being insensitive to bulk CrO_x content.

The error associated with microprobe determinations of chromium oxide in the glass phase was estimated to be 0.2 wt%. Values predicted by the MPE model for conditions where crystalline phases were present agreed with experimental values to within 0.3 to 0.5 wt%.

In summary, an increase in temperature led to an increase in the solubility of chromium oxide in the glass phase. This favourable effect was found to be stronger at lower oxygen partial pressure and higher bulk CrO_x content. MPE-predicted values agree well with the broad trend of the experimental data.

5.2.2 The effect of bulk FeO_x/MgO ratio on the solubility of CrO_x in the glass phase

Figure 5.5 shows the variation of $[CrO_x]_{glass}$ with the bulk ratio of iron oxide to magnesia at $CO_2/CO=2$ in the gas phase and a constant bulk CrO_x level of approximately 1.5 wt%.

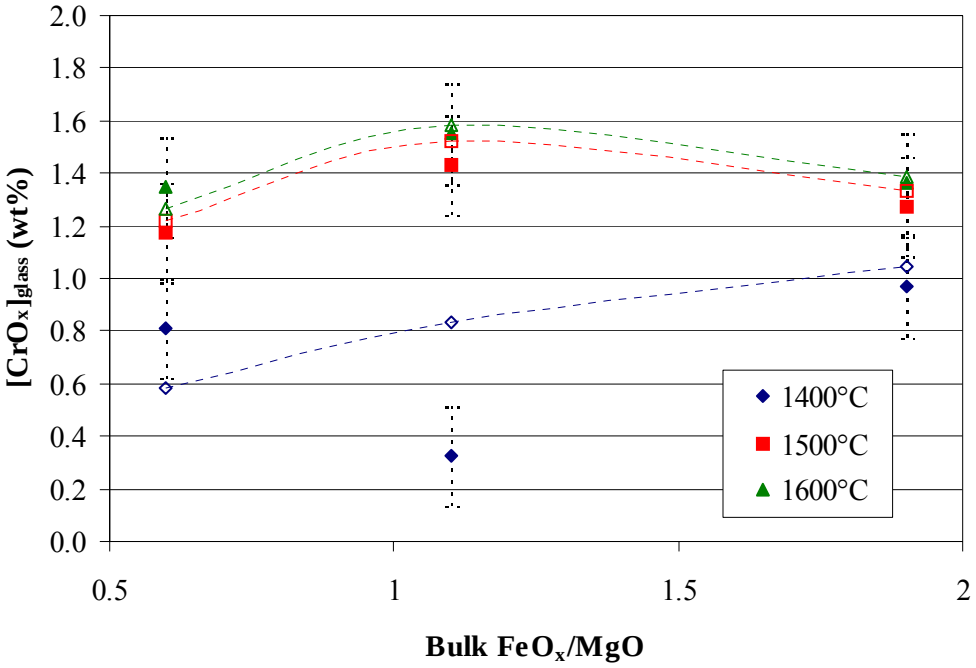

Figure 5.5: Variation of $[CrO_x]_{glass}$ with bulk FeO_x/MgO at $CO_2/CO=2$ and a bulk CrO_x content of 1.5 wt% (experimental values shown with solid markers and MPE-predicted values with open markers and dashed lines)

From Figure 5.5 it appears as though the solubility of CrO_x in the glass phase was not significantly affected by the ratio of total iron to magnesia in the bulk slag, when CO_2/CO and bulk CrO_x levels were constant. At 1600°C all slags with bulk chromium oxide contents of 1.5 wt% were above their liquidus temperatures and therefore, no changes in $[CrO_x]_{glass}$ were expected. At 1500°C the only crystalline phase observed was spinel at $FeO_x/MgO=0.6$. This data point is in excellent agreement with that predicted by the MPE model.

At 1400°C, olivine and spinel were present at FeO_x/MgO ratios of 0.6 and 1.1, while only spinel crystallised at $FeO_x/MgO=1.9$. An increase in the FeO_x/MgO ratio from 0.6 to 1.1 at saturation with olivine and spinel resulted in a decrease in the solubility of CrO_x in the glass phase. A further increase in FeO_x/MgO from 1.1 to 1.9 de-stabilized the olivine phase and led to an increase in chromium oxide solubility. Indications are that the substitution of iron for magnesium in the system stabilized the spinel phase relative to the

olivine phase.

At 1400°C and FeO_x/MgO ratios of 0.6 and 1.1 discrepancies were observed between experimental and predicted data. This may be attributed to the fact that the model predicted the presence of spinel, olivine and pyroxene at a ratio of 0.6 and the presence of spinel and pyroxene at a ratio of 1.1. At a ratio of 1.9, spinel was the only crystalline phase found both experimentally and through the model, and data points are in good agreement. The model does indicate that as the FeO_x/MgO ratio is increased the spinel phase is stabilised relative to other phases, in agreement with experimental observations.

5.2.3 The effect of bulk CrO_x content on the solubility of CrO_x in the glass phase

Figure 5.6 shows the variation of $[CrO_x]_{glass}$ with bulk CrO_x content at a constant CO_2/CO ratio of 2 and bulk FeO_x/MgO ratio of 1.1. The dashed line represents full dissolution of the added chromium oxide. On this line the bulk chromium oxide content is equal to $[CrO_x]_{glass}$ and no crystalline phases exist.

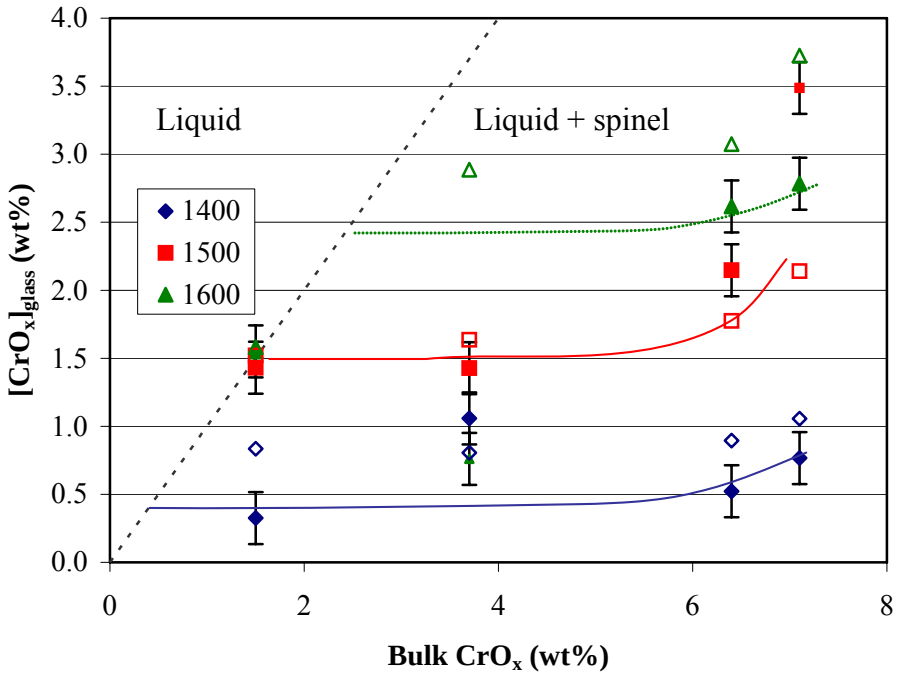

Figure 5.6: Variation of $[CrO_x]_{glass}$ with bulk CrO_x content at a bulk FeOx/MgO ratio of 1.1 and $CO_2/CO=2$ (trend lines are shown as a guide only)

Extrapolation of the 1400°C isotherm revealed that at this temperature the slag has the capacity to dissolve approximately 0.3 wt% CrO_x before any other phases will start to precipitate. Similarly at 1500°C, approximately 1.4 wt% CrO_x dissolved in the glass phase before precipitation of spinel. These observations also indicate that an increase in CrO_x content from approximately 0.3 to 1.4 wt% at a bulk FeO_x/MgO ratio of 1.1 resulted in an increase in liquidus temperature of 100°C.

Limited data suggest that the solubility of CrO_x in the glass phase could be as high as approximately 2.4 wt% at 1600°C and pO_2 of $8.3x10^{-7}$ atm ($CO_2/CO=2$).

At 1500°C good agreement was observed between experimental and predicted values. At both 1400°C and 1600°C the MPE model predicted solubilities to be on average 0.5 wt% higher than experimental values. The fact that the increase in solubility of chromium oxide is not linear with temperature may be due to the fact that the relative amount of spinel crystals decreases as temperature increases.

An observation worth mentioning with regards to spinel composition at 1400°C and constant oxygen partial pressure, was the fact that changes in iron oxide in spinel were negatively correlated with changes in chromium oxide in spinel with variations in the bulk chromium oxide content at 1400°C. This is shown in Figure 5.7.

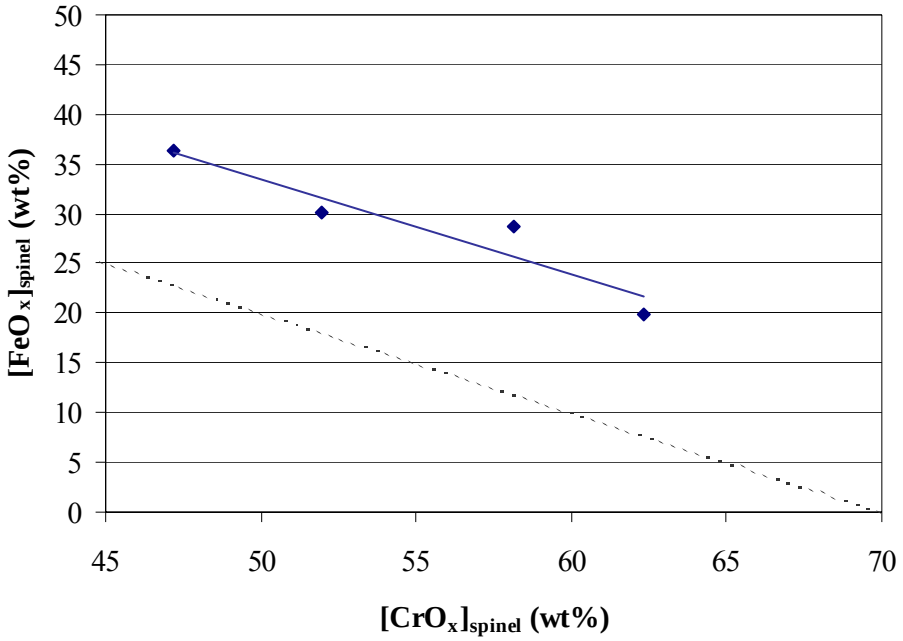

Figure 5.7: The variation of $[FeO_x]_{spinel}$ with $[CrO_x]_{spinel}$ at 1400° and a CO_2/CO ratio of 2 ($pO_2=1.1x10^{-8}$ atm)

Also shown in Figure 5.7 is the dashed line with a slope of -1. It is evident that the sum of $[FeO_x]_{spinel}$ and $[CrO_x]_{spinel}$ is constant, $[FeO_x]_{spinel}$ decreasing with an increase in bulk chromium oxide content. This is probably largely due to an exchange of Cr^{3+} for Fe^{3+} with increasing bulk CrO_x content. This is in accord with observations made by Musić *et al*. (1993) and Riboud and Muan (1964) on the easy exchange of Cr^{3+} and Fe^{3+} in crystalline phases in their studies of the Fe_2O_3-Cr_2O_3 solid solution.

5.2.4 The effect of pO_2 on the solubility of CrO_x in the glass phase

It is expected that a reduction in oxygen partial pressure would lead to an increase in CrO_x dissolved in the glass phase. As discussed earlier it is believed that the solubility of CrO_x in the glass phase increases at lower oxygen partial pressures due to an increase in the Cr^{2+}/Cr^{3+} ratio.

Figure 5.8 shows $[CrO_x]_{glass}$ as a function of oxygen partial pressure at 1500°C.

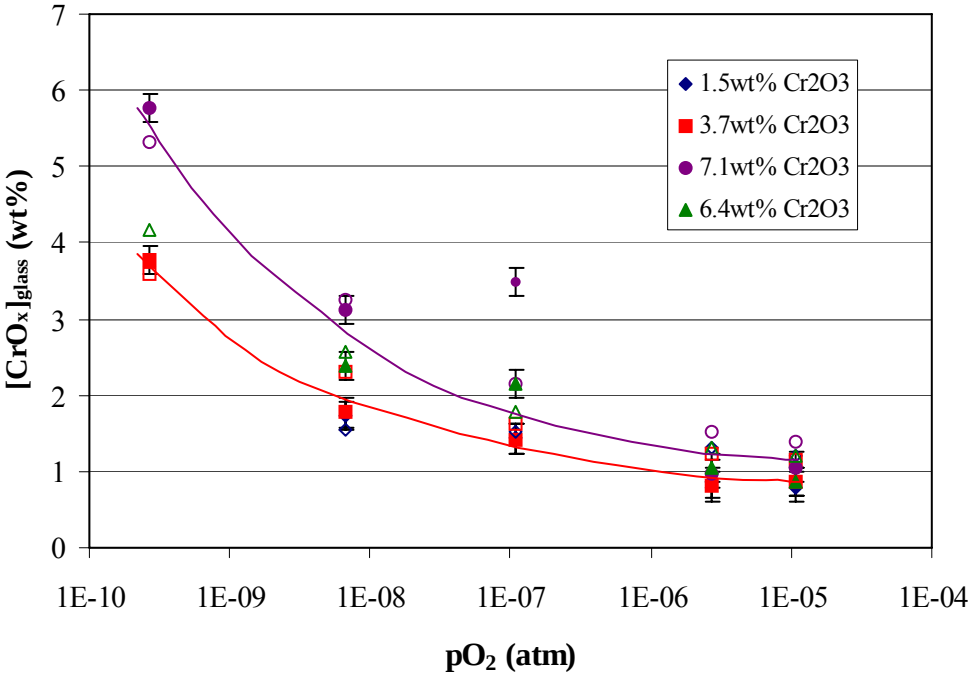

Figure 5.8: The variation of $[CrO_x]_{glass}$ with pO_2 at 1500°C and different bulk chromium oxide contents (lines drawn simply to guide the eyes)

As is evident form Figure 5.8, a decrease in oxygen partial pressure from 10^{-5} to $6.7x10^{-9}$ atm resulted in moderate increases in CrO_x solubility in the glass phase. At bulk CrO_x contents of 1.5 and 3.7 wt%, $[CrO_x]_{glass}$ increased from approximately 0.8 wt% to 1.8wt% (data points coincide). At a bulk CrO_x content of 6.4 wt%, $[CrO_x]_{glass}$

increased from 0.9 to 2.4wt% and at 7.1 wt% bulk CrO_x, $[CrO_x]_{glass}$ increased from 1.1 to 3.1 wt%.

A further decrease in pO_2, from 10^{-8} to approximately $2.7x10^{-10}$ atm, resulted in significant increases in $[CrO_x]_{glass}$. At a bulk CrO_x contents of 3.7 wt% the spinel phase became unstable and all CrO_x dissolved. At 7.1 wt% the solubility of CrO_x in the glass phase increased to 5.8wt%. This trend is in agreement with the results of Murck and Campbell (1986) who found the sharpest increases in the chromium content of the glass phase below oxygen partial pressures of approximately 10^{-8} atm at 1400°C.

According to observations made by Hanson and Jones (1998) the increase in chromium oxide in the glass phase in Fe-free systems is due to an increase in Cr^{2+} in the glass as the Cr^{2+}/Cr^{3+} ratio is influenced by the externally imposed oxygen partial pressure. Because of the fact that there is no reliable method of determining the Cr^{2+}/Cr^{3+} ratio in Fe-bearing systems, the effect of iron on the behaviour of chromium is poorly understood. However, the behaviour of chromium in spinel-saturated liquids was reported to be similar in Fe-free and Fe-bearing systems (Hanson and Jones, 1998).

At 1500°C and bulk CrO_x levels of 1.5 and 3.7 wt% the spinel phase dissolved completely at oxygen partial pressures below $1.1x10^{-7}$ atm, while at higher bulk CrO_x contents the spinel phase remained stable at oxygen partial pressures as low as $6.7x10^{-9}$ atm.

Predictions by the MPE model agree well with experimentally determined data. The discrepancies observed were between 0.1 and 0.5 wt%, while the uncertainty in microprobe determination of chromium oxide was estimated to be in the region of 0.12 wt%.

5.3 Application of the MPE model

As was shown in the previous section, data predicted by the MPE model showed good agreement with experimental data. Therefore, it was decided to run simulations using actual plant data under a number of conditions of temperature, oxygen partial pressure and basicity and qualitatively consider the effects thereof on certain key parameters.

For this purpose a feed composition was selected and converted to the oxides of the system investigated in this study. Copper, nickel, cobalt, sulphur and platinum group metals were excluded. The resultant composition (as weight percentages) is given in Table 5.1.

Table 5.1: Actual feed composition

MgO	**FeO_x***	**SiO_2**	**CaO**	**Al_2O_3**	**CrO_x***
20.4	20.5	49.3	3.1	3.6	3.1

* FeO_x expressed as Fe_2O_3 and CrO_x expressed as Cr_2O_3

The basicity of this slag, defined as $[\frac{MgO + CaO}{SiO_2}]$, is 0.48.

Three different values of basicity were selected. An addition of 10 wt% of CaO to the composition shown in Table 5.1 resulted in a basicity of 0.68 and in order to obtain a basicity of 0.80, an addition of 16 wt% of CaO was required.

5.3.1 The solubility of chromium oxide in the glass phase

The effect of oxygen partial pressure on the solubility of chromium oxide in the glass phase was simulated at temperatures between 1400°C and 1650°C and a basicity of 0.48.

Similar to experimental observations, as discussed in section 5.2.4, a decrease in oxygen

partial pressure resulted in an increase in $[CrO_x]_{glass}$, moreso at lower oxygen partial pressures. At constant oxygen partial pressure, the solubility of chromium oxide was seen to increase with temperature.

The effect of basicity, expressed as on $[CrO_x]_{glass}$ was simulated at a CO_2/CO ratio of 2 and temperatures between 1400 and 1700°C.

An increase in basicity at constant temperature leads to a decrease in the chromium oxide solubility in the liquid phase. At higher basicities, higher operating temperatures are required to maintain chromium oxide solubility.

Conditions favourable for the dissolution of chromium oxide into the glass phase are higher operating temperature, lower oxygen partial pressure and lower basicity.

5.3.2 Slag viscosity

A very useful feature of the MPE model is its ability to predict slag viscosities, taking into account the presence of suspended solid particles in the slag. An increase in temperature was found to cause a decrease in viscosity, obviously due to crystalline phases becoming less stable as temperature is increased. At constant temperature, viscosity was found to increase as oxygen partial pressure increases, this effect being less pronounced at higher operating temperature.

At constant temperature, slag viscosity was seen to decrease with increasing basicity. Once again this effect is less significant at higher temperature.

Conditions that favour lower slag viscosity are higher operating temperature, lower oxygen partial pressure and higher basicity.

Chapter 6

CONCLUSIONS

Chromium oxide was found to partition very strongly into the spinel phase. The highest distribution ratios ($[CrO_x]_{spinel}/[CrO_x]_{glass}$) were found at low temperatures, and high oxygen partial pressures and low bulk chromium oxide contents. The chromium oxide content of the spinel phase was found to vary between 45 and 70 wt%. Significant increases in chromium oxide in the glass phase were observed when $[CrO_x]_{spinel}$ approached its maximum value.

At 1400°C and an oxygen partial pressure of $1.1x10^{-8}$ atm ($CO_2/CO=2$), changes in bulk chromium oxide content caused iron oxide and chromium oxide in the spinel phase to vary in opposite directions with equal amounts on a mass basis. This is consistent with substitution of Fe^{3+} in the spinel phase with Cr^{3+} as bulk chromium oxide content increased.

The solubility of chromium oxide in the glass phase was found to increase with increasing temperature, decreasing oxygen partial pressure and decreasing basicity.

At a bulk FeO_x/MgO ratio of 1.1, a bulk chromium oxide content of 6.4 wt% and a CO_2/CO ratio of 2, the solubility of chromium oxide in the glass phase was found to increase from 0.5 to 2.6 wt% as temperature was increased from 1400°C to 1600°C. An increase in bulk CrO_x content of approximately 1 wt% was found to result in an increase of approximately 100°C in liquidus temperature over the temperature range investigated.

At 1500°C, a decrease in oxygen partial pressure from $1.1x10^{-5}$ and $1.1x10^{-7}$ atm, resulted in an increase in $[CrO_x]_{glass}$ from 0.9 to 1.8 wt% and from 1.1 to 3.1 wt% at bulk CrO_x contents of 3.7 and 6.4 wt%, respectively. A further decrease in oxygen partial pressure from $1.1x10^{-7}$ to $6.7x10^{-9}$ atm resulted in more pronounced increases

in chromium oxide solubility: from 1.8 to 3.7 wt% and 3.1 to 5.8 wt% at bulk CrO_x contents of 3.7 and 6.4 wt%, respectively.

Slag basicity was not varied experimentally, but predictions by the MPE model indicate that the solubility of chromium oxide in the glass phase decreases with increasing basicity at constant temperature. Slag viscosity was predicted to decrease with increasing basicity and decreasing oxygen partial pressure at constant temperature. Both of these effects became less significant as temperature was increased.

At a CO_2/CO ratio of 2 and a basicity of 0.48 the spinel phase was found to precipitate at temperatures up 1600°C, while at basicities of 0.68 and 0.80 the spinel phase was stable at temperatures as high as 1650°C. An increase in basicity thus resulted in the stabilisation of spinel.

In order to improve the tappability of slags and to minimise the entrainment of matte droplets in furnace slag, it is necessary to reduce the amount of solid phases present in melts and to reduce slag viscosity. These two parameters are closely related. Chromium oxide is a key structural component of the spinel phase (Hanson and Jones, 1998) and therefore this may be achieved by modifying furnace conditions such that higher chromium oxide solubilities are achieved, which in turn will limit the formation of spinel crystals in slags.

From the results obtained in this study, one or combinations of the following may be applied to increase the solubility of chromium oxide in molten slags:

- An increase in operating temperature.
- A decrease in chromium oxide content of feed material.
- A decrease in slag basicity.
- A decrease in oxygen partial pressure.

Higher operating temperatures may seem like an obvious solution to limit the formation of solid phases in furnace slags, but other effects need to be taken in to

consideration as well. In order to maintain higher operating temperatures, higher energy-to-feed ratios are required. Higher operating temperatures may have detrimental effects on the integrity of refractory materials in furnaces, or in more modern applications it may cause protective sidewall freeze-linings in furnaces to dissolve. Slag electrical conductivity also has an effect on operating temperature – higher slag conductivities make it difficult to achieve high operating temperatures.

The bulk chromium content of feed concentrates is governed by the ore being mined at the time and cannot be manipulated, except by dilution with low chromium oxide containing concentrates. The high chromium oxide contents of UG2 concentrates, especially those from open-cast mines, may thus be diluted using Merensky concentrates with lower chromium oxide contents. At this stage it is a viable option, but may become problematic in future as the Merensky reef becomes depleted and more of the UG2 reef is mined.

Slag basicity is dependent upon the lime, magnesia and silica contents of concentrates being smelted. The traditional view is that the addition of lime to furnaces, thus increasing slag basicity, decreases liquidus temperatures. Although this may be true for certain applications such as the smelting of Merensky concentrates, data obtained from literature and using the MPE model indicate that lower basicities are favourable to dissolve chromium oxide into the glass phase and to destabilise the spinel phase. This is also in agreement with findings from the literature reviewed. It would be advisable to limit lime additions to as low values as possible. Where CaO is necessary in slags for other reasons, such as to control electrical conductivity, lime additions should be linked to feed concentrate chemistry.

A decrease in oxygen partial pressure is a feasible option to achieve higher chromium oxide solubility and to destabilise spinel crystals. Plant trials have in fact shown that reductants such as carbon or ferrosilicon may be used successfully to reduce Cr^{3+} to Cr^{2+} (Nell, 1998). An undesirable side effect to take into account is that iron may also be reduced to form a primary alloy phase. Such a phase would collect in furnaces and scavenge platinum group metals, thus resulting in decreased recoveries.

It is clear that combinations of the above mentioned factors need to be evaluated and optimised. This could be achieved by carefully monitoring actual furnace operating conditions such as tapping temperatures, slag and matte assays and compositions of the glass and crystalline phases in slags at different reductant additions, lime additions and operating temperatures over an extended period of time. Structured records of such data can be critically assessed and optimum operating conditions determined.

The MPE model is a valuable tool for predicting furnace conditions at different settings of temperature and reductant and lime additions, amongst others. This model can be used to assist in determining which direction changes in furnace setpoints should be made in order to achieve optimum operating conditions.

REFERENCES

Alper A.M, R.N. McNally, R.C. Doman and F.G. Keihn, **Phase Equilibria in the System MgO-$MgCr_2O_4$**, *Journal of the American Ceramic Society*, Vol. 47(4), pp. 30-34, 1964

Amethyst Galleries' Mineral Gallery, **The Mineral Olivine**, *http://mineral.galleries.com/minerals/silicate/olivine/olivine.htm*, 1997

Arculus R.J, M.E. Gillberg and E.F. Osborn, **The System MgO-Iron Oxide-Cr_2O_3-SiO_2: Phase Relations among Olivine, Pyroxene, Silica and Spinel in Air at 1 atm**, *Carnegie Institution of Washington Year Book 73*, pp. 317-322, 1974

Bowen N.L. and J.F. Schairer, **The System MgO-FeO-SiO_2**, *American Journal of Science*, Vol. 29, pp. 151-217, 1935

Chen C, S. Jahanshahi, M. Somerville, S. Sun, T. Tran, D. Xie and L. Zhang, **Final Report – AMIRA P479A Project on Slags, Refractories & Processes**, *Confidential CSIRO Report DMR-2373*, January 2004

Corrans I.J., C.F. Brugman and P.W. Overbeek, **Recovery of Platinum-Group Metals from Ore of the UG-2 Reef in the Bushveld Complex**, *South African Institute of Mining and Metallury*, Vol. 2, pp. 629-634, 1982

Coulson J.M. and Richardson J.F, **Coulson and Richardson's Chemical Engineering Volume 2**, 4th Edition, *Butterworth-Heinemann*, 1996

De Villiers J.P.R. and A. Muan, **Liquidus-Solidus Phase Relations in the System CaO-CrO-Cr_2O_3-SiO_2**, *Journal of the American Ceramic Society*, Vol. 75(6), pp. 1333-1341, 1992

Eguchi M, R. Uchida and M. Chiba, **Phase Equilibria of the FeO-Cr_2O_3-SiO_2 System in Contact with Metallic Iron**, *Bulletin of the Research Institute of Mineral Dressing and Metallurgy, Tohoku University*, Vol. 33(1), 1977

El-Shahat R.M. and J. White, **Phase-equilibrium Relationships in Spinel-Silicate Systems, III. The Ternary System $MgAl_2O_4$-$MgFe_2O_4$-Ca_2SiO_4, the Quaternary System $MgAl_2O_4$-$MgFe_2O_4$-$MgCr_2O_4$-Ca_2SiO_4, and IV. The Pseudo-ternary System $MgAl_2O_4$-$MgCr_2O_4$-$Ca_3MgSi_2O_8$**, *Transactions of the British Ceramic Society*, September, 1966

Fisler D.K, A.J. Mackwell, S. Petch, **Grain boundary diffusion in enstatite**, *Phys Chem Minerals*, Vol. 24, pp. 264-273, 1997

Gilchrist J.D, **Extraction Metallurgy**, 2nd Edition, *Pergamon Press*

Hanson B. and J.H. Jones, **The systematics of Cr^{3+} and Cr^{2+} partitioning between olivine and liquid in the presence of spinel**, *American Mineralogist*, Vol. 83, pp. 669-684, 1998

Hino M, K. Higuchi, T. Nagasaka and S. Ban-Ya, **Phase Equilibria and Thermodynamics of $FeO{\cdot}Cr_2O_3$-$MgO{\cdot}Cr_2O_3$-$MgO{\cdot}Al_2O_3$ Spinel Structure Solid Solution Saturated with $(Cr,Al)_2O_3$**, *ISIJ International*, Vol. 35(7), pp. 851-858, 1995

Jacob K.T, A. Petric, G.M. Kale and G.N.K. Iyengar, **Phase Relations between Al_2O_3-Cr_2O_3 and $FeAl_2O_4$-$FeCr_2O_4$ Solid Solutions at 1823K**, *Ceramics International*, Vol. 13, pp. 123-129, 1987

Jahanshahi S, S. Sun and L. Zhang, **Recent developments in physico-chemical characterisation and modelling of ferroalloy slag systems**, *Proceeding of the 10th INFACON Conference, Cape Town, South Africa*, pp. 316-332, February 2004

Jahanshahi S. and S. Wright, **Redox Equilibria in Al_2O_3-CaO-FeO_x-SiO_2 and Al_2O_3-CaO-FeO_x-MgO-SiO_2 Slags**, *ISIJ International*, Vol. 33(1), pp. 195-203, 1993

Jakeš P. and A.M. Reid, **Chromium partitioning between olivine and pyroxene and the redox state of lunar rocks**, *Abstracts of papers submitted to the Fifth Lunar Science Conference*, p. 381, 1974

Jones R. T, **Slag Chemistry**, *wwwscience.murdoch.edu.au/teach/m358/slagchem.pdf*

Keith M.L, **Phase Equilibria in the System MgO-Cr_2O_3-SiO_2**, *Journal of the American Ceramic Society*, Vol. 37(10), pp. 490-496, 1954

Kim H.G. and H.Y. Sohn, **Effects of CaO, Al_2O_3 and MgO Additions on the Copper Solubility, Ferric/Ferrous Ratio and Minor-Element Behaviour of Iron-Silicate Slags**, *Metallurgical and Materials Transactions B*, Vol. 29B, pp. 583-590, 1998

Kongoli F. and A. Yazawa, **Liquidus surface of FeO-Fe_2O_3-SiO_2-CaO slag containing Al_2O_3, MgO and Cu_2O at various oxygen partial pressures**, *FLOGEN Technologies (http://www.flogen.com)*, 2000

Liddell K.S., L.B. McRae and R.C. Dunne, **Process Routes for the Beneficiation of Noble Metals from Merensky and UG2 Ores**, Mintek Review No. 4, 1986

Liu S, R.J. Fruehan, A. Morales and B. Ozturk, **Measurement of FeO Activity and Solubility of MgO in Smelting Slags**, *Metallurgical and Materials Transactions B*, Vol. 32B, pp. 31-36, 2001

Morita K, A. Inoue, N. Takayama and N. Sano, **The Solubility of $MgO{\cdot}Cr_2O_3$ in MgO-Al_2O_3-SiO_2-CaO Slag at 1600°C under Reducing Conditions**, *Tetsu-to-Hagane*, Vol. 74(6), pp. 999-1005, 1988

Morita K, T. Shibuya and N. Sano, **The Solubility of Chromite in MgO-Al_2O_3-SiO_2-CaO Melts at 1600°C in Air**, *Tetsu-to-Hagane*, Vol. 74(4), pp. 42-49, 1988

Muan A. And E.F. Osborn, **Phase Equilibria at Liquidus Temperatures in the System MgO-FeO-Fe_2O_3-SiO_2**, *Journal of the American Ceramic Society*, Vol. 39(4), pp. 121-140, 1956

Muan A. and S. Sõmiya, **Phase Equilibria in the System Iron Oxide-Cr_2O_3-SiO_2 in Air**, *Journal of the American Ceramic Society*, Vol. 43(10), pp. 531-542

Murck B.W. and I.H. Campbell, **The effects of temperature, oxygen fugacity and melt composition on the behaviour of chromium in basic and ultrabasic melts**, *Geochimica et Cosmochimica Acta*, Vol. 50, pp. 1871-1887, 1986

Musić S, S. Popović and M. Ristić, **Chemical and structural properties of the system Fe_2O_3-Cr_2O_3**, *Journal of Materials Science*, Vol. 28, pp. 632-638, 1993

Nafziger R.H. and A. Muan, **Equilibrium Phase Compositions and Thermodynamic Properties of Olivines and Pyroxenes in the System MgO-"FeO"-SiO_2**, *The American Mineralogist*, Vol. 52, pp. 1364-1385, September-October 1967

Nell J. and J.P.R. de Villiers, **T-P_{O2} Topologic Analysis of Phase Relations in the System CaO-CrO-Cr_2O_3-SiO_2**, *Journal of the American Ceramic Society*, Vol. 76(9), pp. 2193-2200, 1993

Nell J, D. Meyer, T. Goff, M. Rennie and N. Bartie, **Matte-smelting under slightly reducing conditions: A plant campaign**, *Mintek Confidential Communication C2761M*, 1998

Parker R.H, **An Introduction to Chemical Metallurgy**, 2nd Edition, *Pergamon Press*, 1983

Pathy R.V. and R.G. Ward, **Distribution of chromium between liquid iron and simple synthetic slags**, *Journal of The Iron and Steel Institute*, December, pp. 995-1001, 1964

Pei W. and O. Wijk, **Experimental study on the activity of chromium oxide in the CaO-SiO_2-Al_2O_3-MgO_{sat}-CrO_x slag**, *Scandinavian Journal of Metallurgy*, Vol. 23, pp. 228-235, 1994

Perry R.H. and D. Green, **Perry's Chemical Engineers' Handbook**, 6th Edition, *McGraw-Hill Book Company*, 1984

Pretorius E.B, R. Snellgrove and A. Muan, **Oxidation State of Chromium in CaO-Al_2O_3-CrO_x-SiO_2 Melts under Strongly Reducing Conditions at 1500°C**, *Journal of the American Ceramic Society*, Vol. 75(6), pp. 1378-1381, 1992

Pretorius E.B. and A. Muan, **Activity-Composition Relations of Chromium Oxide in Silicate Melts at 1500°C under Strongly Reducing Conditions**, *Journal of the American Ceramic Society*, Vol. 75(6), pp. 1364-1377, 1992

Rait R, S. Jahanshahi and S. Sun, **The effect of Chromium Oxide on the Phase Relations in the CaO-MgO-Al_2O_3-SiO_2-FeO_x System**, *Molten Slags, Fluxes and Salts '97 Conference*, pp. 407-412, 1997

Rankin W.J. and A.K. Biswas, **Oxidation states of chromium in slag and chromium distribution in slag-metal systems at 1600°C**, *Institution of Mining and Metallurgy, Section C*, March, pp. C60-C70, 1978

Rankin W.J. and A.K. Biswas, **The behaviour of chromium in reduced slag-metal systems**, *Arch. Eisenhüttenwes.*, Vol. 50(1), pp. 7-11, 1979

Riboud P.V. and A. Muan, **Effect of Cr_2O_3 on Melting Relations of Iron Oxide at Low Oxygen Pressures**, *Transactions of the Metallurgical Society of AIME*, Vol. 230, pp. 88-90, February 1964

Roeder P.L. and E.F. Osborn, **Experimental Data for the System MgO-FeO-Fe_2O_3-$CaAl_2Si_2O_8$-SiO_2 and their Petrologic Implications**, *American Journal of Science*, Vol. 264, pp. 428-480, 1966

Roscoe, R, *British Journal of Applied Physics*, Vol. 3, pp. 267-269, 1952

Sarkar R, S.K. Das and G. Banerjee, **Effect of addition of Cr_2O_3 on the properties of reaction sintered MgO-Al_2O_3 spinels**, *Journal of the European Ceramic Society*, Vol. 22, pp. 1243-1250, 2002

Schwessinger T. and A. Muan, **Spinel-Silicate Equilibria in the System MgO-FeO-Fe_2O_3-Cr_2O_3-SiO_2**, *Journal of the American Ceramic Society*, Vol. 75(6), pp. 1390-98, 1992

Shim J. and S. Ban-Ya, **The Solubility of Magnesia and Ferric-Ferrous Equilibrium in Liquid Fe_tO-SiO_2-CaO-MgO Slags**, *Tetsu-to-Hagane*, Vol. 67(10), 1981

Speidel D.H. and E.F. Osborn, **Element distribution among coexisting phases in the system MgO-FeO-Fe_2O_3-SiO_2 as a function of temperature and oxygen fugacity**, *The American Mineralogist*, Vol. 52, pp. 1139-1152, July-August 1967

Speidel D.H. and R.H. Nafziger, **P-T-f_{O2} relations in the system Fe-O-MgO-SiO_2**, *American Journal of Science*, Vol. 266, pp. 361-379, May 1968

Stubican V.S. and C. Greskovich, **Trivalent and divalent chromium ions in spinels**, *Geochimica et Cosmochimica Acta*, Vol. 39, pp. 875-881, 1975

Taylor J.R. and A.T. Dinsdale, **A Thermodynamic Assessment of the Cr-Fe-O System**, *Z. Metallkd*, Vol. 84(5), pp. 335-345, 1993

Toker N.Y, L.S. Darken and A. Muan, **Phase Relations and Thermodynamics of the System Fe-Cr-O in the Temperature Range of 1600°C to 1825°C (1873 to 2098K) under Strongly Reducing Conditions**, *Metallurgical Transactions B*, Vol. 22B, pp. 689-703, 1991

Ulmer G.C, **High Temperature Oxides Chapter 6: Chromite Spinels**, *Academic Press*, 1970

Ulmer G.C. and W.B. White, **Existence of Chromous Ion in the Spinel Solid Solution Series $FeCr_2O_4$-$MgCr_2O_4$**, *Journal of the American Ceramic Society*, Vol. 49(1), pp. 50-51, 1966

Verein Deutscher Eisenhuttenleute, **Slag Atlas**, 2nd Edition, *Verlag Stahleisen, Dusseldorf*, 1995

Weisstein E, **Eric Weisstein's World of Science**, *http://scienceworld.wolfram.com/*, 2004

Wilde W.T. and W.J. Rees, **The Ternary System MgO-Al_2O_3-Cr_2O_3**, *Transactions of the British Ceramic Society*, Vol. 42(123), pp. 123-155, 1943

Wright S, L. Zhang, S. Sun, S. Jahanshahi, **Viscosity of a CaO-MgO-Al_2O_3-SiO_2 melt containing spinel particles at 1646K**, *Metallurgical and Materials Transactions B*, Vol. 31B, February, pp. 97-109, 2000

Xiao Y. and L. Holappa, **Determination of Activities in Slags Containing Chromium Oxides**, *ISIJ International*, Vol. 33(1), pp. 66-74, 1993

Yang L. and G.R. Belton, **Iron Redox Equilibria in CaO-Al_2O_3-SiO_2 and MgO-CaO-Al_2O_3-SiO_2 Slags**, *Metallurgical and Materials Transactions B*, Vol. 29B, pp. 837-845, 1998

Zao B, E. Jak and P.C. Hayes, **The Effect of MgO on Liquidus Temperatures of Fayalite Slags**, *Metallurgical and Materials Transactions B*, Vol. 30B, pp. 1017-1026, 1999

Zhang L, S. Jahanshahi, S. Sun, M. Lim, B. Bourke, S. Wright and M. Somerville, **Development and Applications of Models for Pyrometallurgical Processes**, *Material Forum*, Vol. 25, pp. 136-153, 2001

Zhang L, S. Jahanshahi, S. Sun, M. Lim, B. Bourke, S. Wright and M. Somerville, **CSIRO's Multiphase Reaction Models and Their Industrial Applications**, *Journal of Metals*, pp. 51-56, November 2002

APPENDIX A

Calculation of CO_2/CO ratio for the required oxygen partial pressure

The gas-phase reaction relevant to this calculation is the following:

$$\mathbf{CO + ½O_2 \leftrightarrow CO_2}$$

for which $\mathbf{\Delta G°_{rxn} = -67\,500 + 20.75 \times T}$ calories

From thermodynamics: $\mathbf{\Delta G = - RT \ln K}$ where R = 1.987 cal·mol^{-1}·K^{-1}

and $K = \dfrac{pCO_2}{pCO.pO_2^{1/2}}$

Thus:

$$\mathbf{-67\,500 + 20.75 \cdot T = - R\,T \ln K}$$

$$\mathbf{K} = e^{\frac{-67500+20.75T}{-RT}}$$

$$\frac{pCO_2}{pCO} = pO_2^{1/2} \cdot e^{\frac{-67500+20.75T}{-RT}}$$

For any required combination of temperature and oxygen partial pressure, the required ratio of CO_2 to CO can be calculated using the above formula.

Example calculation:

For $pO_2 = 10^{-8}$ atm and

T = 1500°C

$$\frac{pCO_2}{pCO} = (10^{-8})^{1/2} \cdot e^{\frac{-67500+20.75(1500+273.15)}{-(1.987)(1500+273.15)}}$$

$$= 0.61$$

Thus, in order to obtain an oxygen partial pressure of 10^{-8} atm at 1500°C, a CO_2/CO ratio of 0.61 is required.

APPENDIX B

Calibration of equipment

1. Thermocouples

Thermocouples (B-type) were calibrated against the melting point of copper (1083°C, Perry and Green, 1984). High purity electrical copper wire was cut into small pieces and melted in a graphite crucible to just below 1120°C. A photograph of the copper wire and graphite crucible is shown in Figure B1.

Figure B1: Graphite crucible and copper wire

The graphite crucible was manufactured such that a thermocouple could be inserted from the bottom, allowing the thermocouple to act as a pedestal for the crucible. The

thermocouple-crucible arrangement was inserted from the bottom of the furnace tube and secured into place in the hot zone.

After holding the copper at 1118°C for approximately one hour, power to the furnace was switched off and temperature measurements made at intervals of 30 seconds. An example cooling curve obtained in this manner is shown in Figure B2.

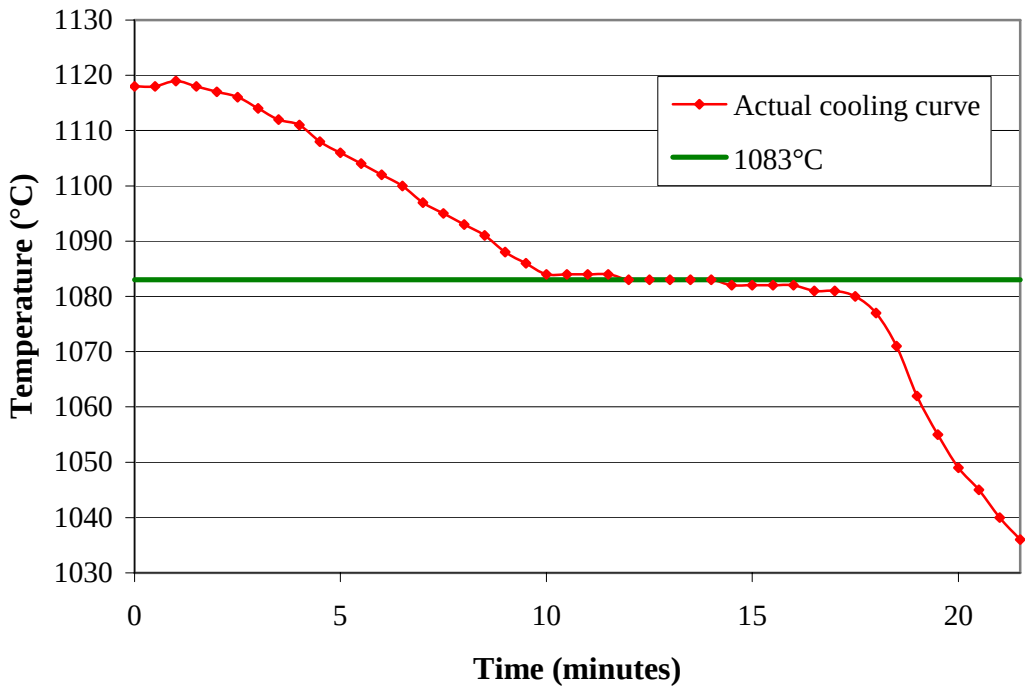

Figure B2: Copper cooling curve for thermocouple calibration

As can be seen from Figure B2, the temperature stabilised at 1084°C for 2 minutes, 1083°C for 2.5 minutes and 1082°C for 2 minutes before starting to cool down further. The fact that the temperature remained constant indicated the change from the liquid state to the solid state.

It is clear that temperatures were measured accurately and no corrections to thermocouple reading were required.

2. Gas flow controllers

Gas flow controllers were calibrated by measuring the flowrates of individual gases at different controller setpoints. This was carried out by connecting the gas outlet to a burette containing a small amount of liquid soap. The velocity of a soap bubble moving through the burette was converted to volume flow using the known volume of the burette.

Different sizes of flow controllers were available depending on the flowrate required for each gas. The total gas flow through the furnace tube was maintained at between 800 and 1000 cm^3/min during experiments. For experiments which required low CO_2/CO ratios, a lower volume controller was used for CO_2. Figure B3 shows calibrations curves for CO_2 with two different flow controllers as well as for CO.

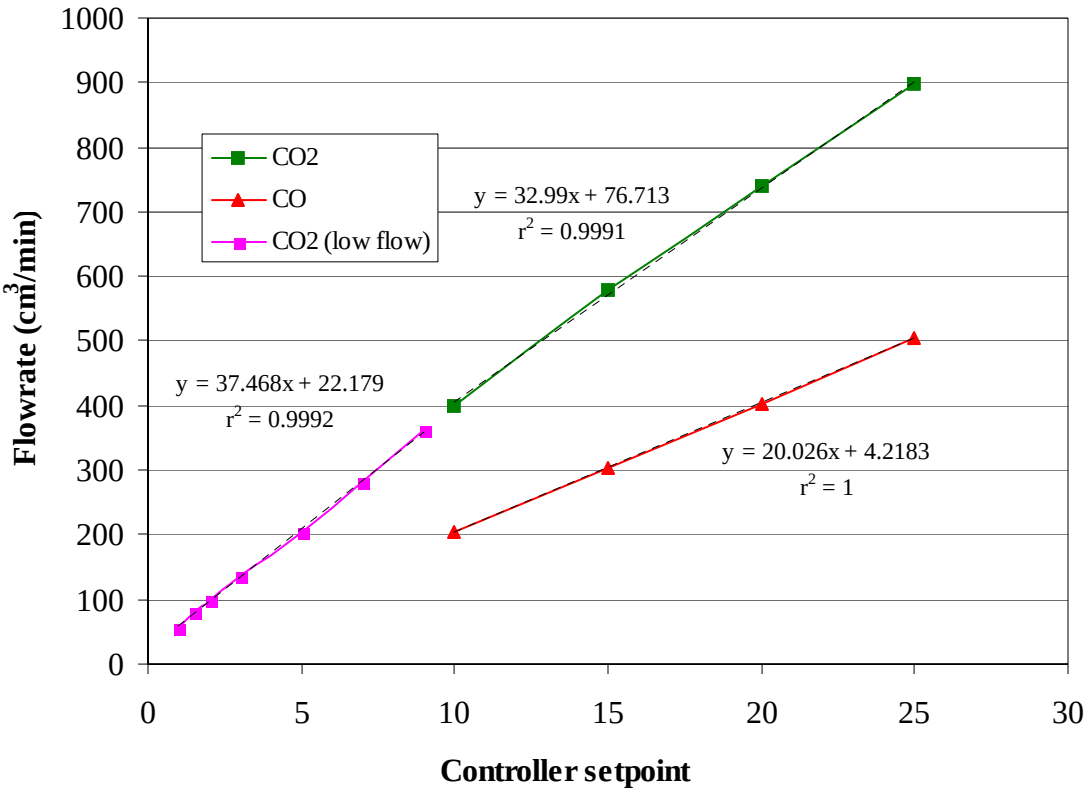

Figure B3: Gas flow calibration for CO and CO_2

As can be seen from Figure B3 calibration curves were linear in all cases. Data were found to be repeatable with increasing and decreasing controller setpoints. In order to achieve the desired ratios of CO_2 to CO in the gas phase, the appropriate controller setpoints were determined from flowrates using plots similar to the above.

3. Hot zone of the tube furnace

The hot zone was determined by measuring temperatures at different depths in the furnace tube. Figure B4 shows the measurements obtained for a heating element setpoint of 950°C.

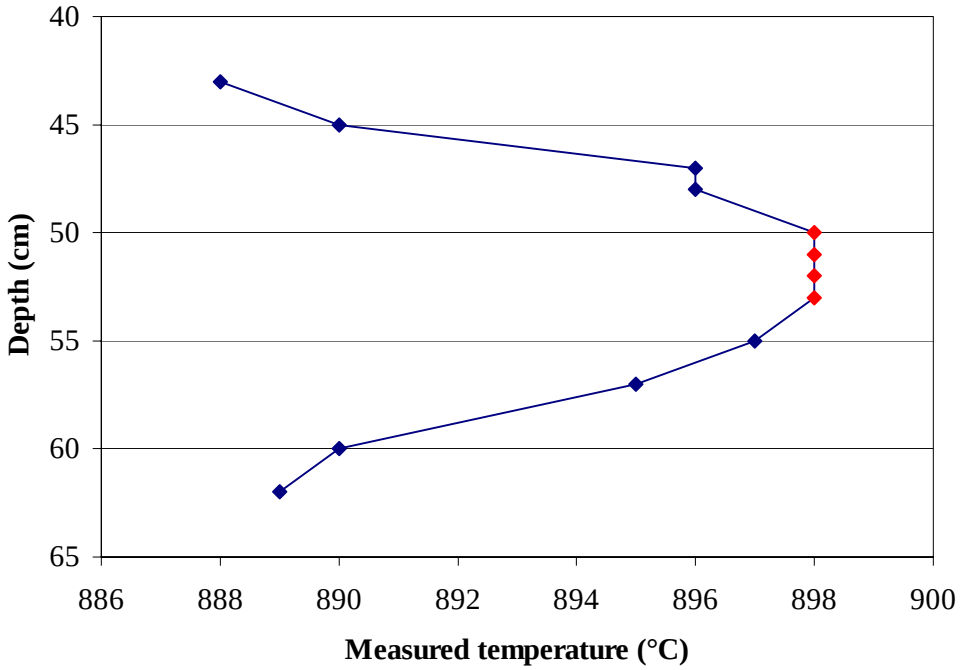

Figure B4: Temperature measurements to determine furnace hot zone

It can be seen clearly that the hot zone was located a depth of between 50 and 53 cm, as measured from the top of the upper end-cap.

4. Preparation of wüstite

As described in Chapter 3, wüstite (FeO) was prepared by reducing pure hematite (Fe_2O_3) at 850°C for 48 hours under an atmosphere with a CO_2/CO ratio of 1.5. Hematite powder was made into small pellets and held in a "wüstite cage" made of stainless steel gauze. The purpose of using gauze was to allow efficient contact between the hematite and the reducing gas phase. A photograph of this container is shown in Figure B5.

Figure B5: "Wüstite cage" for reduction of Fe_2O_3 to FeO

Whether sufficient reduction had taken place was confirmed by means of X-ray Diffraction (XRD) of a hand-ground sample. An example of the spectra obtained is shown in Figure B6.

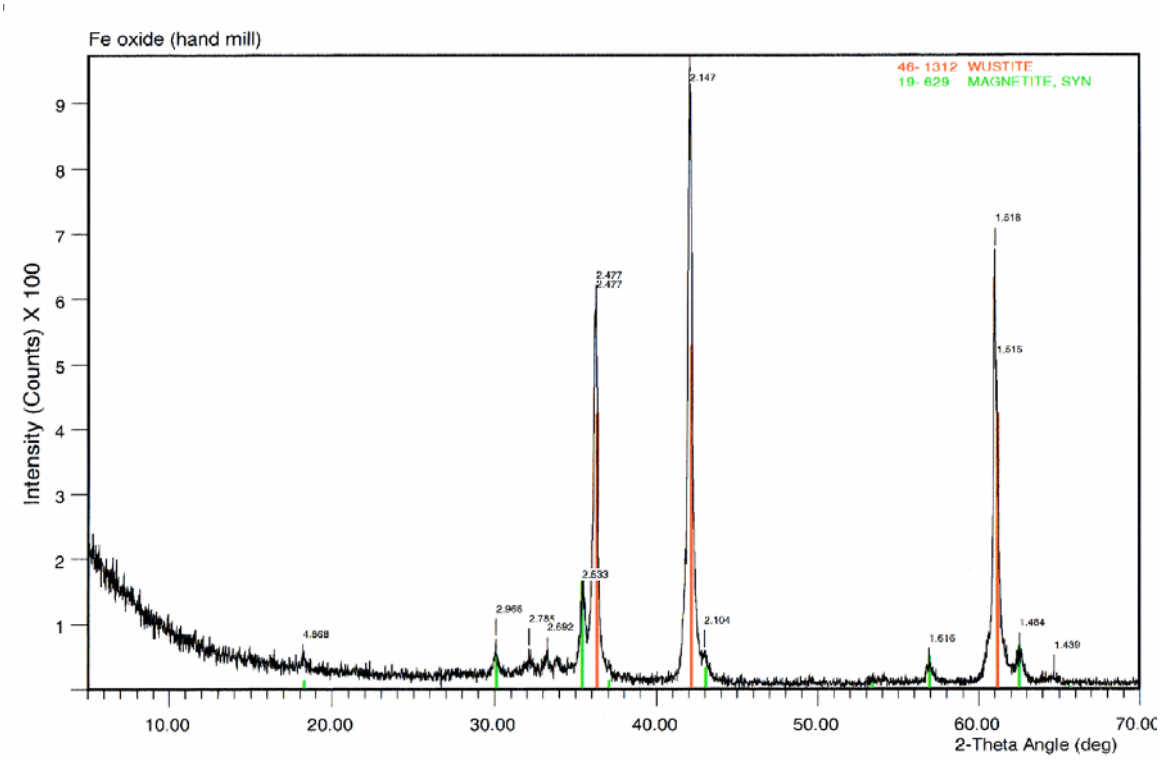

Figure B6: XRD analysis of iron oxide

Figure B6 shows the peaks for wüstite (FeO) as well as magnetite (Fe_3O_4). The XRD results indicate no hematite but that a small residue of unconverted iron oxide remained in the form of magnetite.

APPENDIX C

Photographs of the experimental setup

Figure C1: Vertical tube furnace

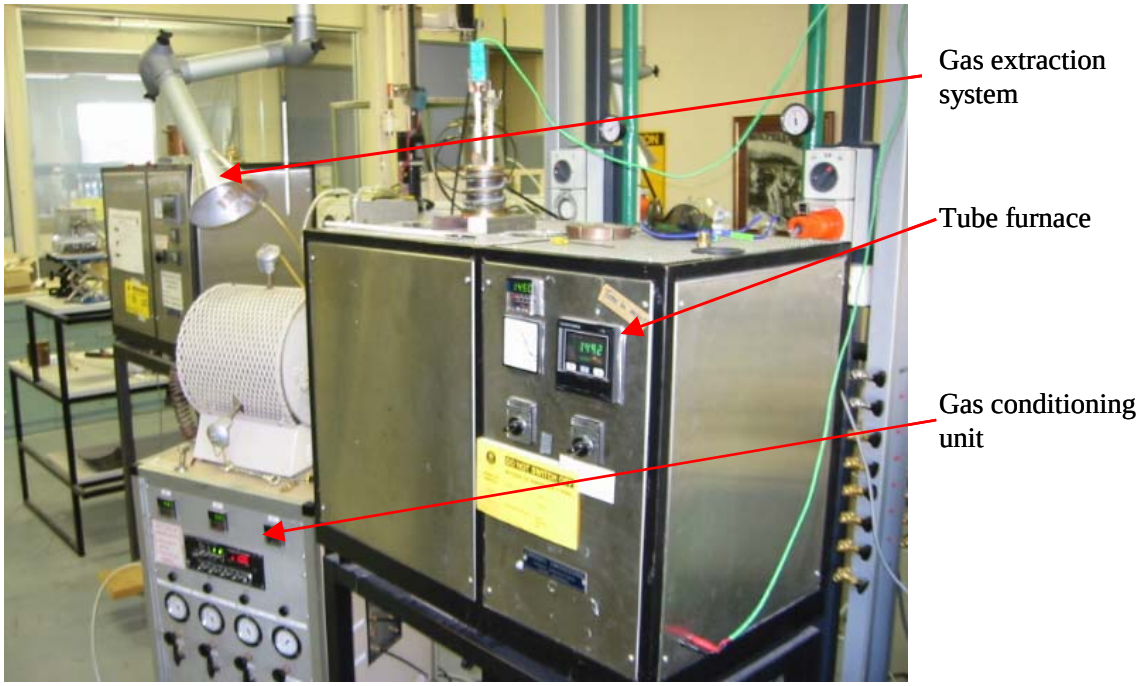

Figure C2: Tube furnace with gas treatment and extraction systems

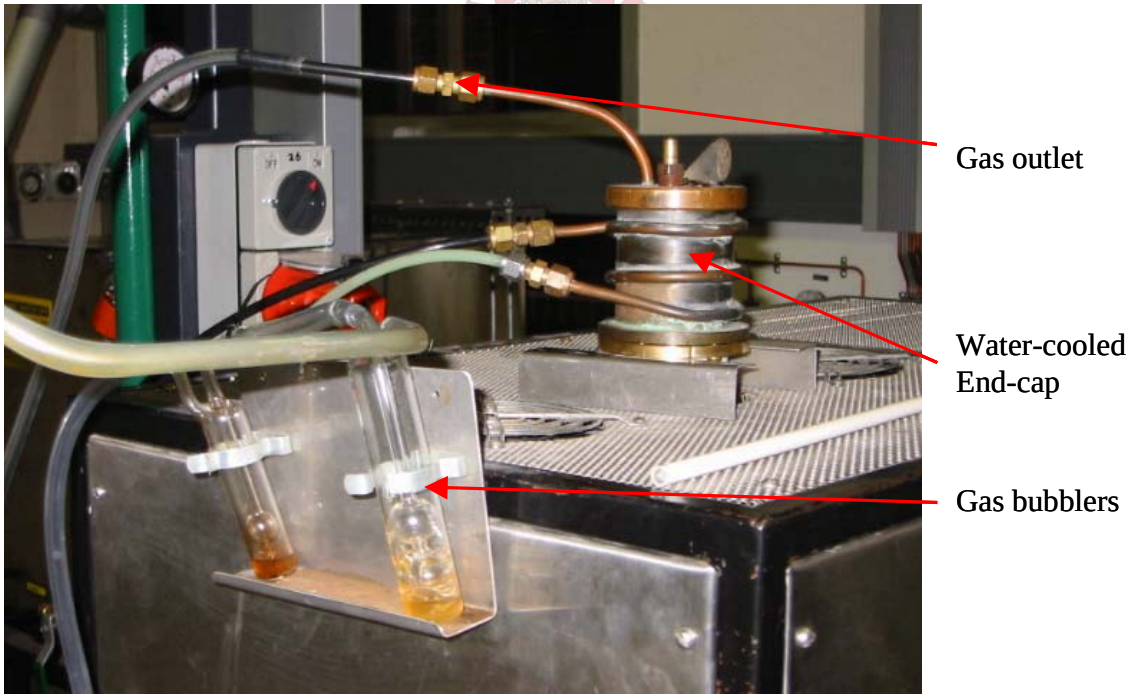

Figure C3: The use of bubblers to monitor the gas seal

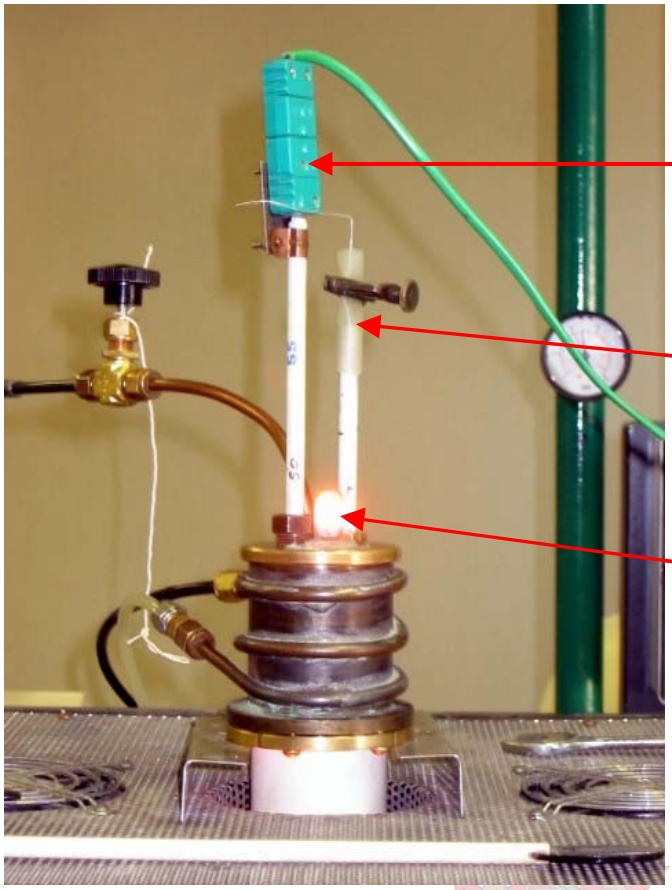

Figure C4: Platinum wire in alumina sheath and prism view of hot zone

Figure C5: Master slag preparation in MgO crucible

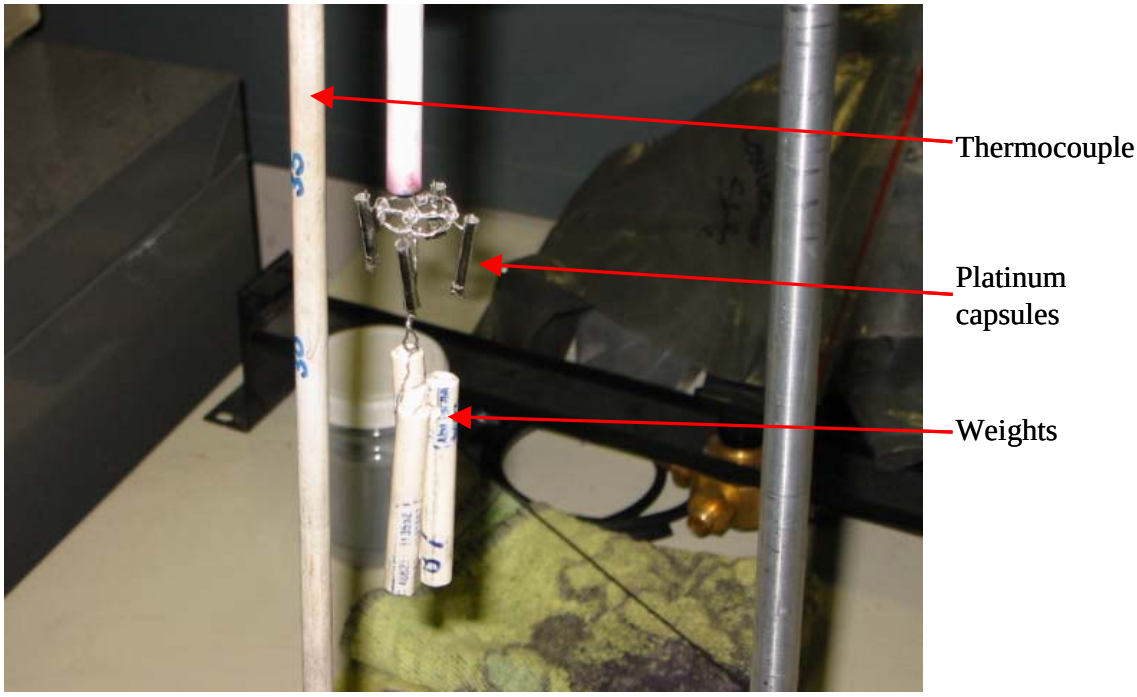

Figure C6: Platinum capsule arrangement

APPENDIX D

Photomicrographs

Figure D1 shows a micrograph of slag obtained by equilibrating master slag 2 for 46 hours at 1400°C and a CO_2/CO ratio of 2 ($pO_2=1.1x10^{-8}$ atm). The crystalline phases identified were spinel and olivine. Olivine crystals appeared to be larger than 200µm in diameter while spinel crystals were significantly smaller.

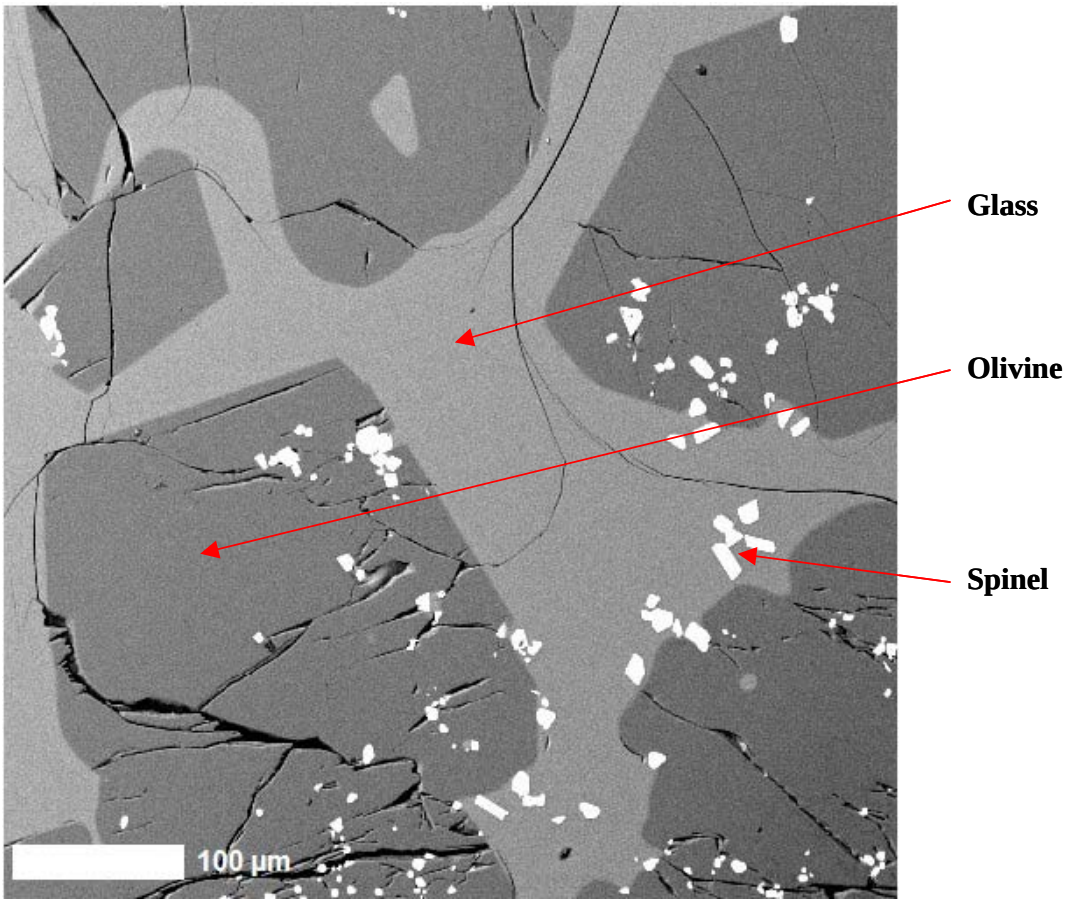

Figure D1: Sample of slag 2 equilibrated for 46 hours at 1400°C and a CO_2/CO ratio of 2

Figure D2 shows a similar micrograph of master slag 1, quenched after 24 hours of reaction from 1400°C and a CO_2/CO ratio of 2 (pO_2=1.1x10^{-8} atm). In this case olivine crystals were significantly smaller than those shown in Figure D1, while spinel crystals were similar in size.

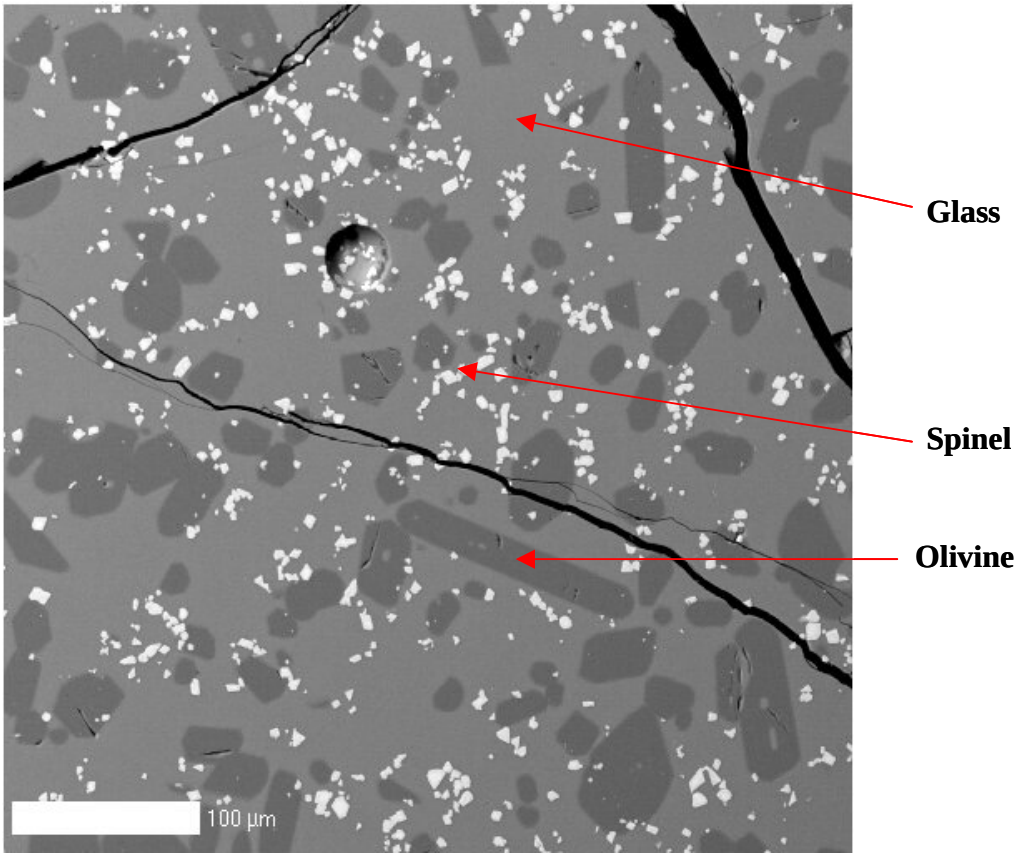

Figure D2: Sample of slag 1 equilibrated for 24 hours at 1400°C and a CO_2/CO ratio of 2

Figure D3 shows a phase map generated using CSIRO's Chimage® software package. An area of 1mm by 1mm was selected and analysed by microprobe in small steps. The resulting point analyses were processed and crystalline phases identified as an iron-magnesium silicate phase (olivine) and a spinel phase.

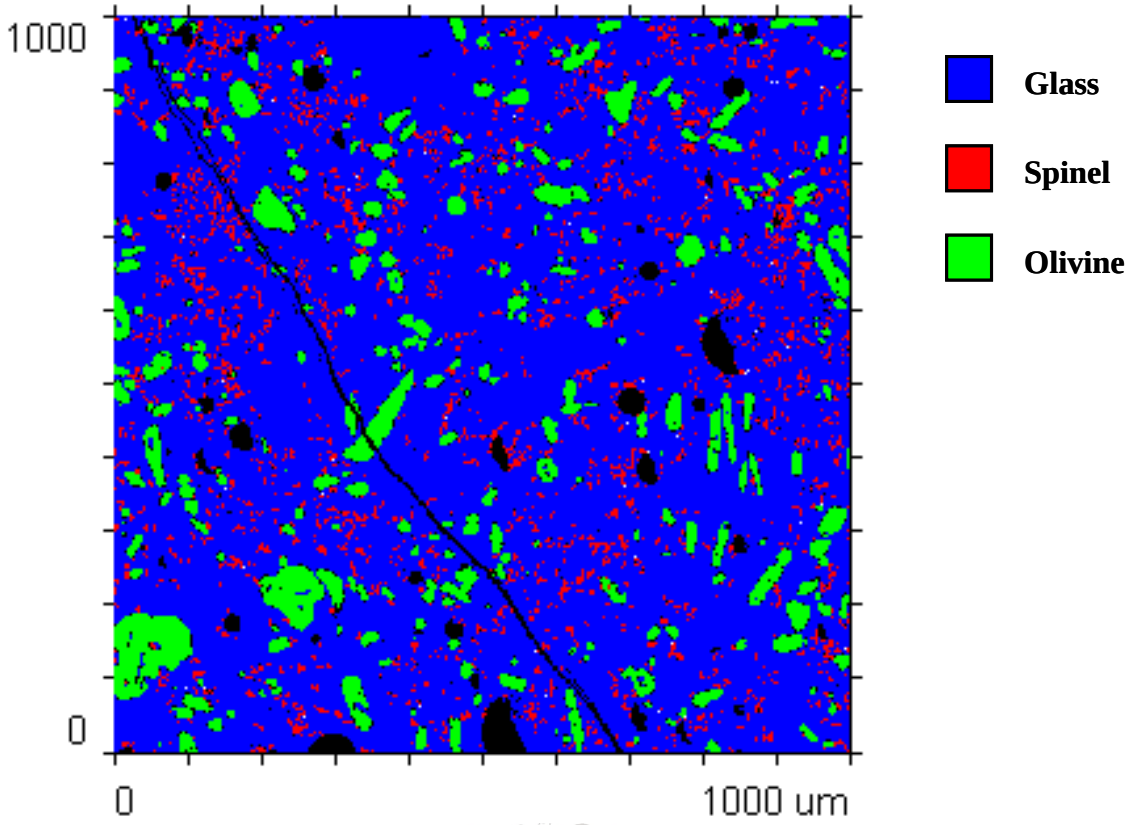

Figure D3: Phase map showing glass, spinel and olivine

APPENDIX E

Results for experiments conducted with a reaction time of 3 hours

1. Master slag compositions

The compositions of master slags used in these experiments are shown in Table E1.

Table E1: Compositions of master slags used for 3-hour experiments

Master Slag	SiO_2 %	Al_2O_3 %	FeO_x*	CaO %	Cr_2O_3 %	MgO %	FeO_x/MgO
1	47.7	4.9	15.3	4.8	1.2	25.1	0.6
2	47.3	4.8	21.0	4.7	1.5	19.2	1.1
3	45.4	4.6	28.2	4.5	1.5	14.6	1.9
4	44.3	4.9	19.9	4.9	3.2	21.8	0.9
5	43.9	4.8	18.1	4.9	5.2	22.0	0.8
6	49.2	4.9	17.0	4.9	6.0	17.2	1.0

* Total iron oxide expressed as FeO

It should be noted that bulk slag compositions after reaction were not determined in any of the 3-hour experiments because of samples being too small.

2. Experiments conducted at 1400°C

Results for experiments conducted at 1400°C and CO_2/CO ratios of 0.5, 2, 5 and 20 are shown in Table E2.

Table E2: Results for experiments conducted at 1400°C with a reaction time of 3 hours

CO_2/CO	Master slag	Phase	MgO	Cr_2O_3	FeO_x	SiO_2	CaO	Al_2O_3
0.5	4	Glass	7.18	0.36	58.13	26.27	2.96	5.11
		Spinel	2.86	35.37	59.78	0.04	0.04	1.91
		Olivine	25.24	0.38	43.34	30.85	0.10	0.08
	5	Glass	7.53	0.44	54.71	28.61	3.30	5.42
		Spinel	2.98	34.48	60.17	0.08	0.05	2.24
	6	Glass	7.34	0.58	50.79	33.02	3.11	5.16
		Spinel	3.06	37.31	57.79	0.07	0.05	1.72
2	1	Glass	7.84	0.41	53.36	29.39	3.20	5.80
		Spinel	2.92	25.25	69.18	0.05	0.04	2.56
		Olivine	28.16	0.35	37.16	34.13	0.10	0.10
	2	Glass	7.06	0.30	59.91	25.88	2.44	4.41
		Spinel	2.40	21.21	74.44	0.05	0.04	1.87
	3	Glass	4.70	0.24	68.42	21.12	1.97	3.56
		Spinel	1.54	13.37	83.85	0.04	0.03	1.17
	4	Glass	7.50	0.88	48.74	32.07	3.94	6.87
		Spinel	2.60	38.80	55.77	0.05	0.04	2.74
		Olivine	21.47	0.85	48.81	28.61	0.13	0.12
	5	Glass	7.87	0.89	46.42	33.56	4.37	6.89
		Spinel	2.90	42.02	51.26	0.07	0.06	3.69
		Olivine	22.31	0.91	47.37	29.12	0.13	0.17
	6	Glass	7.08	1.68	51.68	31.56	3.03	4.97
		Spinel	2.61	46.59	47.49	0.08	0.04	3.19
5	4	Glass	7.19	0.45	51.90	32.35	3.06	5.06
		Spinel	2.94	42.52	52.73	0.05	0.05	1.72
	5	Glass	6.47	0.40	59.67	25.12	3.12	5.21
		Spinel	2.39	35.74	59.14	0.06	0.05	2.63
		Olivine	20.39	0.40	52.97	26.03	0.11	0.10
	6	Glass	6.86	0.56	56.48	27.29	3.45	5.36
		Spinel	2.69	41.20	53.62	0.04	0.05	2.40
		Olivine	21.89	0.48	49.76	27.67	0.11	0.09
20	4	Glass	7.26	0.46	58.28	25.76	3.02	5.22
		Spinel	2.78	32.28	62.47	0.05	0.05	2.38
		Olivine	24.27	0.57	45.35	29.57	0.12	0.12
	5	Glass	7.78	0.59	54.89	28.05	3.29	5.40
		Spinel	3.05	37.86	56.70	0.06	0.05	2.29
		Olivine	25.85	0.53	42.32	31.05	0.11	0.14
		Pyroxene	12.48	0.65	47.78	31.37	2.61	5.10
	6	Glass	7.60	0.57	51.22	32.24	3.12	5.25
		Spinel	3.06	39.09	55.68	0.22	0.06	1.89
		Pyroxene	4.65	18.62	53.13	18.19	1.79	3.63

3. Experiments conducted at 1500°C

Results for experiments conducted at 1500°C are shown in Table E3. At a CO2/CO ratio of 2, the spinel phase for master slag 5 could not be analysed due to spinel crystals being too fine.

Table E3: Results for experiments conducted at 1500°C with a reaction time of 3 hours

CO_2/CO	Master slag	Phase	MgO	Cr_2O_3	FeO_x	SiO_2	CaO	Al_2O_3
0.5	4	Glass	8.41	0.64	58.45	25.33	2.67	4.50
		Spinel	3.17	35.35	58.75	0.05	0.04	2.64
	5	Glass	8.81	0.70	55.41	27.46	2.90	4.72
		Spinel	3.43	42.17	51.96	0.05	0.04	2.35
	6	Glass	7.04	0.90	52.31	31.70	2.99	5.06
		Spinel	3.11	42.97	52.04	0.04	0.05	1.79
2	1	Glass	10.45	0.68	52.16	28.84	2.80	5.08
		Spinel	3.76	38.10	54.83	0.06	0.04	3.21
	2	Glass	6.97	0.66	61.12	24.62	2.34	4.28
		Spinel	2.79	32.55	62.41	0.15	0.05	2.05
	3	Glass	4.54	0.51	69.55	20.09	1.86	3.44
		Spinel	1.86	24.65	72.01	0.04	0.03	1.41
	4	Glass	8.19	0.71	59.18	24.72	2.64	4.55
		Spinel	3.12	41.56	51.46	0.12	0.05	3.69
	5	Glass	8.45	0.94	56.81	26.39	2.82	4.59
		Spinel	not analysed					
	6	Glass	6.99	1.02	52.27	31.54	3.03	5.16
		Spinel	2.99	47.63	47.16	0.05	0.05	2.12
5	4	Glass	8.23	0.67	59.34	24.74	2.61	4.42
		Spinel	2.95	39.39	53.91	0.06	0.04	3.64
	5	Glass	8.86	0.73	56.15	26.89	2.85	4.53
		Spinel	3.13	44.04	49.37	0.06	0.04	3.36
	6	Glass	7.00	0.89	54.09	30.32	2.90	4.80
		Spinel	2.90	46.99	47.83	0.05	0.05	2.19
20	4	Glass	8.75	0.65	58.67	24.74	2.64	4.55
		Spinel	3.20	36.39	56.94	0.06	0.04	3.36
	5	Glass	9.10	1.05	55.28	27.04	2.82	4.72
		Spinel	3.36	42.27	51.44	0.05	0.04	2.84
	6	Glass	7.34	0.98	52.80	30.83	2.99	5.07
		Spinel	3.14	45.14	49.54	0.17	0.06	1.96

4. Experiments conducted at 1550°C

Table E4 shows the results for experiments conducted at 1550°C.

Table E4: Results for experiments conducted at 1550°C with a reaction time of 3 hours

CO_2/CO	Master slag	Phase	MgO	Cr_2O_3	FeO_x	SiO_2	CaO	Al_2O_3
0.5	4	Glass	8.18	0.84	58.89	25.05	2.61	4.44
		Spinel	3.22	39.22	54.83	0.06	0.04	2.63
	5	Glass	8.84	0.93	55.76	27.04	2.83	4.61
		Spinel	3.32	43.54	50.37	0.05	0.04	2.68
	6	Glass	7.02	1.11	53.28	30.81	2.91	4.87
		Spinel	3.13	46.73	48.28	0.05	0.05	1.76
2	1	Glass	10.46	0.93	52.42	28.50	2.75	4.93
		Spinel	3.91	41.97	50.82	0.09	0.05	3.18
	2	Glass	6.92	0.90	61.24	24.37	2.32	4.26
		Spinel	2.90	38.18	56.75	0.05	0.04	2.07
	3	Glass	4.53	0.79	69.73	19.72	1.84	3.39
		Spinel	1.95	27.81	68.72	0.03	0.03	1.46
	4	Glass	8.48	1.08	58.51	24.67	2.64	4.61
		Spinel	3.35	46.85	45.26	0.07	0.05	4.42
	5	Glass	8.61	1.55	54.26	27.95	2.79	4.85
		Spinel	3.44	51.94	40.34	0.06	0.05	4.17
	6	Glass	6.97	1.31	53.83	30.06	2.91	4.91
		Spinel	2.97	52.96	41.68	0.12	0.06	2.20
5	4	Glass	7.05	1.16	53.21	30.69	2.91	4.97
		Spinel	3.21	45.68	49.27	0.04	0.05	1.74
	5	Glass	8.21	0.90	59.03	24.65	2.60	4.60
		Spinel	3.30	37.37	56.52	0.09	0.06	2.65
	6	Glass	8.88	0.95	55.64	26.96	2.85	4.71
		Spinel	3.52	41.56	52.26	0.05	0.04	2.57
20	4	Glass	8.23	1.16	59.07	24.46	2.58	4.50
		Spinel	3.29	40.00	53.97	0.05	0.04	2.65
	5	Glass	8.91	0.91	55.83	26.82	2.82	4.70
		Spinel	3.51	43.53	50.31	0.05	0.04	2.56
	6	Glass	7.04	1.46	53.29	30.39	2.90	4.92
		Spinel	3.22	47.19	47.73	0.07	0.04	1.76

5. Experiments conducted at 1600°C

Table E5 shows the results for experiments conducted at 1600°C.

Table E4: Results for experiments conducted at 1600°C with a reaction time of 3 hours

CO_2/CO	Master slag	Phase	MgO	Cr_2O_3	FeO_x	SiO_2	CaO	Al_2O_3
0.5	4	Glass	8.12	1.22	59.39	24.34	2.54	4.39
		Spinel	3.41	43.90	50.00	0.07	0.05	2.58
	5	Glass	8.67	1.36	56.31	26.35	2.75	4.56
		Spinel	3.55	47.27	46.50	0.06	0.05	2.57
	6	Glass	6.89	1.62	53.98	29.90	2.83	4.78
		Spinel	3.22	50.24	44.75	0.05	0.05	1.70
2	1	Glass	10.46	1.39	52.23	28.20	2.73	5.00
		Spinel	4.11	48.73	44.12	0.06	0.04	2.95
	2	Glass	6.86	1.29	61.34	23.97	2.31	4.23
		Spinel	3.00	42.66	52.25	0.04	0.04	2.00
	3	Glass	4.53	1.15	69.85	19.27	1.84	3.35
		Spinel	2.11	34.22	62.09	0.04	0.03	1.51
	4	Glass	8.43	1.71	57.56	24.91	2.61	4.79
		Spinel	3.52	55.02	36.89	0.08	0.06	4.43
	5	Glass	9.18	1.72	55.27	26.16	2.87	4.81
		Spinel	3.63	53.63	38.50	0.06	0.05	4.13
	6	Glass	7.31	1.95	53.09	29.67	2.93	5.05
		Spinel	3.13	55.95	38.69	0.05	0.05	2.14
5	4	Glass	8.32	1.51	58.64	24.46	2.57	4.51
		Spinel	3.38	51.84	41.00	0.06	0.05	3.66
	5	Glass	8.94	1.52	55.56	26.55	2.82	4.61
		Spinel	3.40	52.30	40.29	0.05	0.04	3.91
	6	Glass	7.04	1.99	54.15	29.27	2.84	4.71
		Spinel	2.94	55.72	39.18	0.04	0.04	2.07
20	4	Glass	8.11	1.22	59.62	24.12	2.53	4.40
		Spinel	3.27	44.79	48.48	0.06	0.04	3.36
		Pyroxene	8.33	1.14	58.58	24.86	2.60	4.48
	5	Glass	8.85	1.14	56.49	26.15	2.83	4.54
		Spinel	3.39	45.77	47.72	0.06	0.05	3.01
	6	Glass	7.02	1.59	53.93	29.77	2.87	4.82
		Spinel	3.11	51.33	43.64	0.04	0.05	1.82

6. Summary of phases observed

A summary of the phases observed under each of the experimental conditions investigated can be found in Table E5.

Table E5: Summary of phase observed under each experimental condition with a reaction time of 3 hours

Master slag	Temperature (°C)	CO_2/CO ratio			
		0.5	2	5	20
1	1400	-	GSO	-	-
	1500	-	GS	-	-
	1550	-	GS	-	-
	1600	-	GS	-	-
2	1400	-	GS	-	-
	1500	-	GS	-	-
	1550	-	GS	-	-
	1600	-	GS	-	-
3	1400	-	GS	-	-
	1500	-	GS	-	-
	1550	-	GS	-	-
	1600	-	GS	-	-
4	1400	GSO	GSO	GS	GSO
	1500	GS	GS	GS	GS
	1550	GS	GS	GS	GS
	1600	GS	GS	GS	GSP
5	1400	GS	GSO	GSO	GSOP
	1500	GS	GS	GS	GS
	1550	GS	GS	GS	GS
	1600	GS	GS	GS	GS
6	1400	GS	GS	GSO	GSP
	1500	GS	GS	GS	GS
	1550	GS	GS	GS	GS
	1600	GS	GS	GS	GS